

AD-A134 299

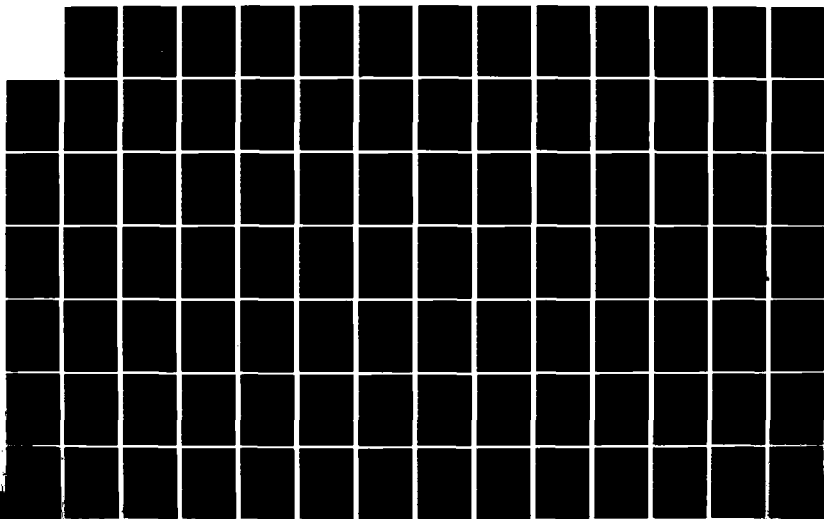
THEORETICAL STUDIES RELATING TO THE INTERACTION OF
RADIATION WITH MATTER: (U) NEW YORK UNIV NY DEPT OF
PHYSICS P R BERMAN 15 SEP 83 N00014-77-C-0553

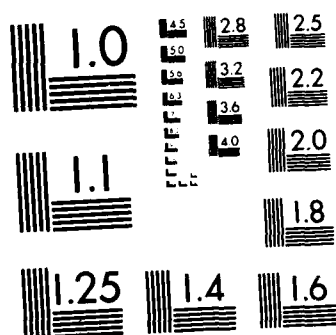
1/2

UNCLASSIFIED

F/G 20/8

NL





MICROCOPY RESOLUTION TEST CHART
NATIONAL BUREAU OF STANDARDS-1963-A

REPORT DOCUMENTATION PAGE		READ INSTRUCTIONS BEFORE COMPLETING FORM
1. REPORT NUMBER AR 6	2. GOVT ACCESSION NO.	3. RECIPIENT'S CATALOG NUMBER
4. TITLE (and Subtitle) Theoretical Studies Relating to the Interaction of Radiation with Matter: Atomic Collision Processes Occurring in the Presence of Radiation Fields		5. TYPE OF REPORT & PERIOD COVERED Interim 8/1/82 - 7/31/83
7. AUTHOR(s) P.R. Berman		6. PERFORMING ORG. REPORT NUMBER
9. PERFORMING ORGANIZATION NAME AND ADDRESS Prof. P.R. Berman Physics Dept. New York University 4 Washington Place, New York, N.Y. 10003		8. CONTRACT OR GRANT NUMBER(s) N00014-77-C-0553
11. CONTROLLING OFFICE NAME AND ADDRESS Office of Naval Research Resident Representative New York 715 Broadway, N.Y., N.Y. 10003		10. PROGRAM ELEMENT, PROJECT, TASK AREA & WORK UNIT NUMBERS
14. MONITORING AGENCY NAME & ADDRESS (if different from Controlling Office)		12. REPORT DATE Sept. 15, 1983
		13. NUMBER OF PAGES 105
		15. SECURITY CLASS. (of this report) Unclassified
		15a. DECLASSIFICATION/DOWNGRADING SCHEDULE
16. DISTRIBUTION STATEMENT (of this Report) Approved for public release; distribution unlimited		
17. DISTRIBUTION STATEMENT (of the abstract entered in Block 20, if different from Report)		
18. SUPPLEMENTARY NOTES		
19. KEY WORDS (Continue on reverse side if necessary and identify by block number) Laser Spectroscopy, Optical Collisions, Radiative Collisions, Two-Level System, Atomic Coherence, Degenerate Four-Wave Mixing, Photon as Catalyst, Saturation Spectroscopy		
20. ABSTRACT (Continue on reverse side if necessary and identify by block number) Work is reported in the areas of:- <ul style="list-style-type: none"> (1) Saturation Spectroscopy (2) Heating and Cooling via Laser-Assisted Collisions (3) Creation of Electronic State Coherences via Laser-Assisted Collisions (4) Two-Level Atom Plus Radiation Pulse (5) Photon as Catalyst (6) Collisional Effects in Four-Wave Mixing 		

MIC FILE COPY

AD-A134 299

NOV 3 1983

S A

Annual Report (AR6)

Title: "Theoretical Studies Relating to the Interaction of Radiation
with Matter: Atomic Collision Processes Occurring in the
Presence of Radiation Fields"

Supported by the U.S. Office of Naval Research

Contract No.: N00014-77-C-0553

Report of Period: August 1, 1982 - July 31, 1983

Reproduction in whole or in part is permitted for any purpose of the
United States Government.

Approved for public release; distribution unlimited.



A-1

Research has been carried out in the areas of (1) Saturation spectroscopy including effects of level degeneracy, (2) Heating and cooling of vapors using collisionally-aided radiative excitation, (3) Creation of electronic state coherences in laser-assisted collisions, (4) Two-level problem plus radiation pulse, (5) Photon as catalyst effect and (6) Collisional processes in 4-wave mixing experiments.

(1) Saturation Spectroscopy Including Effects of Level Degeneracy
(C. Feuillade, P. Berman).

Owing to a favorable resonance transition frequency, Na has been the favorite choice of experimentalists in laser spectroscopic studies. The fine and hyperfine structure of Na leads to a multitude of levels, even in the Na ground state. There have been no rigorous calculations that properly incorporate the effects of fine and hyperfine structure, collisional effects and optical pumping effects with Na as the active atom in a laser spectroscopy experiment. However, it is clear that optical pumping of the ground state, in particular, can severely modify the laser spectroscopic line shapes.

Due to the fundamental importance of the Na system in laser spectroscopy, we have begun a project to include all fine and hyperfine structure of the 3S, 3P and 4D levels of Na, interacting with two laser fields. Both steady state and transient solutions will be sought, to clearly isolate the effects of optical pumping. Eventually, collisional effects will be included.

The first stage of this calculation has now been completed.¹ Using both an irreducible tensor and standard (m-basis) representation for atomic density matrix elements, we have derived expressions for the probe absorption line shape when a pump field of arbitrary strength and polarization drives a transition between two levels (each containing a number of degenerate magnetic sublevels) and a probe field of arbitrary strength and polarization drives a coupled transition. In essence, the calculation is one describing the saturation spectroscopy of three-level systems including effects of level degeneracy. The probe absorption line shape is calculated

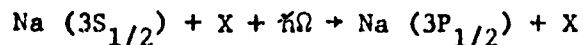
for each velocity subclass of atoms but, at this stage of our work, no average over the atomic velocity distribution has been included. Results are presented for weak probe fields as a function of pump field strength, polarization and detuning. Effects of optical pumping are included.

The results clearly display the effects of pump field strength (Rabi splittings), pump field polarization (position and number of Rabi split resonance peaks) pump field detuning (position of resonance peaks) and optical pumping (relative strengths of the resonance peaks). We have shown that it is advantageous to use the m-basis rather than the irreducible tensor representation provided that the laser fields are either circularly or linearly polarized, if collisional effects are unimportant. We have also shown how to predict the position of the resonance peaks using a dressed-atom approach.²

As they stand, the calculations can be used to describe the interactions of laser fields with an atomic beam. The next step in the calculation will be to include an average over an atomic velocity distribution so that laser field-atomic vapor interactions can be properly modeled.

(2) Heating and Cooling of Vapors Using Collisionally-Aided Radiative Excitation (E. Giacobino, P. Berman).

Several years ago³, we predicted that cooling or heating of an atomic vapor could be achieved using Collisionally-Aided Radiative Excitation (CARE). In Prof. Stroke's laboratory, we are now trying to carry out an experiment of this type. The reaction under investigation is



where X is a rare gas atom.

The energy defect between the photon energy $\hbar\Omega$ and the $3P_{1/2} - 3S_{1/2}$ transition frequency is provided by a corresponding change in the translational energy of the Na - rare gas system. To probe this energy change, the velocity distribution of the excited state Na atom is monitored using the transition to the 4D state. Calculations were made which indicated that heating of the Na should be detectable by this scheme using a positive

energy defect and heavy rare gas perturbers. Experimental confirmation of the heating effect has now been achieved.^{4*} With Ar or Xe rare gas perturbers, the excited state Na velocity distribution was considerably broader than the thermal one, while with He perturbers [the "light" He takes up the excess energy rather than the "heavy" Na] the normal thermal width was observed.

We are still interested in producing a macroscopic heating or cooling of the vapor using CARE. It may be possible to produce such an effect using a high density sodium cell. In that case, CARE is produced via resonant collisions which have a relatively large cross section. Order of magnitude calculations have been carried out^{5*} which indicate that measurable temperature differences can be achieved with Na densities of order $10^{15}/\text{cm}^3$. An experimental test of the predictions is envisioned.

(3) Creation of Electronic State Coherences in Laser-Assisted Collisions. (P. Berman, E. Giacobino).

We have proposed a new method for generating electronic state coherences using laser assisted collisions.^{6*} Both Collisionally-Aided Radiative Excitation (CARE) and Radiatively-Aided Inelastic Collisions (RAIC) can be used to generate such coherences. Two pulsed laser fields are incident on two atoms undergoing a collision.

In CARE (Fig. 1a),

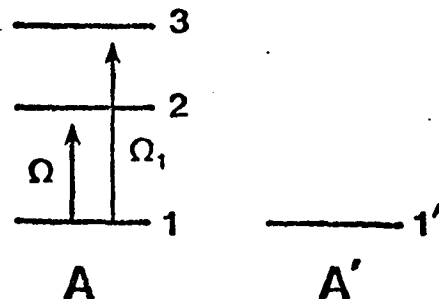


Fig. 1a

* An asterisk on a reference indicates that the reference is appended to this report.

the reaction is

$$A_1 + A'_1 + \hbar\Omega + \hbar\Omega_1 \rightarrow A_1(23) + A'_1,$$

where A and A' are the atoms undergoing the collision and the notation A(ij) is meant to indicate a coherence between states i and j. The frequency difference $\Omega_1 - \Omega$ must be close to the resonance frequency ω_{32} for the coherence to be generated.

In RAIC (Fig. 1b),

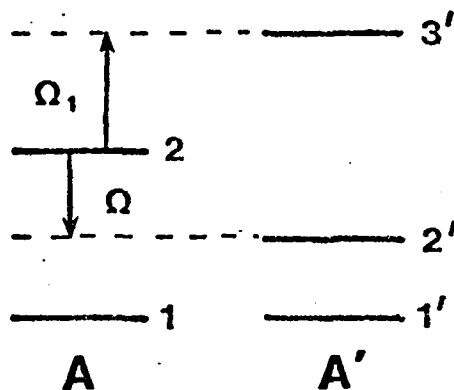


Fig. 1b

a typical reaction is $A_2 + A'_1 + \hbar\Omega + \hbar\Omega_1 \rightarrow A_1 + A'(2'3')$ producing a $2'3'$ coherence in atom A'. This is a somewhat novel way to produce electronic state coherences. In certain cases, it may be possible to produce coherence between states of opposite parity, which could then radiate sum frequency radiation. This process is under investigation.

(4) Two-level Atom Plus Radiation Pulse (E. Robinson, P. Berman).

Research continues in the fundamentally important problem of a two-level system coupled by a radiation pulse. In the large detuning limit, we were able to show that certain classes of coupling pulses having the same asymptotic Fourier transforms will yield transition probabilities that are related to each other by a simple scaling transformation.^{7*} Methods for evaluating the transition probabilities in the large-detuning limit have also been developed, and we are trying to compare our results

with those of other authors.^{8,9} In particular, if we would like to understand the details of Crother's calculations⁸ to see if they can be applied to the general theory of laser-assisted collisions.

Work continues on an eigenvalue method for solving the two-level problem. Eigenvalue expansions for the probability amplitudes have been obtained, approximate positions of the eigenvalues (i.e. those field strengths leading to zero transition probability) determined, and expressions for the transition probability to third order in the detuning were derived.^{10*,11}

(5) Photon as Catalyst Effect (A. Lau).

Using experimentally determined values for energies, transition moments and decay rates, the rate for bound-continuum transitions in I_2 resulting from the photon as catalyst effect have been calculated.^{12*} By stimulated emission, the laser field takes an I_2 bound state to a virtual intermediate state from which a transition to the continuum can occur by the absorption of another photon. There is no net photon absorption - the laser field acts as a "catalyst".

(6) Collisional Processes in 4-Wave Mixing Experiments. (P. Berman)

In collaboration with J. Lam (Hughes Research), we are continuing to attempt to develop a consistent theory of collision-induced structure in 4-wave mixing experiments that was discussed in last year's Annual Report.¹³ That there is still considerable experimental interest in this area is evidenced by the recent work in Bloembergen's group.¹⁴

(7) Miscellaneous

Our review article on laser-assisted collisions has been published.^{15*}

References

1. C. Feuillade and P.R. Berman, Phys. Rev. A (to appear).
2. P.R. Berman and R. Salomaa, Phys. Rev. A 25, 2667 (1982).
3. P.R. Berman and S. Stenholm, Opt. Commun. 24, 155 (1978).

4. E. Giacobino, M. Tawil, P.R. Berman, O. Redi and H.H. Stroke, Phys. Rev. A (to appear as Rapid Communication in October, 1983); E. Giacobino, M. Tawil, O. Redi, R. Vetter, H.H. Stroke and P.R. Berman, to appear in Laser Spectroscopy VI, edited by H.P. Weber (Springer, Berlin, 1983).
5. E. Giacobino and P.R. Berman, in NBS Special Publication 653, edited by W.D. Phillips (U.S. Govt. Printing Office, Washington, D.C. 1983) pp. 112-118.
6. P.R. Berman and E. Giacobino, Phys. Rev. A (to appear).
7. E.J. Robinson and P.R. Berman, Phys. Rev. A27, 1022 (1983).
8. D.S.F. Crothers, J. Phys. B5, 1680 (1972); B6, 1418 (1973).
9. M.G. Payne and M.H. Nayfeh, Phys. Rev. A13, 595 (1976); L. Vainshtein, L. Presnyakov and I. Sobelman, Sov. Phys., - JETP 16, 370 (1963).
10. E.J. Robinson, to appear in Proceedings of Fifth Rochester Conference on Coherence and Quantum Optics.
11. E.J. Robinson, Phys. Rev. A (to appear).
12. A.M.F. Lau, S.N. Dixit, and J. Tellinghuisen, Phys. Rev. A (submitted).
13. Report AR5 (1982).
14. L.J. Rothberg and N. Bloembergen, to appear in Laser Spectroscopy VI, op. cit.
15. P.R. Berman and E.J. Robinson, in Photon Assisted Collisions and Related Topics, edited by N.K. Rahman and C. Guidotti (Harwood Academic Pub., Chur, Switz., 1982) pp. 15-34.

COMBINED RADIATION FIELD - COLLISIONAL EXCITATION OF ATOMS

PAUL R. BERMAN and EDWARD J. ROBINSON
Physics Department, New York University, 4 Washington
Place, New York, New York 10003 U.S.A.

Abstract The physical principles underlying the combined radiation field - collisional excitation of atoms are reviewed. A discussion of both collisionally-aided radiative excitation ("optical collisions") and radiatively-aided inelastic collisions ("radiative collisions") is presented.

INTRODUCTION

The purpose of this paper is to present a simple discussion of atomic transitions induced by the simultaneous action of a laser field and a collision.

Consider a reaction of the general form

$$A_i + B_i + \hbar\Omega \rightarrow A_f + B_f, \quad (1)$$

where $A_{i,f}$ and $B_{i,f}$ are internal states of two atoms A and B undergoing a collision and Ω is the frequency of an applied radiation field. If, in the absence of the collision, one finds

$$A_i + \hbar\Omega \rightarrow A_i$$

$$B_i + \hbar\Omega \rightarrow B_i$$

while, in the absence of the external field, one has

$$A_i + B_i \rightarrow A_i + B_i,$$

the reaction (1) is of a type that requires the simultaneous presence of both a collisional interaction and external radiation field if either or both final atomic states are to differ from the initial ones. One may then speak of "laser-assisted collisions" or "collisionally-assisted light absorption". These are processes which have been the focus of a large number of experimental¹⁻¹⁶ and theoretical¹⁷⁻⁴⁶ investigations in the last decade. In this work, we discuss the physical principles underlying such reactions; more detailed theoretical treatments may be found in the literature.

Reactions of the form (1) may be further classified into two categories. The first of these we refer to as Collisionally-Aided Radiative Excitation³⁷ (CARE) and has been designated by others as "optical collisions".¹⁹ The CARE reaction is easy to visualize (see Fig. 1). An atom A

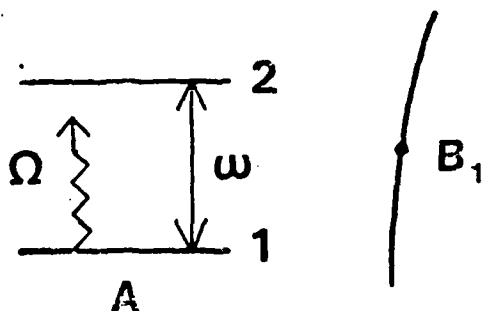


Figure 1. A schematic representation of the CARE reaction $A_1 + B_1 + \hbar\Omega \rightarrow A_2 + B_1$. A laser field of frequency Ω is incident on atom A and can drive the 1-2 transition when atom A undergoes a collision with a ground state perturber B.

is irradiated by a laser field whose frequency Ω is close

enough to that of a resonance. This is a good approximation to the exact resonance, but small corrections may be made compared to the natural linewidth of the transition, but small corrections may be made. With such a large laser field, the probability to excite atom A during a collision with a laser field, the probability is enhanced. The energy of the atomic transition is changing, depending on the change in the energy of the atoms.

The second category is referred to as Radiatively-Assisted Collisional Excitation or "LICET - Laser Induced Collisional Excitation Transfer".³ Atoms A and B₁ and, as a consequence of a collision, a laser field interaction between A_f and B_f. The probability of this process is assumed to be high, in the absence of the photon as a product of the transition A₁ + B₁ → A_f + B_f. The cross section will be large if the laser field is to be resonant with the transition and final components of the transition, with the

COMBINED RADIATION FIELD - COLLISIONAL EXCITATION

enough to that of an atomic transition for a two-level approximation to be valid. The field's frequency is detuned from exact resonance by an amount Δ which is large compared to the natural and Doppler widths of the transition, but small compared to the thermal energy divided by \hbar . With such a large detuning, the probability for the field to excite atom A is negligibly small. However, if A undergoes a collision with atom B while interacting with the field, the probability for excitation can be greatly enhanced. The energy mismatch $\hbar\Delta$ between the photon and atomic transition energies is compensated for by a corresponding change in the translational energy of the colliding atoms.

The second class of reactions of the type (1) we refer to as Radiatively-Aided Inelastic Collisions³⁷ (RAIC) and has been designated by others as "radiative collisions"¹⁷ or "LICET - Laser Induced Collisional Excitation Transfer".³ Atoms A and B are prepared in initial states A_i and B_i and, as a consequence of the combined atom-atom and atom-field interactions, they emerge in some new final states A_f and B_f . The process is depicted schematically in Fig. 2.

The transition between initial and final states is assumed to be highly improbable or energetically forbidden in the absence of the applied field. Thus, one can view the photon as providing the energy to assist the inelastic transition $A_i + B_i \rightarrow A_f + B_f$. In general the RAIC cross-section will be largest if the photon frequency is chosen to be resonant with the energy difference between initial and final composite atomic states. However, as in CARE, significant excitation can occur under off-resonance conditions, with the energy mismatch again compensated by a

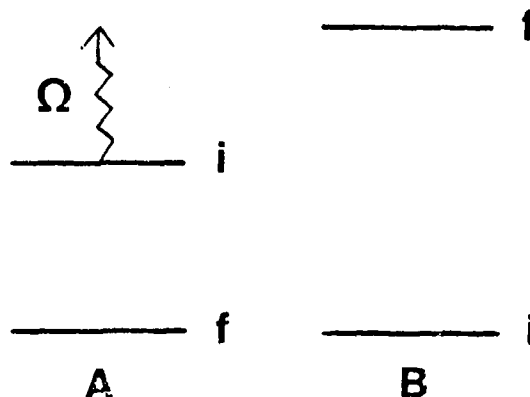


Figure 2. Atoms A and B undergo a collision in the presence of radiation. The field frequency Ω is approximately equal to a transition frequency in the composite AB system. The RAIC reaction is of the form

$$A_i + B_i + \hbar\Omega \rightarrow A_f + B_f.$$

change in translational energy.

Before examining CARE and RAIC in greater detail, it is useful to review the problem of the interaction of a radiation pulse with a two-level atomic system.

ATOM + PULSE

In this section, we examine the interaction of a two-level atom with a radiation pulse whose electric field of polarization \hat{e} may be represented by

$$\underline{E}(t) = \hat{e}E_0(t)\cos(\Omega t),$$

The smooth pulse envelope function $E_0(t)$ is assumed to

COMB

vanish as $\cos(\Omega t)$.
transitions
allowing
the field.
 $t = -\infty$,
state 2 for
the atom-

$$V(t)$$

where \underline{H} is
Schrödinger
tions for
presentati
components

$$\dot{a}_1 =$$

$$\dot{a}_2 =$$

where $\Delta =$
coupling
 $\chi(t)$ is so

The p
following
frequency
ponents ch
of states
justifying
detuning
fication,
smooth pul

COMBINED RADIATION FIELD - COLLISIONAL EXCITATION

vanish as $t \rightarrow \pm\infty$ and to vary slowly in comparison with $\cos(\Omega t)$. The difference $|\Omega - \omega|$, where ω is the atomic transition frequency, is taken to be much less than $(\omega + \Omega)$, allowing one to neglect the "anti-rotating" components of the field. For an atom which is in its lower state 1 at $t = -\infty$, we seek the probability that it is excited to state 2 following its interaction with the pulse. Taking the atom-field interaction to be

$$V(t) = -\underline{\mu} \cdot \underline{E}(t),$$

where $\underline{\mu}$ is the atomic dipole moment operator, one may use Schrödinger's equation to obtain the time evolution equations for the state amplitudes. In the interaction representation and with the neglect of the anti-rotating components of the field, one finds

$$\dot{a}_1 = -i\chi(t) e^{i\Delta t} a_2 \quad (2a)$$

$$\dot{a}_2 = -i\chi(t) e^{-i\Delta t} a_1, \quad (2b)$$

where $\Delta = \Omega - \omega$ is the detuning, $\chi(t) = \mu E_0(t)/2\hbar$ is the coupling parameter, and $\mu = \langle 1 | \underline{\mu} \cdot \hat{e} | 2 \rangle = \mu^*$. The frequency $\chi(t)$ is sometimes referred to as the Rabi frequency.

The problem is conveniently described in terms of the following parameters: (1) the pulse duration T , (2) the frequency $f = \dot{\chi}(t)/\chi(t)$ which determines the frequency components characterizing the pulse, (3) the natural lifetimes of states 1 and 2 which are taken to be much longer than T , justifying the omission of decay terms in Eqs. (2), (4) the detuning Δ , and (5) the Rabi frequency $\chi(t)$. As a simplification, we set $f \approx T^{-1}$, which is a good approximation for smooth pulses.

If the detuning and envelope function are such that $|\Delta|T \gg 1$, the pulse contains negligibly small Fourier components at the frequency needed to compensate for the detuning. In this limit, the pulse is said to be adiabatic. That is, the excitation probability following the passage of the pulse is vanishingly small, *i.e.*, proportional to $\exp(-2|\Delta|T)$ for typical envelope functions. It is interesting to note that the excitation probability remains exponentially small regardless of field strength $\chi(t)$, reflecting the fact that the Fourier components needed to effect the excitation are essentially absent. As the field strength $\chi(t)$ increases, the excitation probability, which is proportional to $A^2 = |\int_{-\infty}^{\infty} \chi(t) dt|^2$ for $A^2 \ll 1$, exhibits some type of saturation behavior for $A^2 > 1$. Thus, without some additional interaction, an adiabatic pulse cannot appreciably excite the atom. The "additional interaction" can be provided by a collision.

CARE

Assume that the atom undergoes a collision with a perturber during its interaction with the adiabatic radiation pulse. This collision occurs on a time scale τ_c (typically 10^{-12} sec for the thermal atoms under consideration here) which is short compared to T (typically 10^{-9} sec). The perturber can be considered as providing an effective time-dependent potential which modifies the energy separation of states 1 and 2 in a transient manner. If $\hbar V_1(t)$ is the collision-induced modification of level 1's energy, then the instantaneous transition frequency is

$$\omega(t) = \omega + V_{LS}(t),$$

where

$$V_{LS}(t) = V$$

It is implicit in the case of the electronic configuration of the field (see

The effect of the collision on the Fourier components of the probability of collisional action of the

$$A_1 + B_1 +$$

The state amplitudes

$$\dot{a}_1 = -i\chi$$

$$\dot{a}_2 = -i\chi$$

subject to the

$$a_1(-\infty) =$$

In order to the various duration, τ_c , and v_r the important

COMBINED RADIATION FIELD - COLLISIONAL EXCITATION

where

$$V_{LS}(t) = V_2(t) - V_1(t).$$

It is implicitly assumed that $V_1(t) \neq V_2(t)$, as is generally the case if levels 1 and 2 belong to different electronic configurations.⁴⁷ The collision does not have sufficient energy to couple levels 1 and 2 in the absence of the field (see Fig. 1).

The effect of the collision-induced transient variation of the transition frequency is to introduce appreciable Fourier components into the excitation mechanism at frequencies up to $\omega_c = \tau_c^{-1} \gg T^{-1}$. These added Fourier components lead to a new contribution to the excitation probability which is much larger than the $\exp(-2|\Delta|T)$ term associated with the atom-adiabatic pulse interaction. This "collisionally-assisted" contribution leads to a CARE reaction of the form

$$A_1 + B_1 + n\Omega \rightarrow A_2 + B_2.$$

The state amplitudes now evolve according to

$$\dot{a}_1 = -i\chi(t)\exp[i\Delta t - i\int_0^t V_{LS}(t')dt']a_2 \quad (3a)$$

$$\dot{a}_2 = -i\chi(t)\exp[-i\Delta t + i\int_0^t V_{LS}(t')dt']a_1, \quad (3b)$$

subject to the initial conditions

$$a_1(-\infty) = 1, a_2(-\infty) = 0. \quad (3c)$$

In order to discuss CARE, it is useful to again refer to the various time scales in the problem. The collision duration, $\tau_c(b, v_r) = b/v_r$, where b is the impact parameter and v_r the interatomic speed associated with a collision, is an important time parameter. Although $\tau_c(b, v_r)$ varies

from collision to collision, we can define a representative time $\tau_c \equiv \tau_c(b_0, \bar{v}_r)$ in which \bar{v}_r is the average interatomic relative speed and b_0 is an impact parameter chosen to guarantee that τ_c is "representative". Generally speaking, b_0 will be that impact parameter for which the phase $\int_{-\infty}^{\infty} V_{LS}(b, \bar{v}_r, t) dt$ takes on a value of order unity; a typical value for b_0 is 10^{-7} cm. The dimensionless parameters which enter our considerations are $|\Delta|T$ which turns out to be unimportant, $|\Delta|\tau_c$ which critically categorizes the detuning, $\chi(t)T$ which represents the strength of the atom-field interaction before and after the collision, and χT which represents the strength of the atom-field interaction during the collision. The field strength $\chi(t)$ is approximately constant during a collision and χ represents some characteristic value of $|\chi(t)|$ for the pulse. As noted above, $\tau_c/T \ll 1$.

Weak Fields: $\chi T \ll 1$

For weak fields, the excitation probability can be calculated from Eqs. (3) using first-order perturbation theory. The results depend critically on the value of $|\Delta|\tau_c$.

If $|\Delta|\tau_c \ll 1$, the only change in state amplitude a_2 during the collision arises from the level-shifting term. The collision acts to provide a sudden change in the phase ϕ of a_2 , given by $\phi(b, v_r) = \int_{-\infty}^{\infty} V_{LS}(b, v_r, t) dt$. This impulse destroys the adiabatic response of the two-level system, and gives a final state amplitude

$$a_2 = -i \left[\int_{-\infty}^{t_c} \chi(t') e^{-i\Delta t'} dt' + e^{i\phi} \int_{t_c}^{\infty} \chi(t') e^{-i\Delta t'} dt' \right] \\ = -2i [\chi(t_c)/\Delta] e^{-i\Delta t_c} e^{i\phi/2} \sin(\phi/2),$$

where t_c is the time at which the collision occurs. Setting $|\chi(t_c)| \equiv \chi$, one obtains the excitation probability

COMBINED RADIATION

$$|a_2(b, v_r, \infty)|^2$$

and the corresponding

$$\sigma_c(v_r) = 2\pi \int_0^{\infty} |a_2(b, v_r, \infty)|^2 b db \\ = 2(\chi T)^2$$

The result (4-5) is smaller than any compact cross-section, the Fourier transform over the range of χ .

The impact parameter b is chosen in the manner. If we were to average, find a probability. The CARE cross-section for excitation probability ($\approx \pi b_0^2$).

If $|\Delta|\tau_c > 1$, the excitation by the detuning is not valid. The collision is too fast that appreciable detuning is induced. If this were the CARE transition $\tau_c(b, v_r)$. However, the origin may be seen. In drawing the curve $V_{LS}(t) < 0$; the curve is an obvious general

COMBINED RADIATION FIELD - COLLISIONAL EXCITATION

$$|a_2(b, v_r, \infty)|^2 = 4(\chi/\Delta)^2 \sin^2[\phi(b, v_r)/2] \quad (4)$$

and the corresponding CARE cross section

$$\sigma_c(v_r) = 2\pi \int_0^\infty |a_2(b, v_r, \infty)|^2 b db \quad (5a)$$

$$= 2(\chi/\Delta)^2 (\pi b_0^2). \quad (5b)$$

The result (4-5) is known as the "impact limit" since τ_c is smaller than any other time scale in the problem. The impact cross-section is independent of the sign of Δ since the Fourier transform of the collision interaction is flat over the range of Δ represented by $|\Delta|\tau_c \ll 1$.

The impact result can be viewed in an alternative manner. If we were to suddenly interrupt the atom-radiation pulse interaction at any time t_c , we would, on average, find a population $[\chi(t_c)/\Delta]^2$ in the upper state. The CARE cross-section is equal to the product of this excitation probability and the collision cross section ($= \pi b_0^2$).

If $|\Delta|\tau_c > 1$, the phase induced in a_2 during the collision by the detuning is not negligible, and the impact result is not valid. As we have seen, one consequence of the collision is to shorten the relevant time from T to τ_c , so that appreciable Fourier components up to τ_c^{-1} are introduced. If this were all that occurred, one would expect a CARE transition probability that varied as $\exp[-2|\Delta|\tau_c(b, v_r)]$. However, there is an additional effect, whose origin may be seen in Fig. 3, which modifies this result. In drawing the energy levels in Fig. 3, we have chosen $V_{LS}(t) < 0$; the case for arbitrary $V_{LS}(t)$ may be treated by an obvious generalization of the method given below.

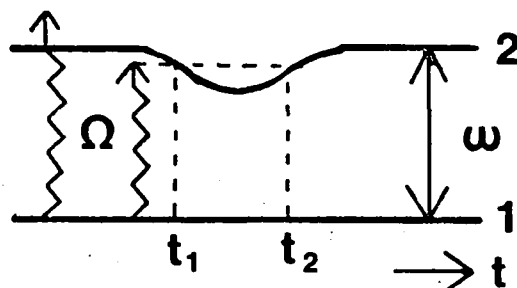


Figure 3. Energy levels of atom A during a collision. "Instantaneous resonances" [$\Omega = \omega(t)$] can occur for detunings $\Delta < 0$ only; for $\Delta > 0$, the collision detunes the atomic transition further from resonance.

The CARE cross section is a strongly asymmetric function of Δ when $|\Delta|\tau_c > 1$. For a given $\Delta < 0$, collisions can always produce $\omega(t) = \Omega$ for short times during the collision;⁴⁸ i.e., the systems become instantaneously resonant with the field. Such times are labeled t_1 and t_2 in Fig. 3. The phase of a_2 varies rapidly owing to the factor $\exp(-i\Delta t)$, except at t_1 and t_2 , where the oscillation is suppressed by the factor $\exp[i\int_{t_1}^{t_2} V_{IS}(t')dt']$. The major contributions to the excitation amplitude are provided by these times of stationary phase. The corresponding CARE cross-section varies as an inverse power law in $|\Delta|$, instead of the exponential that characterizes other regimes. The fact that the points of stationary phase provide the major contributions to $a_2^{(\infty)}$ is linked to the condition $|\Delta|\tau_c > 1$. That is, the (pulse + collision) does not contain the Fourier components at Δ to appreciably excite the atom; in this case the instantaneous resonances become a critical feature. In the

COMBINED

impact limit, the have appreciable presence or absence affect the excitation

In contrast, collision pushes the (Fig. 3). The fact that the nonresonant off exponential after one average. Thus, the CARE with an inverse and an exponential file is shown

$\sigma(\Delta^2)$
10⁻⁵
10⁻¹⁰

Figure 4. CARE in the weak section is as R^{-6} (R is $b_0 = 1.1 \times 10^{-7}$

COMBINED RADIATION FIELD - COLLISIONAL EXCITATION

impact limit, the system of (pulse + collision) does have appreciable Fourier coefficients at Δ so that the presence or absence of instantaneous resonances does not affect the excitation amplitude.

In contrast to the $\Delta < 0$ case, for $\Delta > 0$ the collision pushes the levels further away from resonance (see Fig. 3). The net result of this level displacement is that the nonresonant side of the CARE cross section falls off exponentially as a fractional power of $|\Delta|\tau_c$, even after one averages over impact parameter.^{19,46,49,50} Thus, the CARE cross-section exhibits a marked asymmetry, with an inverse power law dependence on $|\Delta|$ on one side, and an exponential decay on the other. A typical profile is shown in Fig. 4.

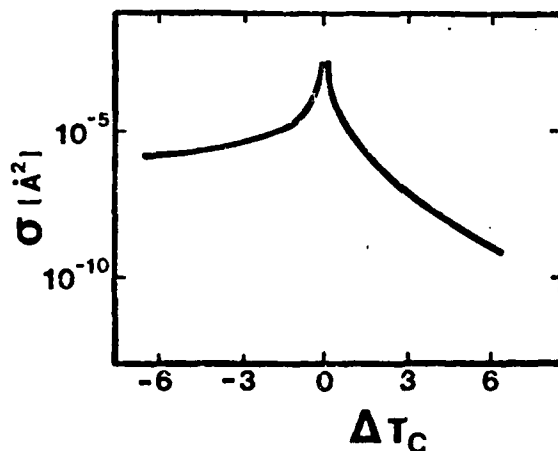


Figure 4. CARE cross section as a function of $|\Delta|\tau_c$ in the weak field limit, $\chi\tau_c = 1.0 \times 10^{-4}$. This cross section is drawn for a level-shifting term which varies as R^{-6} (R is the interatomic separation) and a value $b_0 = 1.1 \times 10^{-7}$ cm (see Ref. 37).

It should be noted that CARE cross-section in the weak-field regime can also be obtained using traditional pressure broadening theories of linear absorption or emission.⁴⁹⁻⁵²

Strong Fields: $\chi T > 1$

As long as $\chi < |\Delta|$, the previous perturbative treatment is valid and the CARE cross-section is proportional to χ^2 . If both $\chi T > 1$ and $\chi > |\Delta|$, the perturbation theory fails, and a strong field theory is required. Space limitations preclude a detailed description of such a theory, which is conveniently developed using a quantized-field dressed-atom approach, but we cite some of the results.

For $\chi > |\Delta|$ and $\chi \tau_c < 1$ (which implies $|\Delta| \tau_c \ll 1$), one is still in the impact domain since the collision time τ_c is the shortest time scale in the problem. If the atom - radiation pulse interaction is interrupted at some arbitrary time, one would find an upper state population approximately equal to 1/2 since the field is sufficiently strong ($\chi T > 1$) to lead to equal populations, on average, in levels 1 and 2. (This factor of 1/2 should be compared with the average population $(\chi/\Delta)^2$ found in the weak field case). Thus, in this limit, the CARE cross-section is approximately equal to $\pi b_0^2/2$, independent of both Δ and χ .

For $\chi > |\Delta|$ and $\chi \tau_c > 1$, an impact theory can no longer be used. During the collision, the field is strong enough to lead to rapid oscillations (so-called Rabi oscillations) in the state amplitudes. Since $\chi > |\Delta|$, these Rabi oscillations provide the dominant phase variation for the state amplitudes; the effective detuning in the problem becomes χ instead of $|\Delta|$. There is no possi-

COMBINED RE

bility of "instability of the excitation". Just as in the CARE cross-section parameter falls of $\chi \tau_c$.¹⁹

RAIC

A typical RAIC

$$A_1 + B_1 + \dots$$

is illustrated final state in intermediate states; these states are in nonresonant problem to that effective operator product of the sional interaction

$$U(t) = \dots$$

where $\bar{\omega}$ is seen ($\bar{\omega} \gg \chi$) and $U(t) = 0$ in the action occurs time T plays a scale in the

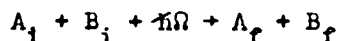
The initial combined AB system

COMBINED RADIATION FIELD - COLLISIONAL EXCITATION

bility of "instantaneous resonances" here; consequently, the excitation probability varies as $\exp[-2\chi\tau_c(b, v_r)]$. Just as in the weak-field result for the $\Delta > 0$ case, the CARE cross-section obtained after averaging over impact parameter falls off exponentially as a fractional power of $\chi\tau_c$.¹⁹

RAIC

A typical RAIC reaction of the form



is illustrated in Fig. 2. In going from the initial to final state in the composite AB system, a number of intermediate states may play a role. However, by summing over these states and neglecting the effect of small variations in nonresonant energy denominators, one may reduce the problem to that for a two-level system coupled by an effective operator $U(t)$ which is proportional to the product of the radiation field amplitude and the collisional interaction. Explicitly we write

$$U(t) = \hbar(\chi/\bar{\omega}) V_c(t),$$

where $\bar{\omega}$ is some representative frequency denominator ($\bar{\omega} \gg \chi$) and $V_c(t)$ is the collisional interaction. Since $U(t) = 0$ in the absence of a collision, the RAIC interaction occurs during the collision only. Thus the pulse time T plays no role at all in RAIC - the relevant time scale in the problem is the collision duration τ_c .

The initial and final state amplitudes for the combined AB system (see Fig. 2) obey the equations

$$\dot{a}_i = -i(\chi/\bar{\omega})V_c(t)\exp[i\Delta t - i\int_0^t V_{LS}(t')dt'] a_f \quad (6a)$$

$$\dot{a}_f = -i(\chi/\bar{\omega})V_c(t)\exp[-i\Delta t + i\int_0^t V_{LS}(t')dt'] a_i, \quad (6b)$$

where

$$\Delta = \pi\Omega - (E_f - E_i)$$

and $V_{LS}(t)$ is the same collisional energy level shift encountered in CARE. An additional contribution to level shifts resulting from the AC Stark effect will not be discussed here, but can be included by redefining the energy levels at their Stark-shifted values.

Weak Fields

A perturbative treatment is valid provided $|a_f(t)| \ll 1$, in which case

$$|a_f(\infty)| = |(\chi/\bar{\omega})\int_{-\infty}^{\infty} V_c(t)\exp[-i\Delta t + i\int_0^t V_{LS}(t')dt']dt|.$$

If $|\Delta|\tau_c \ll 1$, the amplitude for excitation is independent of Δ . For $|\Delta|\tau_c > 1$, one again finds an asymmetric line owing to the effects of instantaneous resonances which occur for one sign of Δ but not the other.⁵³

The functional forms of $V_c(t)$ and $V_{LS}(t)$ determine where the maximum RAIC cross section occurs as a function of Δ . In a typical situation, the time-dependence of $V_c(t)$ and $V_{LS}(t)$ is roughly similar and the maximum RAIC cross section occurs for $\Delta \approx 0$. However, the RAIC maximum may occur for $\Delta \neq 0$ if the duration associated with $V_c(t)$ is much smaller than that associated with $V_{LS}(t)$, as might be the case in RAIC charge transfer³³, where, for an interatomic separation $R(t)$, $V_c(t) \propto \exp[-CR(t)]$, while $V_{LS}(t) \propto [R(t)]^{-n}$. Under these conditions, the

COMBINED RADIATION

collisional coupling producing a relatively high energy levels. Since the composite AB system time that the collisional coupling is producing that the final state is placed from $\Delta = 0$.

Strong Fields

To get some idea of the behavior of (6) in the limit that the term set equal to zero probability varies as

$$|a_2(b, v_r, \infty)|^2 \propto$$

where

$$\phi_R(b, v_r) = (\chi/\bar{\omega})$$

The RAIC cross-section parameter for which power law potential V and b_R^2 varies as (χ/v_r) cross-section, which fields, varies as γ^{2n} intensity for $n=3$ in fields, owing to the parameter collisions minor role for such determined by the inverse $v_r^{\alpha+1} \chi^{-\alpha}$; the RAIC strength.

COMBINED RADIATION FIELD - COLLISIONAL EXCITATION

$$a_f \quad (6a)$$

$$a_i \quad (6b)$$

collisional coupling is significant only when $V_{LS}(t)$ is producing a relatively large variation in the atoms' energy levels. Since the effective level separation of the composite AB system is no longer $E_f - E_i$ during the time that the collisional coupling occurs, it is not surprising that the maximum RAIC cross section can be displaced from $\Delta = 0$.

Strong Fields

To get some idea of strong field effects, consider Eqs. (6) in the limit that $\Delta = 0$ and with the level-shifting term set equal to zero. In that case, the upper state probability varies as

$$|a_2(b, v_r, \infty)|^2 = \sin^2[\phi_R(b, v_r)],$$

where

$$\phi_R(b, v_r) = (\chi/\omega) \int_{-\infty}^{\infty} V_c(b, v_r, t) dt.$$

The RAIC cross-section is equal to πb_R^2 where b_R is an impact parameter for which ϕ_R is of order unity. For a power law potential $V_c(t) \propto [R(t)]^{-n}$, $n \geq 3$, $\phi_R \propto \chi/b^{n-1}v_r$ and b_R^2 varies as $(\chi/v_r)^{2\alpha}$ with $\alpha = (n-1)^{-1}$. The RAIC cross-section, which is proportional to χ^2 for weak fields, varies as $\chi^{2/(n-1)}$ (i.e. as the square root of the intensity for $n=3$) in the strong field limit. For strong fields, owing to the fact that $b_R \propto \chi^\alpha$, large impact parameter collisions only are important and V_{LS} plays a minor role for such collisions. The line width is determined by the inverse collision time $\tau_c^{-1} = v_r/b_R \propto v_r^{\alpha+1} \chi^{-\alpha}$; the RAIC profile narrows with increasing field strength.

The ratio b_R/b_0 can be used as a measure of the field strength. If $b_R > b_0$, one is in the strong field region since the upper state amplitude saturates at radii where the level-shifting effect is unimportant. On the other hand, for $b_R \ll b_0$, the collisional coupling can not overcome the effects of level-shifting and a perturbative treatment is valid. Typically⁴, the transition from weak to strong field occurs for field strengths of order 10^8 W/cm^2 . The strong field effects in RAIC and CARE are fundamentally different. In RAIC, the upper state probability is truly saturated by the field-collisional interaction. In CARE, on the other hand, the upper state probability amplitude is always small if $\chi\tau_c \gg 1$. It is the rapid Rabi oscillations that lead to a decreasing CARE cross section with increasing χ when $\chi\tau_c \gg 1$ and $\chi/|\Delta| > 1$.

CONCLUSION

We have presented explanations of the physical processes underlying combined radiation field-collisional excitation of atomic systems. Alternative approaches could involve a "dressed-atom" description or a molecular-state basis calculation. For a meaningful theoretical description of CARE and RAIC, one must use accurate interatomic potentials and average all results over the spatial and temporal extent of the laser pulse. It may be noted, however, that experimental investigations of CARE and RAIC have revealed many of the qualitative features discussed above.

This work is supported by the U.S. Office of Naval Research. The content of this paper is based, in part, on

COMBINED RA

a lecture given
January, 1980.

REFERENCES

1. S. E. Hare, Lidow, J. Lasers and T. Jagger, York, 1977
2. R.W. Falc Harris, P.
3. Ph. Caluz 462 (1978)
4. S.E. Hare, J. Lukasi and G. A. by H. Wal Berlin, 1
5. S. E. Hare Green, D. Wright, at Seventh 1 edited by York, 1980
6. C. Brechi Rev. A 21
7. J. C. Whit 5, 120 (1
8. D. L. Rou Phys. Rev.
9. J. L. Car 667 (1970)
10. A. M. Bon Fedorov, 909 (1970)
11. R. D. Dri 595 (1977)
12. J. L. Car Rev. A 12
13. M. G. Ray Phys. B 1
14. P. F. Li Phys. Rev.

COMBINED RADIATION FIELD - COLLISIONAL EXCITATION

a lecture given by PRB at the College de France in January, 1980.

REFERENCES

1. S. E. Harris, R. W. Falcone, W. R. Green, D. B. Lidow, J. C. White, and J. F. Young, in Tunable Lasers and Applications, edited by A. Mooradian, T. Jaeger, and P. Stokseth (Springer-Verlag, New York, 1976) p. 193, and references therein.
2. R.W. Falcone, W. R. Green, J. C. White, and S. E. Harris, Phys. Rev. A **15**, 1533 (1977).
3. Ph. Cahuzac and P. E. Toschek, Phys. Rev. Lett. **36**, 462 (1978).
4. S.E. Harris, J. F. Young, W. R. Green, R. W. Falcone, J. Lukasik, J. C. White, J. R. Willison, M. D. Wright, and G. A. Zdasiuk, in Laser Spectroscopy IV, edited by H. Walther and K. W. Rothe (Springer-Verlag, Berlin, 1979) pp. 349-359, and references therein.
5. S. E. Harris, J. F. Young, R. W. Falcone, W. R. Green, D. B. Lidow, J. Lukasik, J. C. White, M. D. Wright, and G. A. Zdasiuk, Proceedings of the Seventh International Conference on Atomic Physics, edited by D. Kleppner and F.M. Pipkin (Plenum, New York, 1981) pp. 407-428, and references therein.
6. C. Brechignac, Ph. Cahuzac, and P. E. Toschek, Phys. Rev. A **21**, 1969 (1980).
7. J. C. White, R. R. Freeman and P. F. Liao, Opt. Lett. **5**, 120 (1980).
8. D. L. Rousseau, G. D. Patterson, and P. F. Williams, Phys. Rev. Lett. **34**, 1306 (1975).
9. J. L. Carlsten and A. Szöke, Phys. Rev. Lett. **36**, 667 (1976); J. Phys. B **9**, L231 (1976).
10. A. M. Bonch-Bruевич, S. G. Przhibel'skii, A. A. Fedorov, and V. V. Khromov, Sov. Phys.-JETP **44**, 909 (1976).
11. R. D. Driver and J. L. Snider, J. Phys. B **10**, 595 (1977).
12. J. L. Carlsten, A. Szöke, and M. G. Raymer, Phys. Rev. A **15**, 1029 (1977).
13. M. G. Raymer, J. L. Carlsten, and G. Pichler, J. Phys. B **12**, L119 (1979).
14. P. F. Liao, J. E. Bjorkholm, and P. R. Berman, Phys. Rev. A **20**, 1489 (1979).

Theory of electronic state coherences produced in
combined laser field - collisional reactions

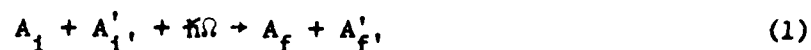
P.R. Berman and E. Giacobino^{*}

Physics Department, New York University, 4 Washington Place, New York, New York 10003

A method for producing electronic state coherences using either CARE (Collisionally-Aided Radiative Excitation or "optical collision") or LICET (Laser-Induced Collisional Energy Transfer or "radiative collision") is proposed. Two atoms, A and A', collide in the presence of two pulsed laser fields having frequencies Ω and Ω_1 . It is shown that, by choosing $(\Omega_1 \pm \Omega)$ such that an energy conserving transition can occur in the composite AA' system, one can create an electronic state coherence in the A or A' atoms. The coherence can be produced between states of the same or of opposite parity; if it is between states of opposite parity, coherent emission at frequency $(\Omega \pm \Omega_1)$ is generated.

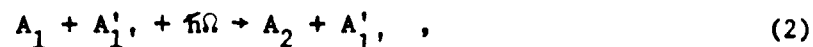
I. Introduction

Over the past ten years¹, there has been increased interest in reactions of the form



in which two atoms or molecules (A and A') collide in the presence of a laser field and undergo a transition from initial state ($A_1 A'_1$) to final state ($A_f A'_f$). It is assumed that the energy difference between the final and initial states in each of the atoms as well as in the combined system is such that no transition occurs in the absence of either the collision or the radiation field. Since the simultaneous action of both the collision and radiation field is needed to produce the transition, we refer to reactions of type (1) as Combined Field-Collisional Transitions (CFCT). It has been common practice to further separate the CFCT into two categories.

The first of these, Collisionally-Aided Radiative Excitation (CARE)², (also referred to as "optical collisions"³), characterizes processes in which the internal state of one of the reactants remains unchanged. That is, CARE reactions are of the form



subject to the condition that direct excitation of atom A by the radiation field in the absence of the collision is energetically forbidden. In CARE the collision provides translational kinetic energy to compensate for the mismatch between the field frequency Ω and the 1-2 transition frequency of

atom A. The CARE cross-section falls to zero for atom-field detunings which correspond to energies that are larger than those available in the colliding atoms' center-of-mass frame.

The second type of CFCT, Laser-Induced Collisional Energy Transfer (LICET)⁴ [also referred to as Radiatively-Aided Inelastic Collisions (RAIC)² and "radiative collisions"⁵], characterizes processes in which both reactants change their internal states [see Eq. (1)]. The photon energy $\hbar\Omega$ is approximately equal to the difference between the final and initial state internal energies of the atoms. As such, the radiation field provides the energy to drive what would normally be an energetically forbidden inelastic collision.⁶

In principle, CFCT's can be produced using either CW or pulsed laser fields. To date, LICET has been seen with pulsed excitation only, while CARE has been observed with both CW and pulsed laser fields. In this work we shall consider situations involving pulsed laser fields only. The transition from initial to final state occurs during the application of the pulsed laser fields; we calculate the final state density matrix elements characterizing the atoms immediately after the passage of the radiation pulses.

The calculation of CARE and LICET cross sections with pulsed laser excitation has been the subject of a large number of theoretical and experimental studies.¹ In a typical calculation or experiment, one determines the excitation cross section as a function of the strength and frequency

of the radiation field, and attempts to gain some information concerning the initial and final state A-A' interatomic potentials. While most of the calculations and experiments have concentrated on final state populations, there has been some recent work devoted to the investigation of the possibility of creating coherences using CFCT with pulsed laser fields. It has been shown^{7,8} that, in cases where the final states consist of a number of degenerate magnetic sublevels, CFCT can create coherences among these sublevels. The existence of such CFCT-induced magnetic state coherences has been experimentally established for both CARE⁹ and LICET.¹⁰

In this article, we present a theory of a new type of CFCT, in which it should be possible to produce electronic-state coherences using pulsed laser excitation. The types of reactions to be considered are conveniently represented in Figs. 1-3. In all cases, atoms A and A' are undergoing a collision at some time during the application of one or more laser pulses. The laser pulse durations T are much greater than the duration of a collision, but much smaller than the lifetimes of the relevant atomic levels. Following the pulses, we wish to determine whether or not any electronic state coherences have been created by the CFCT. By convention, a state written as A(fg), implies that the A atoms possess a coherence between states f and g.

Corresponding to each figure, one can write a reaction that could possibly lead to electronic-state coherences. For Fig. 1, the CARE reaction is

$$A_1 + A_1' + \hbar\Omega \rightarrow A(12) + A_1' , \quad (3)$$

for Fig. 2, the CARE reaction is

$$A_1 + A_1' + \hbar\Omega + \hbar\Omega_1 \rightarrow A(2'3') + A_1' , \quad (4)$$

and, for Fig. 3, the LICET reaction is

$$A_2 + A_1' + \hbar\Omega + \hbar\Omega_1 \rightarrow A_1 + A'(2'3') . \quad (5)$$

A calculation of the actual macroscopic coherence, if any, generated by reactions (3-5) is given in Secs. III and IV, following a discussion in Sec. II, of the approximations and assumptions of the theory. In Sec. V, we indicate methods for detecting the CFCT-induced coherence. The choice of detection scheme depends on whether the coherence is created between states of the same or of opposite parity.

The level scheme of Fig. 2 has been analyzed for CW laser fields by Bloembergen and coworkers¹¹, Grynberg¹², and others¹³; in some sense, our analysis for this case represents the pulsed field analogue of their work. It may also be noted that our theory, while containing some features found in calculations involving "adiabatic following" in two and three-levels systems¹⁴, differs considerably in spirit and content from those calculations. There is a somewhat closer connection between the underlying theory in our work and that exposed in the recent article of Agarwal and Cooper¹⁵, but the approach and emphasis of the two calculations differ appreciably.

II. Notation, Approximations and Assumptions

The main goal of this article is to illustrate the manner in which CFCT using pulsed laser fields can create electronic state coherences. Consequently, we shall make a number of assumptions and approximations to simplify the theoretical development. Most of these assumptions can be relaxed in a more complete theory, but the basic physical content of the theory would remain unchanged.

Before listing our assumptions and approximations, it is useful to introduce some notation. The atoms A and A' of Figs. 2 and 3 are subjected to two laser pulses having amplitudes $\mathcal{E}(t)$ and $\mathcal{E}_1(t)$, frequencies Ω and Ω_1 , and propagation vectors \vec{k} and \vec{k}_1 , respectively. (The atoms of Fig. 1 are subjected to one pulse only). The laser pulses have duration T while the collision duration is τ_c . The detunings Δ and Δ_1 refer to atom-field detunings for single-photon transitions [e.g., in Fig. 2 $\Delta = \Omega - \omega_{21}$, $\Delta_1 = \Omega_1 - \omega_{31}$; $\omega_{ij} = (E_i - E_j)/\hbar$] and χ and χ_1 refer to the Rabi frequencies [evaluated using values of $|\mathcal{E}(t)|$ or $|\mathcal{E}_1(t)|$ averaged over the pulse duration] for single-photon transitions. Spontaneous decay rates are denoted by γ and collision rates by Γ . The most probable atomic speed is u .

The following assumptions or approximations are made: (1) The laser pulse duration is short enough to neglect any spontaneous emission during the pulse,

$$\gamma T \ll 1. \quad (6)$$

(2) The detunings $|\Delta|$ and $|\Delta_1|$ are sufficiently large such that

$$|\Delta| T \gg 1 ; |\Delta_1| T \gg 1. \quad (7)$$

This condition will ensure that there is negligible excitation in the absence of the collision provided that we also require $|\Delta|$ and $|\Delta_1|$ to be larger than the Doppler widths associated with the transitions, i.e.

$$|\Delta| \gg k u ; |\Delta_1| \gg k_1 u. \quad (8)$$

(3) The collision occurs on a time scale short compared with the pulse duration

$$\tau_c / T \ll 1. \quad (9)$$

(4) The collision may be treated in the impact approximation, implying that

$$\Gamma \tau_c \ll 1, \quad (10)$$

$$|\Delta| \tau_c \ll 1 ; |\Delta_1| \tau_c \ll 1, \quad (11)$$

$$\chi \tau_c \ll 1 ; \chi_1 \tau_c \ll 1. \quad (12)$$

Conditions (11) and (12) simplify the mathematical development, but are not essential to the theory. (5) The ground-state lifetimes are infinite.

(6) Two-photon processes are resonant or nearly-resonant. For Fig. 2 this assumption takes the form

$$|\Omega - \Omega_1 - \omega_{32}| T \ll 1, \quad (13)$$

while for Fig. 3a or Fig. 3b, it is

$$|\Omega \mp \Omega_1 - \omega_{3,2}| T \ll 1. \quad (14)$$

where the "-" sign refers to Fig. 3a and the "+" sign to Fig. 3b.

Conditions (13) and (14) ensure that the coherences which are created do not "wash out" during the laser pulse duration T . In parallel with conditions (13) and (14), we must require that the Doppler shifts associated with two-photon transitions that are accumulated during the laser pulse be negligible. For the case of Figs. 2 and 3a, we assume

$$|\vec{k} - \vec{k}_1|uT \ll 1 \quad (15)$$

while for Fig. (3b), the condition is

$$|\vec{k} + \vec{k}_1|uT \ll 1 \quad (16)$$

(7) In order to be able to calculate the coherences using perturbation theory, we assume that

$$[(|\chi|^2 + |\chi_1|^2 + |\chi\chi_1|)/\Delta^2]\Gamma T \ll 1 \quad (17)$$

and¹²

$$(|\chi| + |\chi_1|^2)/\Delta T \ll 1. \quad (18)$$

(8) Finally, we must require that

$$\Gamma T \ll 1 \quad (19)$$

to ensure that the coherence does not decay during the radiation pulse. Together with Eq. (7), Eq. (19) implies that

$$\Gamma \ll |\Delta| ; \Gamma \ll |\Delta_1| . \quad (20)$$

III. Generation of Coherences Using CARE.

A. Figure 1

We first turn our attention to the situation depicted in Fig. 1.

A laser pulse of the form

$$\vec{E}(\vec{R}, t) = \frac{1}{2} \vec{\mathcal{E}}(\vec{R}, t) \hat{x} e^{i(\vec{k} \cdot \vec{R} - \Omega t)} + \text{c.c.} \quad (21)$$

is incident on a vapor containing A and A' atoms. In a field interaction representation to be defined below and in the absence of collisions, density matrix elements of atom A evolve according to

$$\dot{\tilde{\rho}}_{12} = - \left(\frac{1}{2} \gamma_2 + i\Delta \right) \tilde{\rho}_{12} - i\chi^*(t)(\rho_{11} - \rho_{22}) \quad (22a)$$

$$\dot{\rho}_{22} = -\gamma_2 \rho_{22} + i[\chi(t)\tilde{\rho}_{12} - \chi^*(t)\tilde{\rho}_{21}] \quad (22b)$$

where γ_1 is the spontaneous decay rate of level 1,

$$\tilde{\rho}_{12} = \rho_{12} e^{i(\vec{k} \cdot \vec{R} - \Omega t)}, \quad (23)$$

$$\chi(t) = \langle 2 | p_x | 1 \rangle \vec{\mathcal{E}}(\vec{R}, t) / 2\hbar, \quad (24)$$

$$\Delta = \Omega - \omega_{21} \quad (25)$$

and p_x is the x component of the atomic dipole moment operator.

In writing Eqs. (22), γ_1 has been set equal to zero and the Doppler shift has been neglected relative to $|\Delta|$ [Eq. (8)]. In the impact approximation [Eqs. (10-12)], collisions are incorporated into Eq. (22) by the addition of a term $(-\Gamma_{12}\tilde{\rho}_{12})$ to the right hand side of Eq. (22a) [Γ_{ij} is the rate at which collisions destroy ij coherence¹⁶]. If, in addition, we use condition (17) to set $\rho_{11} = 1$ and $\rho_{22} = 0$ in Eq. (22a) (perturbation limit), the appropriate equations to be solved during the laser pulse are

$$\dot{\tilde{\rho}}_{12} = - \left(\frac{1}{2} \gamma_2 + \Gamma_{12} + i\Delta \right) \tilde{\rho}_{12} - i\chi^*(t) \quad (26a)$$

$$\dot{\tilde{\rho}}_{22} = - \gamma_2 \rho_{22} + i[\chi(t)\tilde{\rho}_{12} - \chi^*(t)\tilde{\rho}_{21}] \quad (26b)$$

$$\tilde{\rho}_{21} = (\tilde{\rho}_{12})^* \quad (26c)$$

subject to the initial condition

$$\tilde{\rho}_{12}(T^-) = \tilde{\rho}_{22}(T^-) = 0, \quad (26d)$$

where T^- is some time before the laser pulse.

Although we are primarily interested in the coherence $\tilde{\rho}_{12}$ at a time T^+ following the passage of the laser pulse, it is instructive to first calculate $\rho_{22}(T^+)$. To second order in χ , one can iterate Eqs. (26) to obtain

$$\rho_{22}(T^+) = \int_{-\infty}^{T^+} e^{-\gamma_2(T^+-t')} \chi(t') dt' \int_{-\infty}^{t'} \chi^*(t'') e^{-\left(\frac{1}{2}\gamma_2 + \Gamma_{12} + i\Delta\right)(t'-t'')} dt'' + \text{c.c.} \quad (27)$$

where T^- has been set equal to $-\infty$ without loss of generality. Since $\chi(t'')$ is slowly varying compared with $\exp(i\Delta t'')$, the t'' integration is conveniently carried out using integration by parts as

$$\begin{aligned} \int_{-\infty}^{t'} \chi^*(t'') e^{-\left(\frac{1}{2}\gamma_2 + \Gamma_{12} + i\Delta\right)(t'-t'')} dt'' &= \chi^*(t') \left(\frac{1}{2}\gamma_2 + \Gamma_{12} + i\Delta\right)^{-1} \\ &\quad - \dot{\chi}^*(t') \left(\frac{1}{2}\gamma_2 + \Gamma_{12} + i\Delta\right)^{-2} \\ &\quad + O[\ddot{\chi}^*(t') \left(\frac{1}{2}\gamma_2 + \Gamma_{12} + i\Delta\right)^{-3}] \end{aligned} \quad (28)$$

Substituting this result into Eq. (27), noting that

$$\int_{-\infty}^{T^+} e^{-\gamma_2(T^+-t')} \chi(t') \dot{\chi}^*(t') dt' + \text{c.c.} = -\gamma_2 \int_{-\infty}^{T^+} |\chi(t')|^2 e^{-\gamma_2(T^+-t')} dt', \quad (29)$$

using Eqs. (6) and (20), and setting $T^+ = \infty$, one finds

$$\begin{aligned} \rho_{22}^{(\infty)} &= \left[\frac{2\Gamma_{12} + \gamma_2}{\Delta^2} - \frac{\gamma_2}{\Delta^2} \right] \int_{-\infty}^{\infty} |\chi(t)|^2 dt \\ &= \frac{2\Gamma_{12}}{\Delta^2} \int_{-\infty}^{\infty} |\chi(t)|^2 dt. \end{aligned} \quad (30)$$

Equation (30) vanishes if there are no collisions, $\Gamma_{12} = 0$. In that case, a more careful evaluation of Eq. (27) yields

$$\begin{aligned} \rho_{22}^{(\infty)} &\approx \left| \int_{-\infty}^{\infty} e^{-i\Delta t} \chi(t) dt \right|^2 \\ &\text{for } \Gamma_{12} = 0. \end{aligned} \quad (31)$$

This result is consistent with conservation of energy considerations. If there are no collisions, then the excitation probability for a detuning Δ is determined by the Fourier transform of the pulse envelope function evaluated at Δ . If $|\Delta|T \gg 1$ as assumed in this work, the field does not possess the proper frequency components to excite the atom [typically, the excitation probability varies as $\exp(-2|\Delta|T) \ll 1$]. Once collisions are present, however, the effective time scale of the problem is changed from the pulse duration T to the collision duration τ_c . The collision does possess the Fourier components to excite the transition ($\tau_c^{-1} \gg |\Delta|$) and, moreover, provides a mechanism (change in center-of-mass translational energy of the colliding atoms) allowing for conservation of energy in the total (absorption + collision) process. The corresponding collision enhanced excitation probability is indicated in Eq. (30).

It might be thought that collisions could also lead to a non-negligible macroscopic coherence ρ_{12} following the radiation pulse. Collisions do, in fact, produce non-negligible coherence each time they occur during the radiation pulse, but, on averaging over the various times during the radiation pulse at which they occur, one finds that the coherence is negligible. Formally, the result follows directly from Eq. (26a), i.e.

$$\tilde{\rho}_{12}(T^+) = -ie^{-i\Delta T^+} \int_{-\infty}^{T^+} e^{-(\frac{1}{2}\gamma_2 + \Gamma_{12})(T^+ - t')} e^{i\Delta t'} \chi^*(t') dt' \quad (32)$$

Using Eqs. (6) and (20), and letting $T^+ \rightarrow \infty$ in the integral, we obtain a coherence

$$\tilde{\rho}_{12}(T^+) = -ie^{-i\Delta T^+} \int_{-\infty}^{\infty} \chi^*(t') e^{i\Delta t'} dt' \quad (33)$$

which, for $|\Delta|T \gg 1$, is negligibly small.

B. Figure 2

In order to produce coherences which do not dephase during the radiation pulse, one can use the level scheme depicted in Fig. 2. Levels 2 and 3 are assumed to have the same parity which is opposite to that of level 1. Laser fields of the form

$$\vec{E}(\vec{R}, t) = \frac{1}{2} \vec{E}(\vec{R}, t) \hat{x} e^{i(\vec{k} \cdot \vec{R} - \Omega t)} + c.c. \quad (34a)$$

$$\vec{E}_1(\vec{R}, t) = \frac{1}{2} \vec{E}_1(\vec{R}, t) \hat{x} e^{i(\vec{k}_1 \cdot \vec{R} - \Omega_1 t)} + c.c. \quad (34b)$$

are simultaneously incident on the vapor. We wish to calculate the coherence $\rho_{23}(T^+)$ using perturbation theory. In a field interaction re-

representation defined by

$$\tilde{\rho}_{12} = \rho_{12} e^{i(\vec{k} \cdot \vec{R} - \Omega t)} \quad (35a)$$

$$\tilde{\rho}_{13} = \rho_{13} e^{i(\vec{k}_1 \cdot \vec{R} - \Omega_1 t)} \quad (35b)$$

$$\tilde{\rho}_{23} = \rho_{23} e^{+i[(\vec{k}_1 - \vec{k}) \cdot \vec{R} - (\Omega_1 - \Omega)t]} \quad (35c)$$

density matrix elements evolve according to

$$\dot{\tilde{\rho}}_{12} = -\left(\frac{1}{2}\gamma_2 + \Gamma_{12} + i\Delta_v\right)\tilde{\rho}_{12} + i\chi_{21}^*(t)(\rho_{22} - \rho_{11}) + i\chi_{31}^*(t)\tilde{\rho}_{32} \quad (36a)$$

$$\dot{\tilde{\rho}}_{13} = -\left(\frac{1}{2}\gamma_3 + \Gamma_{13} + i\Delta_v'\right)\tilde{\rho}_{13} + i\chi_{31}^*(t)(\rho_{33} - \rho_{11}) + i\chi_{21}^*(t)\tilde{\rho}_{23} \quad (36b)$$

$$\dot{\tilde{\rho}}_{23} = -\left[\frac{1}{2}(\gamma_2 + \gamma_3) + \Gamma_{23} + i(\Delta_v' - \Delta_v)\right]\tilde{\rho}_{23} + i\chi_{21}(t)\tilde{\rho}_{13} - i\chi_{31}^*(t)\tilde{\rho}_{21} \quad (36c)$$

$$\tilde{\rho}_{ji} = (\tilde{\rho}_{ij})^* \quad (36d)$$

where

$$\Delta_v = \Omega - \omega_{21} - \vec{k} \cdot \vec{v}, \Delta_v' = \Omega_1 - \omega_{31} - \vec{k}_1 \cdot \vec{v} \quad (37)$$

and

$$\begin{aligned} \chi_{21}(t) &= \langle 2 | p_x | 1 \rangle \mathcal{E}(\vec{R}, t_c) / 2\hbar \\ \chi_{31}(t) &= \langle 3 | p_x | 1 \rangle \mathcal{E}_1(\vec{R}, t_c) / 2\hbar \end{aligned} \quad (38)$$

Equations for ρ_{22} and ρ_{33} need not be written since populations in these states created by CARE excitation will not appreciably affect $\tilde{\rho}_{13}$ when condition (18) holds.¹² To calculate $\tilde{\rho}_{23}$, we set $\rho_{22} = \rho_{33} = \tilde{\rho}_{32} = \tilde{\rho}_{23} = 0$,

and $\rho_{11} = 1$ in Eqs. (36a) and (36b), owing to the perturbation limit.

With these simplifications, Eqs. (36) reduce to

$$\dot{\tilde{Q}}_{12} = -\left(\frac{1}{2}\gamma_2 + \Gamma_{12} + i\Delta_v\right)\tilde{Q}_{12} - i\chi_{21}^*(t) \quad (39a)$$

$$\dot{\tilde{Q}}_{13} = -\left(\frac{1}{2}\gamma_3 + \Gamma_{13} + i\Delta_v'\right)\tilde{Q}_{13} - i\chi_{31}^*(t) \quad (39b)$$

$$\dot{\tilde{Q}}_{23} = -\left[\frac{1}{2}(\gamma_2 + \gamma_3) + \Gamma_{23} + i(\Delta_v' - \Delta_v)\right]\tilde{Q}_{23} + i\chi_{21}(t)\tilde{Q}_{13} - i\chi_{31}^*(t)\tilde{Q}_{21} \quad (39c)$$

$$\tilde{Q}_{ji} = (\tilde{Q}_{ij})^* \quad (39d)$$

The calculation of the coherence $\tilde{\rho}_{23}$ parallels that for ρ_{22} given above in Sec. A. If there are no collisions, the coherence created is negligible. With collisions present, Eqs. (39a) and (39b) are integrated by parts twice and the resulting values for $\tilde{\rho}_{12}$ and $\tilde{\rho}_{23}$ (neglecting terms of order $\ddot{\chi}/|\Delta|^3$ or $\ddot{\chi}'/|\Delta'|^3$) are substituted into Eq. (39c) which is then integrated to yield

$$\begin{aligned} \tilde{Q}_{23}(\vec{R}, T^+) &= \Delta^{-2} \int_{-\infty}^{T^+} d\tau' \left\{ \left[\frac{1}{2}(\gamma_2 + \gamma_3) + \Gamma_{12} + \Gamma_{13} + i(\Delta_v' - \Delta_v) \right] \chi_{21}(\tau') \chi_{31}^*(\tau') \right. \\ &\quad \left. + \chi_{21}(\tau') \dot{\chi}_{31}^*(\tau') + \dot{\chi}_{21}(\tau') \chi_{31}^*(\tau') \right\} \\ &\quad \times \exp\left(-\left[\frac{1}{2}(\gamma_2 + \gamma_3) + \Gamma_{23} + i(\Delta_v' - \Delta_v)\right](T^+ - \tau')\right). \end{aligned} \quad (40)$$

In arriving at Eq. (40), we have used the fact that

$$\left| \frac{\Delta_v^1 - \Delta_v}{\Delta_v} \right| \ll 1 \quad (41)$$

which follows from Eqs. (7), (13) and (15). The last two terms in Eq.

(40) may be integrated by parts to give

$$\begin{aligned} & \int_{-\infty}^{T^+} [\chi_{21}(t') \dot{\chi}_{31}^*(t') + \dot{\chi}_{21}(t') \chi_{31}^*(t')] \\ & \times \exp \left\{ - \left[\frac{1}{2}(\gamma_2 + \gamma_3) + \Gamma_{23} + i(\Delta_v^1 - \Delta_v) \right] (T^+ - t') \right\} dt' \\ & = - \left[\frac{1}{2}(\gamma_2 + \gamma_3) + \Gamma_{23} + i(\Delta_v^1 - \Delta_v) \right] \int_{-\infty}^{T^+} \chi_{21}(t') \chi_{31}^*(t') \\ & \times \exp \left\{ - \left[\frac{1}{2}(\gamma_2 + \gamma_3) + \Gamma_{23} + i(\Delta_v^1 - \Delta_v) \right] (T^+ - t') \right\} dt'. \end{aligned} \quad (42)$$

Combining Eqs. (42) and (40), using conditions (6), (13) and (15) to set the exponential appearing in the integrand equal to unity and taking $T^+ \rightarrow \infty$, one finds

$$\tilde{g}_{13}(\vec{R}, T^+) = \frac{\Gamma_{12} + \Gamma_{13} - \Gamma_{23}}{\Delta^2} \int_{-\infty}^{\infty} \chi_{21}(\vec{R}, t) \chi_{31}^*(\vec{R}, t) dt \quad (43)$$

where the spatial dependence of the fields has been made explicit. Equation (43) gives the coherence created by CARE.

The result (43) can be viewed as the pulse analogue of pressure-induced extra resonances discussed by Bloembergen et al¹¹, Grynberg¹² and others.¹³ A steady-state value for $\tilde{\rho}_{23}$ calculated assuming a repetition rate for the radiation pulses has the same structure as one of the terms contributing to $\tilde{\rho}_{23}$ given in the works cited above.¹¹⁻¹³ There is an additional term, however, which appears in the CW calculation that does not appear in our pulsed version. This additional term does not vanish in the absence of collisions. Such terms appear typically in steady-state theories (for example, a two-level atom driven by an off-resonance CW field acquires a steady-state population χ^2/Δ^2 for any Δ). However, even though such terms appear, one must probe the system on a time scale shorter than $1/|\Delta|$ in order to isolate their contribution. (i.e. to "see" the population in the two-level example mentioned above one must turn off the field in a time which is small compared with $|\Delta|^{-1}$).

It might also be noted that the coherence $\tilde{\rho}_{23}$ can be seen in the CW experiments only if $|\Delta_v - \Delta_v^1| \lesssim (\frac{1}{2} \gamma_2 + \Gamma_{23})$. The pulsed version creates coherences over the much larger range of detunings $|\Delta - \Delta_1| \lesssim T^{-1}$. Methods for detecting the coherence are discussed in Sec. V.

IV. Creation of Coherences Using LICET (Figure 3)

In Fig. 3a or Fig. 3b, a coherence $\tilde{\rho}_{2,3}$, is generated by the LICET reaction

$$A_2 + A'_1 + \hbar\Omega + \hbar\Omega_1 \rightarrow A_1 + A'(2'3') . \quad (44)$$

Once created, the coherence $\tilde{\rho}_{2,3}$, oscillates at frequency $\omega_{3,2} \approx \Omega_1 - \Omega$ (Fig. 3a) or $\omega_{3,2} \approx \Omega_1 + \Omega$ (Fig. 3b) so that it is possible to generate coherences at either the sum or difference frequencies of the applied laser fields. (In CARE, it is also possible to generate a coherence at the sum frequency if one starts with atom A in an excited state).

To obtain equations describing the time evolution of atomic state density matrix elements during the passage of the laser pulses which produce the LICET reaction, it is useful to note an important difference between CARE and LICET. In CARE, non-negligible excited state density matrix elements of atom A (see Fig. 2) are produced during the laser pulses even in the absence of collisions. However, in the absence of collisions, these excited state density matrix elements adiabatically follow the field and vanish at time T^+ immediately after the passage of the laser pulses. Collisions break this adiabatic following and lead to non-vanishing excited state density matrix elements at time T^+ . Consequently, the equations that determine the time evolution of excited state density matrix elements in CARE contain a collision-independent contribution (the adiabatic - following term) plus a collisional contribution. In general, the collisional term can depend on the laser field strength and the atom-field detuning; however, in the impact approximation, the collisional contribution is independent of the

field variables and can be represented simply by the rates Γ_{ij} found in Eqs. (36).

On the other hand, atom A' excited-state density matrix elements produced in LICET (Fig. 3) result solely from the combined radiation field-collisional excitation; they are negligibly small during the passage of the laser pulses if no collision occurs. The coherence $\tilde{\rho}_{2,3}$ can be created directly during a collision; the average value for $\tilde{\rho}_{2,3}(\vec{R}, T^+)$ produced by this "direct" excitation channel is calculated below. The coherence $\tilde{\rho}_{2,3}(\vec{R}, T^+)$ can also be produced by an "indirect" process involving (a) the generation of populations $\rho_{2,2}$ or $\rho_{3,3}$ by LICET at some time during the laser pulses followed by (b) the laser fields, acting in the absence of collisions, to generate the coherence $\tilde{\rho}_{2,3}$ from the difference $(\rho_{3,3} - \rho_{2,2})$. In this indirect process, the population and coherence are created sequentially during the same laser pulses. The contribution to $\tilde{\rho}_{2,3}$ from the indirect process, while easily calculable, can be neglected relative to that of the direct process when condition (18) holds.

In light of the above discussion, we proceed to obtain the LICET-induced coherence $\tilde{\rho}_{2,3}$ as follows: (1) the value of $\tilde{\rho}_{2,3}(b, v_r, t_c, \vec{R})$ resulting from a single collision characterized by impact parameter b and relative speed v_r is calculated for a collision occurring at a time t_c and position \vec{R} . (2) From this value for $\tilde{\rho}_{2,3}(b, v_r, t_c, \vec{R})$, we find the average 2'-3' coherence following the laser pulses as

$$\begin{aligned} \tilde{\rho}_{2,3}(\vec{R}, T^+) = N_A \int_0^\infty 2\pi b db \int_0^\infty W(v_r) v_r dv_r \\ \times \int_{T^-}^{T^+} dt_c \tilde{\rho}_{2,3}(b, v_r, t_c, \vec{R}) \end{aligned} \quad (45)$$

where N_A is the density of A-atoms and $W(v_r)$ is the relative speed distribution.

The calculation of $\tilde{\rho}_{2,3}(b, v_r, t_c, \vec{R})$ is most conveniently carried out using state amplitudes rather than density matrix elements. The laser fields incident on the atoms are again given by Eq. (34). When a collision occurs during the laser pulses, the state amplitudes change as a result of three effects.⁷ First, there is a shifting of the levels owing to the light-shift operator; for the perturbation calculation of this paper, this term can be neglected. Second, there is a shifting of the levels owing to a collisional operator. The collisional level shifts become important for collisions with impact parameters less than or of the order of some critical impact parameter b_0 (typically of the order of the Weisskopf radius associated with theories of pressure broadening). For collisions with $b > b_0$, the collisional level shifts can be ignored; for collisions with $b < b_0$ there is a rapid phase variation of $\tilde{\rho}_{2,3}(b, v_r, t_c, \vec{R})$ with b , leading to destructive interference in the integral (45). Thus, in calculating $\tilde{\rho}_{2,3}(\vec{R}, T^+)$, we should set the lower limit of the b integration to b_0 and neglect the effects of the collisional shift operator in treating collisions with $b > b_0$. Third, there is the LICET transition operator which couples the initial and final states of the AA' system and gives

rise to the coherence $\tilde{\rho}_{2,3}$.

Matrix elements of the LICET transition operator between the initial state $|2\ 1'\rangle$ and final state $\langle 1f'|$ ($f' = 2'$ or $3'$) are given by⁷

$$T_{f'}(b, v_R, t_c, \vec{R}; t) = -i \left[\mathcal{E}_{f'}(\vec{R}, t_c) / 2\hbar \right] \\ \times \sum_{e e'} \left(\frac{\langle 1f' | p_x + p_x' | e e' \rangle \langle e e' | \mathcal{U}[\vec{R}_{AA'}(t)] | 21' \rangle}{\hbar (\omega_{e2} + \omega_{e'1'})} \right. \\ \left. + \frac{\langle 1f' | \mathcal{U}[\vec{R}_{AA'}(t)] | e e' \rangle \langle e e' | p_x + p_x' | 21' \rangle}{\hbar (\omega_{e1} + \omega_{e'f'})} \right) , \quad (46)$$

where

$$\mathcal{E}_{f'}(\vec{R}, t_c) = \begin{cases} \mathcal{E}(\vec{R}, t_c) & f' = 2' \\ \mathcal{E}_1(\vec{R}, t_c) & f' = 3' \end{cases} , \quad (47)$$

\mathcal{U} is the AA' collisional Hamiltonian evaluated along the classical collision trajectory $\vec{R}_{AA'}(b, v_R, t)$, and the sum is over all intermediate states e and e' [primed (unprimed) quantities refer to atom A (A')]. Note that $T_{f'}$ represents the combined action of the radiation field and collision and vanishes if either $\mathcal{E}_{f'}$ or \mathcal{U} is zero. In terms of the matrix element (46), the final state amplitude $a_{1f'}(b, v_R, t_c, \vec{R})$, calculated

in lowest order perturbation theory and in the impact approximation

[Eqs. (10-12)], is given by

$$\tilde{a}_{if'}(b, v_n, t_c, \vec{R}) = e^{-i\Delta_v(f')t_c} T_{f'}(b, v_n, t_c, \vec{R}), \quad (48)$$

where¹⁷

$$\Delta_v(f') = \begin{cases} \Delta - \vec{k} \cdot \vec{v} = \Omega - (\omega_{2'1'} - \omega_{21}) - \vec{k} \cdot \vec{v} \\ \Delta_1 - \vec{k}_1 \cdot \vec{v} = \Omega_1 - (\omega_{3'1'} - \omega_{31}) - \vec{k}_1 \cdot \vec{v} \end{cases}, \quad (49)$$

$$T_{f'}(b, v_n, t_c, \vec{R}) = \int_{t_c^-}^{t_c^+} T_{f'}(b, v_n, t_c, \vec{R}; t) dt, \quad (50)$$

and t_c^- and t_c^+ represent times before and after a collision centered at $t = t_c$. The value of $\tilde{\rho}_{2,3}$ produced by this collision is

$$\tilde{\rho}_{2,3}(b, v_n, t_c, \vec{R}) = e^{-i[\Delta_v(2') - \Delta_v(3')]t_c} T_{2,3}(b, v_n, t_c, \vec{R}), \quad (51)$$

where

$$T_{2,3}(b, v_n, t_c, \vec{R}) = T_c(b, v_n, t_c, \vec{R}) [T_3(b, v_n, t_c, \vec{R})]^*. \quad (52)$$

In carrying out the integration (45), we can take the exponential factor in Eq. (51) to be constant, owing to conditions (14) and (15). Setting $t_c = 0$ without loss of generality, we find the value of $\tilde{\rho}_{2,3}(\vec{R}, T^+)$ following the

laser pulses from Eqs. (45) and (51) to be

$$\tilde{S}_{2,3}(\vec{R}, T^+) = N_A \int_{b_0}^{\infty} 2\pi b db \int_0^{\infty} W(v_R) v_R dv_R \\ \times \int_{T^-}^{T^+} dt_c T_{2,3'}(b, v_R, t_c, \vec{R}) \quad (53)$$

where $T_{2,3'}$ is calculated from Eqs. (52), (50) and (46).

Without going into a detailed evaluation of Eq. (51), one can note several general features of the result. First, the magnitude $|\tilde{\rho}_{2,3'}(\vec{R}, T^+)|$ is of the same order of magnitude as the populations ($\rho_{2,2'}$ or $\rho_{3,3'}$) induced by the LICET reaction. Second, states 2' and 3' can be of the same or opposite parity - the relative parity of the two levels determines which part of the interatomic potential (i.e. dipole-dipole; dipole-quadrupole, etc.) contributes in Eq. (46). Third, the LICET cross section is significantly enhanced if the energy of the intermediate levels (e or e') in Eq. (46) is such as to lead to a "small" energy denominator in Eq. (49)¹⁸; in that case, a single term dominates the summation in Eq. (46). The existence of nearly resonant intermediate levels has played a key role in all experimental observations of LICET to date.

The types of level schemes which lead to near-resonant enhancement have been discussed in a previous work.⁷ To illustrate this feature, we consider the level schemes depicted in Figs. 4 and 5. In Fig. 4, contribution to Eq. (46) with level r' as intermediate state is dominant. One

can view the LICET process as a collisional exchange which takes atom A from state 1 to f and atom A' from state $1'$ to r' (the r' state is virtual) followed by the field \vec{E} taking atom A' from r' to $2'$ (leading to the amplitude $\tilde{a}_{f2'}$) or the field \vec{E}_1 taking atom A' from r' to $3'$ (leading to the amplitude $\tilde{a}_{f3'}$). For this type of level scheme, levels $2'$ and $3'$ must be of the same parity. The value of $|\tilde{\sigma}_{2,3}|$ produced in this LICET reaction may be calculated from Eqs. (46)-(53) and is found to be of order⁷

$$|\tilde{\sigma}_{2,3}(\vec{R}, T)| \approx N_A u_r \left| \int_T^T \chi'_{2',r'}(\vec{R}, t_c) \chi'^*_{3',r'}(\vec{R}, t_c) dt_c \right| \times (\omega_{r',1'} - \omega_{2'})^{-2} (b_{r'}/b_0)^2 b_{r'}^2 \quad (54)$$

where

$$\begin{aligned} \chi'_{2',r'}(\vec{R}, t_c) &= \langle 2' | p_{r'} | r' \rangle \vec{E}(\vec{R}, t_c) / 2\hbar \\ \chi'_{3',r'}(\vec{R}, t_c) &= \langle 3' | p_{r'} | r' \rangle \vec{E}_1(\vec{R}, t_c) / 2\hbar \end{aligned} \quad (55)$$

u_r is the most probable relative speed, $b_{r'}$ is a radius which characterizes resonant broadening of the $r'-1'$ transition, and b_0 is a radius at which the collisional level shifting operator becomes important (as such, it is a characteristic radius of foreign gas broadening). Values of $b_{r'}$ in the 10\AA to 20\AA range are typical as are ratios $b_{r'}/b_0 \approx 4$.

It would appear that a coherence between states of opposite parity can be produced by the level scheme shown in Fig. 5 in which there are two nearly resonant intermediate states r' and r'_1 of opposite parity. Assume that states $1, 1', r'_1, 2'$ have parity "+" and states $2, r', 3'$ have parity "-". Then, a dipole-dipole collisional interaction followed by field \vec{E} acting on atom A' leads to a final state amplitude \tilde{a}_{12} , via the pathway $21' \rightarrow 1r' \rightarrow 12'$. Similarly, a dipole-quadrupole collisional interaction followed by field \vec{E}_1 acting in atom A' leads to a final state amplitude \tilde{a}_{13} , via the pathway $21' \rightarrow 1r'_1 \rightarrow 13'$. Since the collision operator \mathcal{U} contains both dipole-dipole and dipole-quadrupole components, the same collision creates both \tilde{a}_{12} , and \tilde{a}_{13} . Consequently, it would appear that a coherence $\tilde{\rho}_{2,3}$, with states $2'$ and $3'$ having opposite parity, can be produced in LICET. The order of magnitude of this coherence is given by an equation analogous to Eq. (54).

Although a given collision produces a coherence $\tilde{\rho}_{2,3}$, one finds that the macroscopic dipole moment, obtained by averaging over all possible collision orientations, vanishes if states $2'$ and $3'$ are of opposite parity.¹⁹ In some sense,⁷ one can view the production of coherence $\tilde{\rho}_{2,3}$ in the A' atoms as a four-wave mixing process; the four fields are the two laser fields and the dipole and quadrupole collisional interactions acting on the A' atoms. The dipole and quadrupole collisional interactions can be thought of as unpolarized "fields";⁷ for isotropic collisions, these fields are incident

from all directions with equal probability and the macroscopic coherence $\tilde{\rho}_{2,3}$, vanishes. However, by velocity selecting either the A or A' atoms (e.g. use velocity selective excitation of the A atoms, use a beam of A or A' atoms, detect only those A' atoms in a given velocity subclass), one creates an anisotropic distribution of collision orientations. In effect, the collisional dipole and quadrupole "fields" are no longer incident with equal probability from all directions and it becomes possible to create a nonvanishing macroscopic $\tilde{\rho}_{2,3}$. A detailed calculation of $\tilde{\rho}_{2,3}$ will be given in a future paper; at this point, however, we note that it appears that it is necessary to be detuned from exact resonance for one of the LICET transitions in order to produce a nonvanishing macroscopic coherence.

V. Detection

The result of the CARE or LICET reaction is to create a coherence in one of the atoms, A or A'. The method of detection depends on whether the final states have the same or opposite parity.

A. Final states having the same parity following the CARE or LICET excitation.

The analysis is the same for both CARE and LICET; to be specific, we analyze the CARE process. Immediately following the laser pulses at $t = T^+$ (which is now arbitrarily set equal to zero), a coherence

$$\rho_{23}(\vec{R}, 0) = \tilde{\rho}_{23}(\vec{R}, T^+ = 0) e^{i(\vec{k} - \vec{k}_1) \cdot \vec{R}} \quad (56)$$

is created. Since states 2 and 3 have the same parity, one uses an interrogation pulse²⁰ to monitor the 2-3 coherence. Several methods are available²⁰, depending on the relative magnitudes of the decay rates and the \vec{k} and \vec{k}_1 vectors. We shall choose one, a detection scheme similar to that employed in the tri-level echo²¹; in using this scheme, we assume that

$$|\vec{k} - \vec{k}_1| u \gg \gamma_{23}^t \quad (57)$$

where

$$\gamma_{23}^t = \frac{1}{2} (\gamma_i + \gamma_j) + \Gamma_{ij} \quad (58)$$

is the total rate at which the ij coherence decays.

The level scheme is as shown in Fig. 6. At time T_1 after the initial laser pulses, a third laser pulse

$$\vec{E}_2(\vec{R}, t) = \frac{1}{2} \vec{E}_2(\vec{R}, t) \hat{x} e^{i(\vec{k}_2 \cdot \vec{R} - \Omega_2 t)} \quad (59)$$

in near resonance with the 2-4 transition, is incident on the sample.

The pulse duration T is assumed to be short enough so that all relaxation processes can be neglected during the pulse [i.e. $\gamma_{1j}^t T \ll 1$;

$|\vec{k} - \vec{k}_1|uT \ll 1$; $k_2 uT \ll 1$; $(\Omega_2 - \omega_{42})T \ll 1$, etc.]. To calculate the response of the system, we set

$$\rho_{43} = \bar{\rho}_{43} e^{i(\vec{k}_f \cdot \vec{R} - \Omega_f t)} \quad (60a)$$

in anticipation of a signal being generated with propagation vector \vec{k}_f and frequency Ω_f . In addition, we write

$$\rho_{24} = \bar{\rho}_{24} e^{-i(\vec{k}_2 \cdot \vec{R} - \Omega_2 t)} \quad (60b)$$

$$\rho_{23} = \bar{\rho}_{23} e^{i[(\vec{k}_f - \vec{k}_2) \cdot \vec{R} - (\Omega_f - \Omega_2)t]}. \quad (60c)$$

At a time T_1^- just before the interrogation pulse is applied,

$\bar{\rho}_{24} = \bar{\rho}_{43} = 0$. The coherence ρ_{23} has evolved freely to a value

$\tilde{\rho}_{23}(\vec{R}, 0) \exp[i(\vec{k} - \vec{k}_1) \cdot (\vec{R} - \vec{v}T_1) - i(\Omega - \Omega_1)T_1 - \gamma_{23}^t T_1]$, which, together with

Eq. (61b), implies that $\bar{\rho}_{23}(T_1^-)$ is equal to

$$\begin{aligned} \bar{\rho}_{23}(T_1^-) &= \tilde{\rho}_{23}(\vec{R}, 0) e^{-i[(\vec{k}_f - (\vec{k}_2 - \vec{k}_1 + \vec{k})) \cdot \vec{R}]} e^{i(\vec{k}_1 - \vec{k}) \cdot \vec{v}T_1} \\ &\times e^{i[\Omega_f - (\Omega_2 - \Omega_1 + \Omega)]T_1} e^{-\gamma_{23}^t T_1}. \end{aligned} \quad (61)$$

The laser field couples the coherences $\bar{\rho}_{23}$ and $\bar{\rho}_{43}$. Following the laser pulse, $\bar{\rho}_{43}$ acquires a value proportional to $\bar{\rho}_{23}(\vec{R}, T_1^-)$; with the neglect of all relaxation during the laser pulse and the use of an optimal pulse (one having a pulse area of $\pi/2$), the value of $\bar{\rho}_{43}$ at a time T_1^+ immediately following the laser pulse is

$$\bar{\rho}_{43}(T_1^+) = i \bar{\rho}_{23}(T_1^-) \quad (62)$$

For $t > T_1$, $\bar{\rho}_{43}$ evolves freely according to

$$\dot{\bar{\rho}}_{43} = - [\gamma_{34}^t - i(\Omega_f - \omega_{43}) + i \vec{k}_f \cdot \vec{v}] \bar{\rho}_{43} \quad (63)$$

Combining Eqs. (61)-(63), one finds that, for $t > T_1$,

$$\begin{aligned} \bar{\rho}_{43}(\vec{R}, v, t) &= i \tilde{\rho}_{23}(\vec{R}, 0) e^{-i [\vec{k}_f - (\vec{k}_2 - \vec{k}_1 + \vec{k})] \cdot \vec{R}} \\ &\times e^{i [\Omega_f - (\Omega_2 - \Omega_1 + \Omega)] T_1} e^{i (\Omega_f - \omega_{43})(t - T_1)} \\ &\times e^{-i [\vec{k}_f(t - T_1) + (\vec{k} - \vec{k}_1) T_1] \cdot \vec{v}} \\ &\times e^{-[\gamma_{23}^t T_1 + \gamma_{34}^t (t - T_1)]} \end{aligned} \quad (64)$$

The coherence $\bar{\rho}_{43}$ generates a radiation field provided that the phase-matching condition

$$\vec{k}_f = \vec{k}_2 - \vec{k}_1 + \vec{k} \quad (65)$$

along with the subsidiary condition

$$(\Omega_f - \omega_{43}) L / c \ll 1 \quad (66)$$

is obeyed (L = sample length). These phase-matching conditions can be achieved by taking copropagating waves with $(\Omega_1 - \Omega) \approx \omega_{32}$ and $\Omega_2 \approx \omega_{42}$. Assuming the phase-matching conditions to hold and that the sample is optically thin, it is easy to show that the power density exiting the sample is given by

$$S(t) = \frac{N_A^2}{4\pi\epsilon_0} |\langle 4 | P_K | 3 \rangle|^2 (2\pi c)^2 k_f^2 L^2 |\langle \bar{\rho}_{43}(\vec{R}, \vec{v}, t) \rangle|^2, \quad (67)$$

where N_A is the atom A density and the average is over the atom A velocity distribution and any changes in $\bar{\rho}_{43}$ caused by the lack of spatial coherence of the laser fields. On integrating over velocities for times $(t - T_1) > 1/k_f u$, one finds a negligibly small $\bar{\rho}_{43}$ except when

$$\vec{k}_f(t - T_1) + (\vec{k} - \vec{k}_1) T_1 = 0. \quad (68)$$

For copropagating waves satisfying Eq. (65), this condition implies that an echo can be produced at a time t_e given by

$$t_e = \left(\frac{k_2}{k_2 - k_1 + k} \right) T_1. \quad (69)$$

An echo is produced provided that $k_1 > k$, an inequality that holds for the system we have chosen. Combining Eqs. (64)-(68), we find that the maximum

value for the echo power density exiting the sample is

$$S_{\text{max}}(t = t_e) = \frac{N_A^2}{4\pi\epsilon_0} | \langle 4 | P_x | 3 \rangle |^2 (2\pi c)^2 k_f^2 L^2 \\ \times e^{-2[\gamma_{23}^T T_1 + \gamma_{34}^T (t_e - T_1)]} \\ \times | \langle \tilde{\rho}_{23}(\vec{R}, 0) \rangle |^2 \quad (70)$$

Assuming that $| \langle \tilde{\rho}_{23}(\vec{R}, 0) \rangle |$ can reach values of order 0.01, one finds power densities of order 1.0 W/cm^2 for active atom densities $N_A \approx 10^{15} \text{ atoms/cm}^3$.

B. Final states having opposite parity.

For the LICET reaction, it is possible to create an optical coherence $\tilde{\rho}_{2',3'}$ in which states 2' and 3' have opposite parity. This coherence can be monitored by detecting the free-induction decay signal emitted by the sample. At time $T^+ = 0$ immediately following the LICET excitation, a coherence

$$\tilde{\rho}_{2',3'}(\vec{R}, 0) = \tilde{\rho}_{2',3'}(\vec{R}, T^+ = 0) e^{i(\vec{k} - \vec{k}_1) \cdot \vec{R}} \quad (71)$$

is created. This coherence then evolves freely so that at a time $t > 0$, one finds phase matching can be achieved with copropagating fields having $k_1 - k = \omega_{3',2'}$. Under phase-matching conditions, the power density exiting the sample is given by an equation analogous to (67). On performing the

necessary velocity integration assuming $(k_1 - k)u' \gg \gamma_{2,3}^t$, (u' = atom A' most probable speed), one may obtain

$$S(t) = \frac{N_{A'}^2}{4\pi\epsilon_0} |\langle 3' | p_A | 2' \rangle|^2 (2\pi c) (k_1 - k)^2 L^2 \times \left[\pi \epsilon_0^{-\frac{1}{2}} (k_1 - k)^2 u'^2 t^2 \right] |\langle \tilde{\phi}_{2,3'}(\vec{R}, 0) \rangle|^2 \quad (72)$$

where $N_{A'}$ is the A'-atom density. Although the value for the coherence $|\tilde{\phi}_{2,3'}(\vec{R}, 0)|$ is smaller than that in the case when levels 2' and 3' have the same parity, (see discussion of Sec. IV), it would appear that there is sufficient signal strength to detect the LICET induced coherent emission.

VI. Conclusion

A method for producing electronic state coherences using Combined Field-Collisional Transitions (CFCT) has been outlined. Such coherences can be produced using either Collisionally-Aided Radiative Excitation (CARE) or Laser-Induced Collisional Excitation Transfer (LICET). The final state coherence may be created between levels having the same or opposite parity. For final states of the same parity, the coherence can be "stored"; at some later time, an interrogation pulse can be used to trigger the emission of dipole radiation. For final states of opposite parity, the system can radiate immediately following the LICET excitation. In this way, one can use LICET for either sum or difference frequency generation.

As noted above, some additional feature must be added to LICET (i.e. velocity selection of either the A or A' atoms) to produce a final state coherences between states of opposite parity. Another way to achieve a final state coherence between states of opposite parity using either CARE or LICET is illustrated in Fig. 7. A coherence is created between two states of atom A (i and i_1) by a CW or pulsed field. From this initial state, a CARE reaction produces a coherence ρ_{23} (Fig. 7a) while a LICET reaction produces a coherence $\rho_{2,3'}$ (Fig. 7b) between states of opposite parity. This technique could be used to produce radiation at the sum frequency of the three laser fields.

In order to produce coherence using CFCT, the laser fields must be temporally and spatially coherent. The relative phase of the two laser

fields cannot vary significantly in times less than the pulse duration or in distances less than a wavelength for the coherence to be produced. Since the production of tri-level echoes requires the same coherence properties and since tri-level echoes are readily observed with non-mode-locked lasers²¹, it would appear that the coherence criteria for creating CFCT induced electronic state coherences can be achieved.

One of the authors (P.R.B.) would like to thank Prof. T. Mossberg for comments concerning methods for detecting coherences produced in CARE.

E.G. would like to thank P. Berman and H.H. Stroke for their kind hospitality during her stay at New York University.

This research is supported by the U.S. Office of Naval Research and, in part, by NSF Grant INT-7921530.

References

* Permanent Address: Laboratoire de Spectroscopie Hertzienne de l'E.N.S.
Universite P. et M. Curie, 4 Place Jussieu 75230 Paris Cedex 05 France.

1. For a general review of this subject area, see Photon-Assisted Collisions and Related Topics edited by N.K. Rahman and C. Guidotti (Harwood Academic Publishers, Chur, Switzerland, 1982).
2. S. Yeh and P.R. Berman, Phys. Rev. A 19, 1106 (1979).
3. V.S. Lisitsa and S.I. Yakovlenko, Zh. Eksp. Teor. Fiz. 66, 1550 (1974) [Sov. Phys. - JETP 39, 759 (1974)].
4. Ph. Cahuzac and P.E. Toschek, Phys. Rev. Lett. 36, 462 (1978).
5. L.I. Gudzenko and S.I. Yakovlenko, Zh. Eksp. Teor. Fiz. 62, 1686 (1972) [Sov. Phys. JETP 35, 877 (1972)].
6. As in CARE, small differences between $\hbar\Omega$ and $[E(\text{final}) - E(\text{initial})]$ can be compensated by a change in the translational energy of the colliding atoms.
7. P.R. Berman, Phys. Rev. A 22, 1838, 1848 (1980).
8. See, for example, E.L. Lewis, M. Harris, W.J. Alford, J. Cooper and K. Burnett, J. Phys. B 16, 553 (1983) and references therein.
9. P. Thomann, K. Burnett and J. Cooper, Phys. Rev. Lett. 45, 1325 (1980); W. Behmenburg and V. Kroop, J. Phys. B 14, 427 (1981); W.J. Alford, K. Burnett and J. Cooper, Phys. Rev. A 27, 1310 (1983).
10. A. Débarre, J. Phys. B 15, 1693 (1982).

References - Con't.

11. See, for example, N. Bloembergen, A.R. Bogdan and M.W. Donner, in Laser Spectroscopy V edited by A.R.W. McKellar, T. Oka and B.P. Stoicheff (Springer-Verlag, Berlin, 1981) pp. 157-165.
12. G. Grynberg, J. Phys. B 14 2089 (1981).
13. For a general review of this subject, see, M. Dagenais, Phys. Rev. A 26, 869 (1982).
14. See, for example, D. Grischkowsky, Phys. Rev. A 7, 2096 (1973); M.D. Crisp, Phys. Rev. A 8, 2128 (1973); D. Grischkowsky, M.M.T. Loy and P.F. Liao, Phys. Rev. A 12, 2514 (1975).
15. G.S. Agarwal and J. Cooper, Phys. Rev. A 26, 2761 (1982).
16. For simplicity, we take Γ_{ij} to be real.
17. The equations are written specifically for Fig. 3a. They can be modified for Fig. 3b by changing the sign of Δ_v^1 .
18. It is implicitly assumed that the energy denominator is greater than \hbar/τ_c ; if this were not the case, collisional exchange in the absence of the radiation fields could occur.
19. Assuming an isotropic distribution of collision orientations, one finds that the same multipole order of the collision interaction must enter into the calculation of each of the final state amplitudes. This result follows directly from Eqs. (A15), (A16), (15) and (21) of the second article in Ref. 7, along with the fact that $kk' \begin{smallmatrix} K \\ A_Q \end{smallmatrix} \propto \delta_{K,k+k'}$, in those equations. One of the authors (PRB) would like to thank Prof. S.E. Harris for a discussion concerning attempts to produce sum frequency generation in centrosymmetric systems.

References - Con't.

20. See, for example, M. Matsuoka, H. Nakatsuka, and J. Okada, Phys. Rev. A 12, 1062 (1975); R.L. Shoemaker and R.G. Brewer, Phys. Rev. Lett. 28, 1430 (1972); R.G. Brewer and E.L. Hahn, Phys. Rev. A 11, 1614 (1975); J.R.R. Leite, R.L. Sheffield, M. Ducloy, R.D. Sharma and M.S. Feld, Phys. Rev. A 14, 1151 (1976); P.F. Liao, J.E. Bjorkholm and J.P. Gordon, Phys. Rev. Lett 39, 15 (1977); A. Flusberg, T. Mossberg, R. Kachru and S.R. Hartmann, Phys. Rev. Lett. 41, 305 (1978).
21. T. Mossberg, A. Flusberg, R. Kachru and S.R. Hartmann, Phys. Rev. Lett. 39, 1523 (1977); T.W. Mossberg, R. Kachru, S.R. Hartmann and A.M. Flusberg, Phys. Rev. A 20, 1976 (1979).

Figure Captions

1. CARE reaction $A_1 + A'_1 + \hbar\Omega \rightarrow A(12) + A'_1$, [the notation $A(ij)$ is used to indicate a coherence between states i and j]. The A and A' atoms collide in the presence of a pulsed laser field whose frequency is represented by an arrow in the figure. As noted in the text, the coherence ρ_{12} vanishes on averaging over times during the laser pulse at which the collision may occur.
2. CARE reaction $A_1 + A'_1 + \hbar\Omega + \hbar\Omega_1 \rightarrow A(23) + A'_1$. A coherence ρ_{23} is created if $\Omega_1 - \Omega \approx \omega_{32}$.
3. LICET reaction $A_2 + A'_1 + \hbar\Omega + \hbar\Omega_1 \rightarrow A_1 + A'(2'3')$. A coherence $\rho_{2'3'}$ is created if $\Omega_1 - \Omega = \omega_{3'2'}$ (Fig. 3a) or $\Omega_1 + \Omega \approx \omega_{3'2'}$ (Fig. 3b).
4. LICET reaction $A_2 + A'_1 + \hbar\Omega + \hbar\Omega_1 \rightarrow A_1 + A'(2'3')$ with a nearly resonant intermediate state. The collisional interaction creates a virtual state with energy close to that of level r' and the field interactions complete the LICET process. States $2'$ and $3'$ must have the same parity.
5. A LICET reaction similar to that shown in Fig. 4, but one for which there are two nearly resonant intermediate states of opposite parity and for which states $2'$ and $3'$ are of opposite parity. The r' and r'_1 levels enhance the excitation probability for states $2'$ and $3'$, respectively.

Figure Captions - Con't.

6. A scheme for detecting the coherence ρ_{23} created by a CARE reaction at $t = 0$. At time T_1 a laser pulse of frequency $\Omega_2 \approx \omega_{42}$ is applied to the atoms. At some time later, an echo signal can be generated at frequency $\Omega_f \approx \omega_{43}$.

7. A method for producing electronic state coherences between states of opposite parity by starting with atom A prepared in a coherent superposition of states i and i_1 .

(7a) CARE reaction $A(i i_1) + A'_1 + \hbar\Omega + \hbar\Omega_1 \rightarrow A(23) + A'_1$;

$$(\Omega + \Omega_1 + \omega_{i_1 i}) \approx \omega_{32}.$$

(7b) LICET reaction $A(i i_1) + A'_1 + \hbar\Omega + \hbar\Omega_1 \rightarrow A_1 + A'(2'3')$;

$$(\Omega + \Omega_1 + \omega_{i_1 i}) \approx \omega_{3'2'}.$$

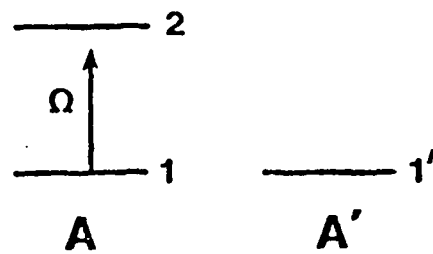


Fig. 1

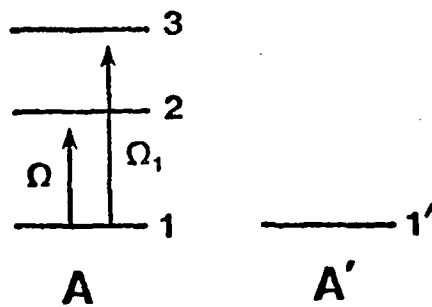


Fig. 2

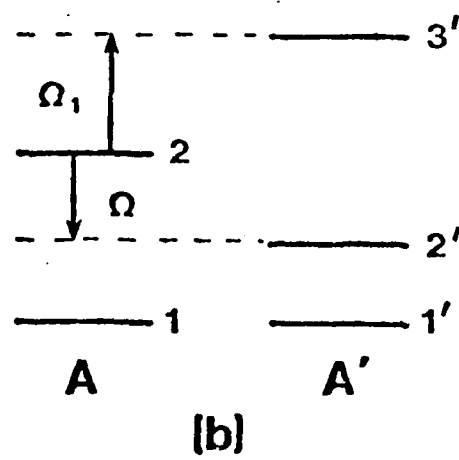
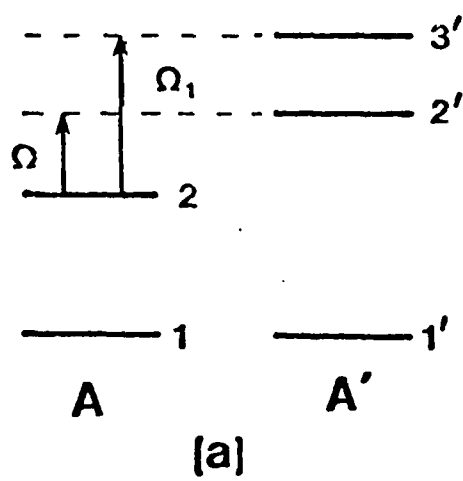


Fig. 3

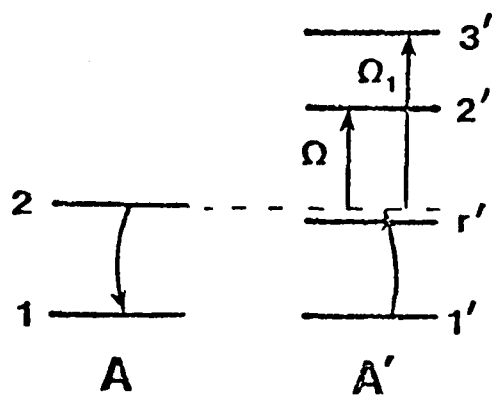


Fig. 4

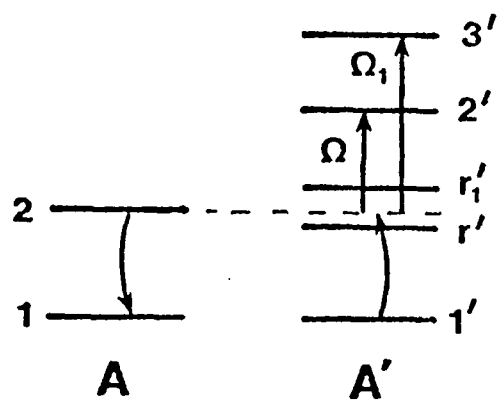


Fig. 5

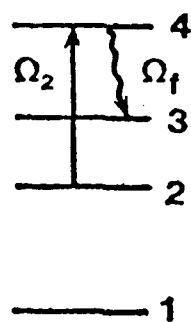


Fig. 6

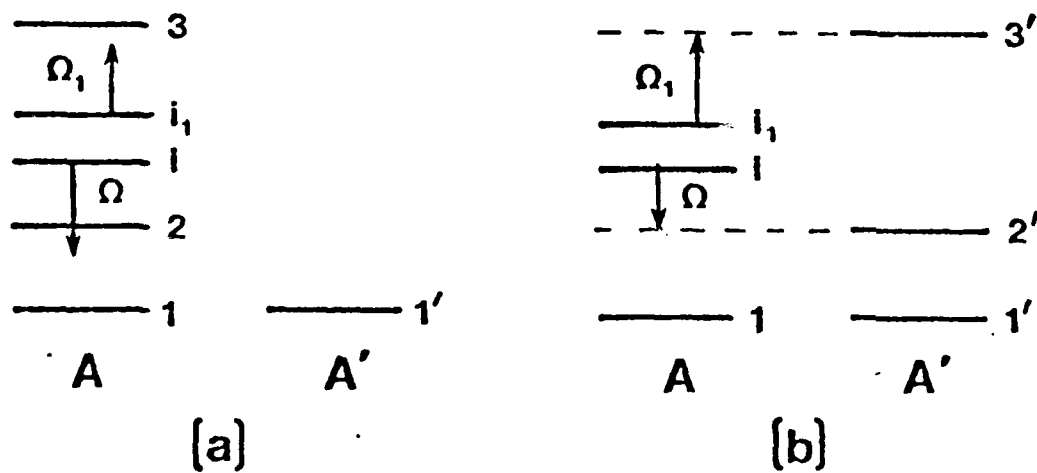


Fig. 7

New results for transition probabilities in two-level systems: The large-detuning regime

E. J. Robinson and P. R. Berman

Department of Physics, New York University, New York, New York 10003

(Received 29 June 1982)

The problem of calculating transition probabilities in two-level systems is studied in the limit where the detuning is large compared to the inverse duration of the interaction. Coupling potentials whose Fourier transforms $\tilde{V}(\omega)$ are of the form $f(\omega)e^{-b\omega}$ for large frequencies give rise to solutions which may be classified into families according to the form of $f(\omega)$. Within each family transition probabilities may be calculated from formulas that differ only in the numerical value of a scaling parameter. In cases where the coupling function has a pole in the complex time plane, the families are identified with the order of this singularity. In particular, for poles of first order, a connection with the Rosen-Zener solution can be made. The analysis is performed via high-order perturbation expansions which are shown to always converge for two-level systems driven by coupling potentials of finite pulse area.

1. INTRODUCTION

In many areas of physics, one encounters problems involving two states of a quantum-mechanical system coupled by a time-dependent potential.¹⁻¹⁰ In the interaction representation, the equations of motion for a_1 and a_2 , the probability amplitudes of levels 1 and 2, are of the form

$$i\dot{a}_1 = V(t)e^{i\omega t}a_2, \quad (1a)$$

$$i\dot{a}_2 = V(t)e^{-i\omega t}a_1, \quad (1b)$$

where ω is the frequency separation of the states and $V(t)$ is the coupling potential. Decay effects are neglected in Eqs. (1) (and throughout this paper), and we work in a system of units in which $\hbar=1$.

Equations of this type arise in many semiclassical problems. A problem of current interest to which they apply is the coupling of two levels of an atom by a laser pulse that has a temporal width which is small compared to the natural lifetimes of the levels. The pulse $V(t)$ is of the form

$$V(t) = 2A(t)\cos\Omega t, \quad (2)$$

where Ω is the central frequency of the pulse, and $2A(t)$ is the envelope function of its amplitude. Assuming that $|\Omega - \omega|/(\Omega + \omega) \ll 1$, one can recast Eqs. (1) in terms of Δ , the detuning of the pulse from resonance (rotating-wave approximation), as

$$i\dot{a}_1 = A(t)e^{i\Delta t}a_2, \quad (3a)$$

$$i\dot{a}_2 = A(t)e^{-i\Delta t}a_1. \quad (3b)$$

Equations (3) or (1) are deceptively simple in form, and one might, at first glance, believe that the system must be completely understood, so that nothing

remains to be investigated about the equations or their solutions. Actually, there is very little known about the overall qualitative nature of the solutions to Eqs. (3) for arbitrary $A(t)$. Apart from any intrinsic interest one might have in the dynamics of two-level systems, such information could be useful, for example, in applications where one wished to choose the pulse shape to maximize the excitation probability for a given detuning Δ .

To appreciate that our assertion concerning the lack of knowledge about the behavior of systems described by Eqs. (3) is valid, one need only recognize that the answer to the following question is not known in general: Starting with initial conditions $a_1(-\infty)=1$ and $a_2(-\infty)=0$, how does the probability amplitude $a_2(t)$ depend qualitatively on the pulse area S , defined by

$$S = \int_{-\infty}^{\infty} A(t)dt,$$

on the detuning, and on the shape of the envelope function $A(t)$? A response to this query can be made for a limited number of cases. Analytic solutions are available if $A(t)$ belongs to a class of functions⁵ (including the hyperbolic secant of Rosen and Zener^{2,3}) mappable into the hypergeometric equation, or if^{9,10}

$$A(t) = (\text{const})\exp(-\alpha|t|),$$

or if $A(t)$ is a step function (Rabi problem), or if the detuning is zero. (Kaplan⁷ has also considered cases where the detuning varies as prescribed functions of the amplitude and obtained closed-form expressions.) In addition, there are approximate solutions available in adiabatic⁴ or perturbative limits. Yet, there remains a wide range of parameters and pulse

shapes for which an answer to the basic question cannot be provided.

In this paper, we shall examine the solutions to Eqs. (3) in the limit where the product of the detuning Δ and the characteristic pulse duration τ has a magnitude greatly in excess of unity. In other words, we are assuming that the pulse does not possess the appropriate Fourier components to significantly compensate for the detuning. In consequence, the transition probability $|a_2(\infty)|^2$ will always be very small (but still great enough to be experimentally measurable in atomic vapors of densities $\sim 10^{12}$ atoms/cm³). We note that numerical solutions of Eqs. (3) in this detuning range may be possible but are very costly in computer time and plagued with technical difficulties.

For the case $\Delta\tau \gg 1$, we shall establish the following results: (1) Low-order perturbative approximations for $a_2(\infty)$ are not valid for arbitrary pulse area S , despite the fact that $|a_2(t)|^2 \ll 1$ for all time. (2) An iterative solution to Eqs. (1) always converges for well-behaved envelope functions. (3) Asymptotic solutions for $a_2(t)$, t finite, may be easily found, but expressions for $a_2(\infty)$ are difficult to obtain. (4) Asymptotic solutions for $a_2(\infty)$ can be obtained for a limited class of pulse-envelope functions using contour integration techniques. This is a broader set than that for which exact solutions are known. (5) The asymptotic dependence of $a_2(\infty)$ depends critically on the nature of the singularities of the pulse-envelope function $A(t)$, analytically continued into the complex plane. (6) If two pulse functions have the same Fourier transforms in the limit of large frequencies and if the dominant dependence of the transform is an exponential decay in the frequency, then the asymptotic forms of the solutions $a_2(\infty)$ for these functions in the limit of large Δ are simply related. In this paper, we address points (1), (2), (3), and (6); methods for actually obtaining asymptotic solutions [points (4) and (5)] will be discussed in a future article. In the present discussion, the initial conditions are taken as $a_1(-\infty) = 1$ and $a_2(-\infty) = 0$.

II. ASYMPTOTIC SOLUTIONS

As we have indicated, the Rosen-Zener^{2,3} (hyperbolic secant coupling pulse) problem is one of the few for which exact solutions are known. In this case, a simple expression gives the transition amplitude as a function of detuning and area for all values of these parameters. Naturally, since this formula

$$a_2(\infty) = iV(2\pi A(\Delta)) \frac{\sin S}{S}, \quad (4)$$

where A is the Fourier transform of $A(t)$, is exact, it is valid in the special case of the asymptotic limit

We shall show that there is an entire class of pulses for which the asymptotic transition amplitude, as a function of S and Δ , may be written by inspection once the Rosen-Zener problem has been solved. We shall also demonstrate that there are other classes of pulses whose solutions as $t \rightarrow \infty$ are unrelated to Rosen-Zener but are connected to each other in the sense that once one has been solved, the solutions for the entire class may be obtained by inspection.

The existence of these related solutions will be established via term-by-term comparison of n th-order perturbation expansions which, under very general conditions, are convergent in two-level problems (see the Appendix). With suitable scaling of the coupling strengths, the series for different members of particular classes will be seen to be identical in the limit of large detunings.

The particular potentials analyzed in this paper are $A(t)$ whose Fourier transforms for large ω assume the form $p(\omega)\exp(-b\omega)$, where p is slowly varying in a frequency interval b^{-1} , and b is a constant. It is convenient to make a variable change, such that $v = b\omega$ and $x = t/b$. Consequently, the exponential decay factor in the Fourier transform becomes $\exp(-v)$ and the equations of motion transform to

$$i\dot{a}_1 = \beta f(x)e^{i\alpha x}a_2, \quad (3a')$$

$$i\dot{a}_2 = \beta f(x)e^{-i\alpha x}a_1, \quad (3b')$$

where $\alpha = b\Delta$ and where the dot now signifies differentiation with respect to x . The quantity β , previously designated as S , is the pulse area. The reduced potential function $f(x)$ is defined such that

$$\int_{-\infty}^{\infty} f(x)dx = 1.$$

The pulse area is invariant under the indicated change of variable. One may also write Eqs. (3) as a pair of uncoupled second-order equations

$$\ddot{a}_1 + \left[\frac{\dot{f}}{f} + i\alpha \right] \dot{a}_1 + \beta^2 f^2 a_1 = 0, \quad (5a)$$

$$\ddot{a}_2 + \left[\frac{\dot{f}}{f} - i\alpha \right] \dot{a}_2 + \beta^2 f^2 a_2 = 0. \quad (5b)$$

There are two aspects to the solutions of Eqs. (3) or (5). These are the calculations of the amplitudes at finite and infinite times, respectively. The former are of interest if the transient solutions are to be used as inputs to other problems, such as multiphoton ionization,¹¹ while the latter, with which we are mainly concerned here, gives the transition amplitude $a_2(\infty)$. The two temporal regimes differ greatly in the methods that must be used to perform accurate calculations.

One may write the solutions to Eqs. (3) as perturbation series in the usual fashion, noting that only even orders enter the expression for a_1 , while only odd orders appear in the formula for a_2 . The expansion for $a_2(t \rightarrow \infty)$ is

$$a_2 = -i \sum_{k=0}^{\infty} a_2^{(2k+1)} \beta^{2k+1} (-1)^k,$$

where

$$a_2^{(2k+1)} = \int_{-\infty}^{\infty} f(x_1) e^{-i\alpha x_1} dx_1 \\ + \prod_{j=2}^{2k+1} \int_{-\infty}^{x_{j-1}} f(x_j) e^{i(-1)^{j+1} \alpha x_j} dx_j.$$

In the Appendix, it is shown that this series converges for all finite pulse areas.

For the remainder of the paper we will restrict ourselves to the case of pulses that are symmetric in time and where $|\alpha| \gg 1$, the adiabatic or asymptotic limit. The Fourier transform will be symmetric in v . We shall begin by comparing the finite and infinite time solutions of the Rosen-Zener problem, which exemplify relevant properties of transition amplitudes induced by smooth pulses.

With initial conditions $a_1(-\infty) = 1$ and $a_2(-\infty) = 0$ with a pulse-envelope function $f(x) = \text{sech}(\pi x/2)/2$, Rosen and Zener^{2,3} obtained an analytic solution to Eqs. (3') of the form

$$a_1(x) = {}_2F_1(a, b, c, z), \quad (6a)$$

$$a_2(x) = iKz^{c-a-b} {}_2F_1(a-c^*+1, b-c^*+1, 2-c^*, z), \quad (6b)$$

or

$$a_1(x) = iKz^{c-a-b} (1-z)^{c^*-a-b} {}_2F_1(1-a, 1-b, 2-c^*, z), \quad (6b')$$

where

$$z = 1 - \frac{\beta}{1 + \frac{1}{2} \frac{i\alpha}{4\pi}} \frac{\tanh \frac{\pi x}{2} + 1}{2}, \quad K = -\frac{\beta}{4\pi \left[\frac{1}{2} - \frac{i\alpha}{4\pi} \right]},$$

and F designates the hypergeometric function. The form of a_2 given by Eq. (6b) is valid for all x , while that given by Eq. (6b') holds only for finite x , unless β corresponds to an eigenvalue, a pulse area for which $a_2 \rightarrow \infty$ vanishes.⁴ We recall that $a_2(\infty)$, the transition amplitude for the Rosen-Zener problem, is given by Eq. (4).

We may obtain the finite time solution by explicitly expanding the ${}_2F_1$ function of Eq. (6b')

$$a_2 = \frac{i\beta}{4\pi} \left[\frac{1}{2} - \frac{i\alpha}{4\pi} \right] e^{-i\alpha x \text{sech} \frac{\pi x}{2}} \left[1 + \frac{\left| 1 + \frac{\beta}{\pi} \right| \left| 1 - \frac{\beta}{\pi} \right|}{3 - \frac{i\alpha}{2\pi}} \left| \tanh \frac{\pi x}{2} + 1 \right| + \dots \right].$$

For large α , it is sufficient to retain the leading term

$$a_2 \sim \frac{\beta}{\alpha} e^{-i\alpha x \text{sech} \frac{\pi x}{2}}.$$

This is equivalent to first-order perturbation theory in the adiabatic limit

$$a_2^{(1)} = -i\beta \int_{-\infty}^x f(x') e^{-i\alpha x'} dx' \\ \sim \beta \frac{f(x)}{\alpha} e^{-i\alpha x},$$

where subsequent parts integrations are neglected, since they are $O(1/\alpha^n)$, $n \geq 1$. We immediately see that this sequence of parts integrations is unsuitable for calculating $a_2(\infty)$, since each term separately

vanishes when $x \rightarrow \infty$. Even including the third- and higher-order terms in the perturbation series via analogous sequences of parts integrations does not enable one to obtain a nonzero amplitude as $t \rightarrow \infty$. Consequently, other methods are necessary to calculate $a_2(\infty)$.

It is clear from the preceding paragraph that for large enough α , first-order perturbation theory is a sufficiently accurate approximation for most purposes, provided x is finite. For infinite times, not only does the adiabatic sequence of parts integrations lead to an incorrect $a_2(\infty)$, but even an exact evaluation of the first-order integral may be insufficient. This is typified by the exact Rosen-Zener amplitude, Eq. (4), in which the factor $\sin \beta$ does not reduce to its first-order limit of β unless $|\beta|$ is

small compared to unity. This failure of the first-order theory occurs no matter how large the detuning becomes. One must retain enough terms in the perturbation expansion to accurately represent the sine function. Thus for the Rosen-Zener pulse, if the coupling is great enough so that saturation effects would appear at resonance, simple first-order theories cannot be used for a nonresonant pulse of the same strength. As we shall see, other smooth pulses also possess this "saturation memory." In fact, in some cases, a higher-order theory is necessary off resonance even for a case where a first-order theory would suffice at resonance. This is exemplified by the formulas of Eqs. (9) below.

Since each coupling function $f(x)$ is different, one might be led to believe that separate calculations must be performed for each individual case. Fortunately, as we have stated earlier, there prove to be classes of pulses where, if one knows the functional dependence of the asymptotic transition amplitude on α and β for one member of the class, one knows it for all members of the class, although the actual time dependence of the potentials may be drastically different. What is significant is that their Fourier transforms assume the same form as $\alpha \rightarrow \infty$.

When Rosen and Zener deduced Eq. (4), they suggested that similar formulas might hold for other

smooth pulses.² This conjecture proves not to hold in general. It is manifestly false for asymmetric pulses and is not even valid for all symmetric pulses.^{5,6} What we shall show is that a kind of Rosen-Zener conjecture does apply at large detunings for pulses in which $f(x)$ has simple poles at $x = i$. This law does not apply to pulses which have higher-order poles at this point, although scaling laws for these do exist, different for each order.

The following theorem will be established. Let two coupling pulses $f(x)$ and $f_0(x)$ have Fourier transforms $\tilde{f}(v)$ and $\tilde{f}_0(v)$. The Fourier transforms of both approach, for large values of the argument, the same asymptotic form $\tilde{f}_a(v)$. If \tilde{f}_a is of the form $\phi(v)e^{-v}$, where $\phi(v)$ is a slowly varying function of v , then the asymptotic transition amplitudes generated by the two pulses will be the same, provided that the pulse areas are both finite. A sufficient condition for the indicated asymptotic behavior of the Fourier transforms is that they be equal, for large v , to a contour integration whose value is given by the product of the residue at $x = i$ and the usual Cauchy factor $2\pi i$. If two such pulses are to have the same $\phi(v)$, they must possess poles of the same order at $x = i$.

The contribution of order $(2k+1)$ to the transition amplitude may be rewritten slightly.

$$a_2^{(2k+1)} = \int_{-\infty}^{\infty} f(x_1) e^{-i\alpha x_1} dx_1 \prod_{j=2}^{2k+1} \lim_{\lambda_j \rightarrow 0} \int_{-\infty}^{x_j-1} f(x_j) e^{i(-1)^{j-1} \alpha + i\lambda_j x_j} dx_j.$$

The factors $e^{i\lambda_j x_j}$ do not affect the integrals. They are used to remove ambiguities as $x_j \rightarrow -\infty$ in the treatment below, where we express the amplitude in terms of integrals in the frequency domain. The limits $\lambda_j \rightarrow 0$ are to be taken before the x_1 integration is performed. Expressing each (x_j) , $j \geq 2$, in terms of its Fourier transform, we find

$$a_2^{(2k+1)} = \frac{1}{(2\pi)^k} \int_{-\infty}^{\infty} f(x_1) e^{-i\alpha x_1} dx_1 \prod_{j=2}^{2k+1} \lim_{\lambda_j \rightarrow 0} \int_{-\infty}^{x_j-1} dx_j \int_{-\infty}^{\infty} \tilde{f}(v_j) e^{i(v_j + (-1)^{j-1} \alpha + i\lambda_j)x_j} dv_j.$$

By working in the frequency domain, we shall be able to examine the structure of the integrals for $a_2^{(2k+1)}$ and establish that the contribution from regions where the asymptotic form of \tilde{f} is not valid is lower by $O(1/\alpha)$ than the contributions from regions where it is valid.

The integrals over the x_j are trivial to perform. We obtain

$$a_2^{(2k+1)} = \lim_{\lambda_l \rightarrow 0} \frac{1}{(2\pi)^{k-1/2}} \int_{-\infty}^{\infty} dv_2 \cdots dv_{2k+1} \tilde{f} \left[\sum_{j=2}^{2k+1} v_j - \alpha \right] \prod_{j=2}^{2k+1} \frac{\tilde{f}(v_j)}{\sum_{l=2k+3-j}^{2k+1} [v_l + (-1)^l \alpha - i\lambda_l]}.$$

We now proceed to determine the asymptotic form of these amplitudes. The analysis is easiest to follow for the third-order contribution $a_2^{(3)}$, but exactly the same reasoning and conclusions will apply for the higher-order terms. (The theorem is true by inspection in first order, since that contribution is, apart from a constant multiplier, just the Fourier transform itself. Thus if two coupling functions have Fourier transforms of the same asymptotic form, their first-order transition amplitudes scale the same way with β and α .) The leading nontrivial term is $a_2^{(3)}$. Changing the dummy variable v_1 to v_3 , we find

$$a_2^{(3)} = \lim_{\lambda_l \rightarrow 0} \frac{1}{2\pi} \int_{-\infty}^{\infty} \int_{-\infty}^{\infty} \frac{\tilde{f}(v_1) \tilde{f}(v_2) \tilde{f}(v_3 + v_2 - \alpha)}{(v_1 - \alpha - i\lambda_1)(v_2 + v_1 - i\lambda_2)} dv_1 dv_2.$$

where, without loss of generality, all λ_j and sums of λ_j have been replaced by the single infinitesimal λ . It is convenient to make the change of variable $y_1 \rightarrow y_1/\alpha$. One finds

$$\begin{aligned} a_2^3 &= \lim_{\lambda \rightarrow 0} \frac{1}{\sqrt{2\pi}} \int_{-\infty}^{\infty} \int_{-\infty}^{\infty} \frac{\tilde{f}(\alpha y_1) \tilde{f}(\alpha y_2) \tilde{f}(\alpha(y_1 + y_2 - 1)) dy_1 dy_2}{(y_1 - 1 - i\lambda)(y_1 + y_2 - i\lambda)} \\ &= \frac{1}{\sqrt{2\pi}} \left[P \int_{-\infty}^{\infty} \int_{-\infty}^{\infty} \frac{\tilde{f}(\alpha y_1) \tilde{f}(\alpha y_2) \tilde{f}(\alpha(y_1 + y_2 - 1)) dy_1 dy_2}{(y_1 - 1)(y_1 + y_2)} \right. \\ &\quad \left. + i\pi \lim_{\lambda \rightarrow 0} \int_{-\infty}^{\infty} dy_2 \left[\frac{\tilde{f}(\alpha) [\tilde{f}(\alpha y_2)]^2}{1 + y_2 - i\lambda} + \frac{[\tilde{f}(\alpha y_2)]^2 \tilde{f}(\alpha)}{-y_2 - 1 - i\lambda} \right] \right], \end{aligned}$$

where P indicates that the integrand excludes infinitesimal regions near $y_1 = -y_2$ and $y_1 = 1$. We may formally integrate the last two terms. If -1 is factored from the second of the two integrals, they combine to become

$$i\pi \lim_{\lambda \rightarrow 0} \int_{-\infty}^{\infty} dy_2 \tilde{f}(\alpha) [\tilde{f}(\alpha y_2)]^2 \left[\frac{1}{1 - y_2 - i\lambda} - \frac{1}{1 + y_2 + i\lambda} \right].$$

It is immediately obvious that if these are partitioned according to the rule

$$\lim_{\epsilon \rightarrow 0} \int_{x_1 - i\epsilon}^{x_1 + i\epsilon} \phi(x) dx = P \int_{x_1 - x_0}^{x_1 + x_0} \phi(x) dx + i\pi \phi(x_0),$$

the principal value contributions exactly cancel, while the $i\pi$ terms are proportional to $e^{-\alpha a}$ and are exponentially small compared to a_2^3 , which decays only like e^{-a} . Terms proportional to exponentials which decay more rapidly than e^{-a} do not contribute to the asymptotic form.

We now proceed to examine the remaining contributions to a_2^3 , where it is again understood that the small regions in the neighborhood of $y_2 = -y_1$ and $y_1 = 1$ are excluded from the integrals. For all regions where $y_1 \leq a/\alpha$, where a is a number greater than unity, $\tilde{f}(\alpha y)$ may be replaced by its asymptotic form $\tilde{f}_a(\alpha y)$. Thus for the entire $y_1 - y_2$ plane, except where $y_1 \sim 0$, $y_2 \sim 0$ (but not both simultaneously) and $y_1 + y_2 \sim 1$, the numerator of the integrand is well represented by its asymptotic form. Furthermore, since at most one of the three Fourier-transform factors departs from its asymptotic form in any given region of space, the area in the $y_1 - y_2$ plane over which one of the \tilde{f} both departs from its asymptotic form and decays no more rapidly than e^{-a} is $O(1/\alpha)$. It is, of course, implicitly assumed that the exact and asymptotic forms of the Fourier transforms remain bounded as their arguments approach zero. For the former, this is equivalent to the requirement, which we have already stated, that β be finite.

Now consider that portion of the $y_1 - y_2$ plane where all factors in the numerator are well approximated by their asymptotic forms. Examine in particular the exponential decay factors

$$e^{-\alpha y_1} e^{-\alpha y_2} e^{-\alpha(y_1 + y_2 - 1)}.$$

The only portion of the plane where the combined effect of the exponential factors leads to an overall decay that is not faster than e^{-a} is the range $0 < y_1 < 1$, $0 < y_2 < 1 - y_1$. The integrand does not change sign in this portion of $y_1 - y_2$ space, which encompasses an area $\sim \frac{1}{2}$ (to be compared with the area of order $1/\alpha$ which was found for the nonasymptotic contribution). Note that there is no portion of the plane in which the integrand decays more slowly than e^{-a} . Thus the nonasymptotic integrand contribution is $O(1/\alpha)$ compared to that of the asymptotic integrand. Similar considerations enable one to deduce that one may also replace the Fourier transforms in the higher-order integrals by their asymptotic forms. We thus conclude that if the time dependences of two coupling functions are such that the asymptotic forms of their Fourier transforms are identical and of the indicated form, the large-detuning transition amplitudes are the same.

As we have indicated, a sufficient condition that two pulses have the same $a_2(\infty)$ for large α is that both asymptotic Fourier transforms be equal to contour integrations given by $(2\pi i)[\text{Res}(x=i)]$. We compare the hyperbolic secant of Rosen and Zener, $f = \frac{1}{2} \text{sech}(\pi x/2)$, with the Lorentzian $f = (1/\pi)(1+x^2)^{-1}$. The corresponding $A(x) = \beta f(x)$ are

$$A_I(x) = \frac{\beta_I}{\pi} (1+x^2)^{-1},$$

$$A_H(x) = \frac{\beta_H}{2} \text{sech} \frac{\pi x}{2}.$$

The transforms for both may be calculated via contour integrations. The Lorentzian case is trivial and applies to all ν , not just large frequencies. We

choose a contour that runs along the real axis from $-R$ to $+R$ and is closed by a semicircle in the upper half plane. The contribution to the contour integral from the arc vanishes as $R \rightarrow \infty$, so that the Fourier transform is identical to the contour integral, whose value is determined by the residue at the simple pole at $x = i$. The result is

$$\tilde{A}_L = \frac{\beta_L}{\sqrt{2\pi}} e^{-\nu} \quad (7a)$$

For the hyperbolic secant we choose a rectangular contour which runs from $-R$ to $+R$ along the real axis, and is continued by rectangular segments parallel to the imaginary axis from the points $(\pm R, 0)$ to the points $(\pm R, 2i)$, and is closed by a line parallel to the real axis which runs from $(R, 2i)$ to $(-R, 2i)$. The two vertical segments give vanishing contributions as $R \rightarrow \infty$, and the horizontal segment off the real axis goes exponentially to zero compared to the segment along the real axis as $\nu \rightarrow \infty$. Thus for the hyperbolic secant, the Fourier transform is identical to that of the Lorentzian in the asymptotic region. For large ν it is given by

$$\tilde{A}_H \approx \frac{2\beta_H}{\sqrt{2\pi}} e^{-\nu} \quad (7b)$$

Since the Rosen-Zener solution gives the transition amplitude for all detunings, according to Eq. (4), as (recall that $\tilde{A} = \beta \tilde{f} = S \tilde{f}$)

$$-i\sqrt{2\pi} \tilde{f}_H(\alpha) \sin \beta_H,$$

this formula must be valid asymptotically also. As we have shown that the asymptotic Fourier transforms of the Lorentzian and hyperbolic secant are proportional for large detunings, the Lorentzian must induce a transition amplitude that obeys a formula similar to Eq. (4). From Eqs. (7), we see that to construct the Lorentzian and hyperbolic secant Fourier transforms so that they are asymptotically identical, it is necessary to choose the Lorentzian pulse area β_L to be twice that of β_H . Since $\tilde{f}_H = 2\tilde{f}_L$ and $\beta_H = \beta_L/2$, the asymptotic transition amplitude for the Lorentzian pulse may be obtained from the known result for the hyperbolic secant pulse as

$$a_{2L} = -i\sqrt{2\pi} 2\tilde{f}_L(\alpha) \sin \frac{\beta_L}{2} \quad (8a)$$

This result has been independently obtained by carrying out an asymptotic solution of Eqs. (3).¹² One can also show that for the pulse

$$A_c = \beta_c x \operatorname{cosech} \pi x,$$

the appropriate scaling law is

$$a_{2c} = -i\sqrt{2\pi} \tilde{f}_c(\alpha) \sin 2\beta_c \quad (8b)$$

For the hyperbolic secant pulse, the transition amplitude vanishes for pulse areas $\beta_H = n\pi$, n integral, for all detunings. The zeros of a_{2L} , on the other hand, occur for $\beta_L = n\pi$ for zero detuning, while those for large detuning are $\beta_L = 2n\pi$. Those of a_{2c} go from $n\pi$ at $\alpha = 0$ to $n\pi/2$ as $\alpha \rightarrow \infty$.

The existence of a pole at $x = i$ is a sufficient, but not a necessary, condition that the asymptotic Fourier transform of a coupling pulse vary as $p(\omega)e^{-\omega}$. For example, the function $(1+x^2)^{-3/2}$ has an asymptotic Fourier transform proportional to $\nu^{1/2}e^{-\nu}$. The factor $\nu^{1/2}$ precludes deducing the asymptotic transition amplitude from the Rosen-Zener formula. Similarly, the squares of the hyperbolic secant and of the Lorentzian each have poles of second order at $x = i$ with the consequence that, for both of these, $\tilde{A}_a \sim \nu^2 e^{-\nu}$, so that while these will have asymptotic transition amplitudes that are related to each other, they cannot be obtained by scaling from Eq. (4). In a future paper, we shall show how to calculate asymptotic transition amplitudes when the coupling pulse has second- and higher-order poles at $x = i$. For now, we merely present the formulas for the transition amplitudes generated by the squares of the hyperbolic secant and Lorentzian

$$a_2(H^2) = -i \frac{2\pi}{C^2} e^{-\alpha} \sin \left[C \left| \frac{\alpha\beta}{\pi} \right|^{1/2} \right] \times \sinh \left[C \left| \frac{\alpha\beta}{\pi} \right|^{1/2} \right], \quad (9a)$$

$$a_2(L^2) = -i \frac{2\pi}{C^2} e^{-\alpha} \sin \left[C \left| \frac{\alpha\beta}{2\pi} \right|^{1/2} \right] \times \sinh \left[C \left| \frac{\alpha\beta}{2\pi} \right|^{1/2} \right], \quad (9b)$$

where $C = 1 + \frac{1}{8} + \frac{1}{56} + \frac{1}{182} + \dots \approx 1.198$. Equation (9a) can be obtained from Eq. (9b) by scaling techniques derived in this paper. Equation (9a) is valid only for $|\beta| < |\alpha|$, and Eq. (9b) for $|\beta| < 2\alpha$.

III. SUMMARY AND CONCLUSION

In this paper, we have demonstrated that pulse shapes $A(t)$ whose Fourier transforms asymptotically approach the form $\phi(\nu)e^{-\nu}$, where ϕ is slowly varying, may be categorized into families which differ according to the function ϕ . Within each family, the transition amplitudes $a_2(x)$ are related by simple scaling laws, so that if one is able to derive an expression for the transition amplitude generated by one member of the family, corresponding formulas for all other members of the family

may be written down by inspection.

A sufficient condition that the Fourier transform be of the required form is that it be obtainable in the asymptotic region as a contour integral evaluated from the residue at a single pole on the imaginary time axis. For the case where $A(t)$ has simple poles, $a_2(\infty)$ may be inferred from the solution of the Rosen-Zener problem,^{2,3} known for 50 years, by a trivial scaling operation.

Our results were obtained by examining the structure of the terms in perturbation expansions for transition amplitudes. (We have demonstrated that these sequences always converge in two-level problems provided that the pulse areas are finite. Low-order approximations, however, are frequently not useful for $t \rightarrow \infty$ even when they are valid at finite

times.) With suitable choices of ratios of pulse areas, corresponding terms in the series for different members of the same family will be identical.

In a future paper,¹² we shall present methods for explicitly calculating transition amplitudes that apply to higher-order, as well as simple poles. Thus we are not restricted in practice to writing scaling laws for pulses which may be compared in the asymptotic region to the hyperbolic secant.

ACKNOWLEDGMENTS

The authors are indebted to Dr. A. Bambini for interesting discussions of this and related problems. This work was supported by the Office of Naval Research.

APPENDIX: CONVERGENCE OF PERTURBATION THEORY FOR THE TRANSITION AMPLITUDE

We demonstrate here that the perturbation series for a_2 converges for all finite pulse areas. The contribution of order $(2k+1)$ is

$$b_1^{(k)} = i\beta^{2k+1} a_2^{(2k+1)} \\ = -i\beta^{2k+1} (-1)^k \int_{-\infty}^{\infty} f(x_1) e^{-i\alpha x_1} dx_1 \prod_{j=2}^{2k+1} \int_{-\infty}^{x_{j-1}} f(x_j) e^{(-1)^{j-1} i\alpha x_j} dx_j. \quad (A1)$$

Now assume that $A(x)$ is of a single algebraic sign. Without loss of generality we may take this to be positive. We compare the series with the corresponding expansion for $\alpha=0$,

$$b_{10}^{(k)} = -i\beta^{2k+1} (-1)^k \int_{-\infty}^{\infty} f(x_1) dx_1 \prod_{j=2}^{2k+1} \int_{-\infty}^{x_{j-1}} f(x_j) dx_j \quad (A2)$$

$$= -i\beta^{2k+1} (-1)^k \int_{-\infty}^{\infty} f(x_1) dx_1 \prod_{j=2}^{2k+1} \int_{-\infty}^{x_{j-1}} f(x_j) dx_j. \quad (A2')$$

Invoking the theorems on repeated integrals of the same function

$$b_{10}^{(k)} = \frac{-i\beta^{2k+1}}{(2k+1)!} (-1)^k \left| \int_{-\infty}^{\infty} f(x) dx \right|^{2k+1},$$

and the terms are recognized as identical to those for the series $-i \sin \beta$. Now consider the series

$$F(\beta) = \sum_{k=0}^{\infty} b_{10}^{(k)} = \sum_{k=0}^{\infty} \frac{\beta^{2k+1}}{(2k+1)!} \left| \int_{-\infty}^{\infty} f(x) dx \right|^{2k+1} = \sum_{k=0}^{\infty} \frac{\beta^{2k+1}}{(2k+1)!}.$$

This is evidently the series for $\sinh \beta$, which converges as long as β is finite. Hence, the series of Eq. (A2) is absolutely convergent. Now

$$b_1^{(k)} = \beta^{2k+1} \int_{-\infty}^{\infty} f(x_1) e^{-i\alpha x_1} dx_1 \prod_{j=2}^{2k+1} \int_{-\infty}^{x_{j-1}} f(x_j) e^{(-1)^{j-1} i\alpha x_j} dx_j \\ \leq \beta^{2k+1} \int_{-\infty}^{\infty} |f(x_1)| dx_1 \prod_{j=2}^{2k+1} \int_{-\infty}^{x_{j-1}} |f(x_j)| dx_j \\ < b_{10}^{(k)},$$

so that the series, Eq. (A1) is also absolutely convergent, and our result is established.

We note that the same arguments will apply to perturbation series at finite times, provided merely

that $\int_{-\infty}^{\infty} f(x') dx' = \beta(x)$ is of one sign and finite. If $f(x)$ changes sign, the results will still be valid provided the generalized area $\int_{-\infty}^{\infty} |f(x')| dx'$ is finite.

A simple case where the convergence theorem does not apply is the coupling function

$$A(x) = (\text{const})(\tanh \pi x / 2) / x,$$

since β is logarithmically divergent. In addition, since the pulse area is proportional to the Fourier transform at zero frequency, the multiple integrals in the frequency domain for the third- and higher-order contributions to the perturbation series contain regions where the integrands blow up, so that the in-

dividual terms beyond first order may not even exist. (The first-order contribution will be finite, since the Fourier transform for this pulse exists for $\nu \neq 0$. In this case, we note that the infinite area does *not* imply a pulse of infinite energy, so that it theoretically could exist. One evidently cannot use the methods developed here to describe the dynamics. At the very least, decay would have to be included in the analysis, and a completely nonperturbative treatment utilized.)

¹L. Allen and J. H. Eberly, *Optical Resonance and Two-Level Atoms* (Wiley, New York, 1975). This work includes an extensive bibliography for the two-level problem.

²N. Rosen and C. Zener, Phys. Rev. **40**, 502 (1932).

³R. T. Robiscoe, Phys. Rev. A **17**, 247 (1978).

⁴R. T. Robiscoe, Phys. Rev. A **25**, 1178 (1982).

⁵A. Bambini and P. P. Berman, Phys. Rev. A **23**, 2496 (1981).

⁶E. J. Robinson, Phys. Rev. A **24**, 2239 (1981).

⁷A. E. Kaplan, Zh. Eksp. Teor. Fiz. **68**, 823 (1975) [Sov. Phys.—JETP **41**, 409 (1976)].

⁸M. G. Payne and M. H. Nayfeh, Phys. Rev. A **13**, 595 (1976).

⁹D. S. F. Crothers and J. G. Hughes, J. Phys. B **10**, L557 (1977).

¹⁰D. S. F. Crothers, J. Phys. B **11**, 1025 (1978).

¹¹E. J. Robinson, J. Phys. B **13**, 2243 (1980).

¹²P. R. Berman and E. J. Robinson (unpublished).

Photon-Catalyzed Bound-Continuum Processes: Post-Saturation Fluorescence
Quenching and Huge Enhancement of Fragments in I_2

Albert M. F. Lau

Department of Physics, New York University

4 Washington Place, New York, N.Y. 10003

S. N. Dixit

Exxon Research and Engineering Company

P. O. Box 45, Linden, N.J. 07036

and

Joel Tellinghuisen

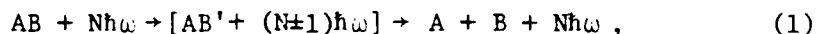
Department of Chemistry, Vanderbilt University

Nashville, TN 37235

Abstract

With accurate experimental values of energies, transition moments and decay rates as input, our calculated results show that photon-catalyzed bound-continuum processes can be observed for the first time using I_2 in a cell or a molecular-beam experiment at laser intensities as low as 10^7 W/cm^2 and 10^5 W/cm^2 , respectively. Two new features, post-saturation quenching of fluorescence and huge (>150 -fold) enhancement of fragments, are shown for the first time.

Interest in laser-induced multiphoton bound-continuum processes (e.g. ionization, autoionization, dissociation and predissociation) in gases¹ and ^{the} condensed phases² continues to grow. In view of the ~~recent~~ high nonlinearity (direct 33-photon ionization) ^{recently} observed in multiphoton bound-continuum processes with net absorption,¹ it is surprising that there is so far no experimental demonstration of the lowest-order (two-photon) process in another kind of multiphoton bound-continuum transitions,



which conserves the total number N of photons in a given mode of the electromagnetic field. In reaction (1), A and B refer to neutral or charged fragments, and the square brackets denote an intermediate state. An example is given in Figure 1. Since the rate in the reaction (1) is enhanced by the photons without their being consumed in the transition (while there are usually some losses or gains due to other unavoidable processes present in an experiment), this multiphoton process has been called the photon-as-catalyst effect (PCE).³ It can be viewed in general as a bound-continuum state mixing due to the external coherent radiation and as a nonstoichiometric use of laser photons.⁴⁻⁸ When a resonant intermediate discrete level in absorptive multiphoton processes (AMP) is imbedded in a vibrational^{4,6} or ionization^{5,7,8} continuum, PCE may occur simultaneously (and sometimes unsuspectedly) with the AMP.

The considerable amount of recent theoretical works³⁻⁸ have heightened the interest for an observation of the PCE. To facilitate this goal, we propose here two such experiments and show their feasibility with detailed analyses on the bound-continuum process: photon-catalyzed predissociation of I_2 in selectively excited $BO_u^+ vJ$

states, as explained in Fig. 1. The unpopulated high-lying $XO_g^+v'J'$ states are chosen as intermediate states.⁴ Our calculation shows for the first time that the PCE could cause a new characteristic post-saturation quenching in the $BvJ \rightarrow Xv_1J_1$ fluorescence (a phenomenon new to AMP as well) and a huge (>150-fold) enhancement of the atomic iodine fragments. Our results indicate that the PCE induced by 1- μ s laser pulses could be observed in a cell experiment monitoring the fluorescence with laser intensity $I \approx 10^7$ W/cm² or ⁱⁿ a molecular-beam experiment monitoring the fragments at $I \approx 10^5$ W/cm². This range is many orders of magnitude lower than the requirements ($\approx 10^{11}$ - 10^{12} W/cm²) calculated for other systems.^{7,8} In this note we describe these key findings.

Our calculation is based on the published analytic results (Eqs. (2.28) and (2.30) of Ref. 5) of a theory of resonant photon-catalyzed bound-continuum transitions (via a bound intermediate state as illustrated in Fig. 1) regardless whether the continuum is vibrational or electronic and whether the system is in the gaseous or the condensed phases. The main approximation is that the laser is a square pulse of constant intensity I and duration τ . According to Section III of Ref. 5, some favorable conditions for observing the PCE are (1) resonant intermediate states; (2) large transition moments; (3) long-lived bound states (and long laser pulse) for long interaction time; and (4) small competing spontaneous bound-free transition ^{rates} I_2 . Indeed I_2 possesses these advantages: (1) the X-B transition frequencies⁹ being in the tunable range of narrow-band dye lasers; (2) favorable electronic transition moments and Franck-Condon factors and densities¹⁰; (3) long lifetimes ($\sim 1\mu$ s) of BvJ and $Xv'J'$ states^{11,12}; and (4) weak natural predissociation ($\leq 10^6$ s⁻¹).¹¹ These explain the low

intensity requirement and huge fragment enhancement in our results. In contrast, the other calculated systems suffer the disadvantages of shorter-lived states, large competing spontaneous autoionization rate and far from resonance⁸ or small transition moments.⁷

Our first set of results is applicable to an I_2 cell experiment in which a resolved $BvJ \rightarrow Xv_1J_1$ fluorescence line is monitored. The BvJ level can be selectively populated from the ground state by a dye-laser pump pulse.¹¹ A second time-delayed dye-laser pulse (the PCE laser) is incident on the excited I_2 , and the monitored fluorescence line is integrated over the PCE-pulse duration τ . The parameters of the level system defined in Fig. 1 (chosen to match the optimum power output of laser dyes and for their favorable Franck-Condon densities) are: $Xv_0J_0 = X, 0, 38$; $\omega_p = 17,688.936 \text{ cm}^{-1}$; $BvJ = B, 18, 37$; $\omega_f = 17,475.806 \text{ cm}^{-1}$; $Xv_1J_1 = X, 1, 38$; $Xv'J' = X, 7, 36$ and the $BvJ-Xv'J'$ frequency $\omega_0 = 16,228.577 \text{ cm}^{-1}$. A first step in the experiment is to tune the PCE-laser frequency ω into resonance with ω_0 . Our calculated results on the integrated fluorescence signal (IFS) versus ω show a (power-broadened) dip at ω_0 . With ω locked at ω_0 , the next step is to increase the PCE-laser intensity I and record the IFS versus I . Our calculated values for the I_2 vapor pressure 0.36 Torr (at 300°K) are plotted in Fig. 2. Considering first the resonance curves (labelled by 0) for 10-ns pulses and starting from the low intensity region, we note the decrease in the IFS due to laser-stimulated $B \rightarrow X$ transfer of population, and then the coherent saturation of the $B - X$ transition, a known phenomenon.¹³ For 1- μs pulses, the resonance IFS has already reached saturation at $I = 10^2 \text{ W/cm}^2$. Then at still higher intensity, if the PCE were to remain negligible, the IFS would stay constant (the

flat dotted curves in Fig. 2). In fact, however, our calculations (the solid lines) reveal a new feature: a laser-intensity-dependent decrease beyond the saturation region. This is due to the fact that the laser-stimulated bound-free absorption in the second (and bottle-neck) stage of the PCE (hence the whole process itself) dominates over all the other loss mechanisms of the bound-state population. The resulting inflection region between the two quenching regimes would be a readily recognizable feature in an experiment. This inflection persists for detunings up to about 0.03 cm^{-1} , but disappears for $\Delta \geq 0.3 \text{ cm}^{-1}$. In the latter case, the mark of PCE is quenching the fluorescence to vanishing values at higher intensity without ever reaching saturation, as shown in Fig. 2. From the $\Delta = 0$ curves, we see that the PCE could be identified at $I \approx 10^8 \text{ W/cm}^2$ for 10-ns pulses and at $I \approx 10^7 \text{ W/cm}^2$ for 1- μs pulses.

If the sharp resonance dips at characteristic frequencies ω_0 and the quenching beyond saturation were observed in an experiment, we think they would constitute sufficiently strong evidence for the PCE. The dependence on ω_0 means that the level $Xv'J'$ must play a critical role. Then from energetic and symmetry considerations, the only possibility of a laser-stimulated decay from the $Xv'J'$ level, and out of the coherently superposed B-X states, is a transition to the $1u$ or A dissociative states. The dependence on the $Xv'J'$ levels would also eliminate the possibility of the observed behavior being caused by (a) single-photon dissociation, nonresonant Raman or Raleigh scattering, all from the BvJ level; or (b) resonant Raman or Raleigh scattering, or resonant multiphoton dissociation or ionization via some discrete levels higher than BvJ , since no higher levels possess the identical spectrum as the B-X transitions.

Our second set of results is applicable to a crossed laser-molecular-beam experiment with the apparatus similar to those in double absorption photofragment spectroscopy, capable of mass, translational-energy and angular-distribution resolution.¹⁴ The molecular beam, the nearly coaxial pump- and PCE-laser beams, and the quadrupole mass spectrometer are oriented along the x, y, z axes respectively (see inset in Fig. 3). The atomic-iodine fragments (as the signal) are collected during the PCE-laser pulse and afterwards. To eliminate the background noise arising from $Xv_0J_0 \rightarrow (1u,A)$ photodissociation fragments due to the weaker pump pulse, its linear polarization \hat{e}' should be oriented along the detection z-axis (under the axial-recoil approximation,¹⁴ fragment angular distribution $\propto \sin^2\theta$, with θ measured from \hat{e}'). For the same purpose, the frequency ω of the time-delayed PCE-laser pulse is chosen to be smaller than the dissociation energy D_0 ($12,440 \text{ cm}^{-1}$) of the ground level. To maximize the PCE-fragment signal the linear polarization \hat{e} of the PCE-laser should be oriented at 45° from the z-axis, since the PCE-fragment angular distribution is given by $\cos^2\phi \sin^2\phi$, with ϕ being measured from \hat{e} .

The level system (see Fig. 1) for the fragment calculation is given by: $Xv_0J_0 = X, 0, 54$; $\omega_p = 17,280.974 \text{ cm}^{-1}$; $BvJ = B, 14, 53$; $\omega_f = 16,856.283 \text{ cm}^{-1}$; $Xv_1J_1 = X, 2, 54$; $\omega_0 = 12,168.112 \text{ cm}^{-1}$ and $Xv'J' = X, 26, 54$. The BvJ level is chosen for its small predissociation rate¹¹ and the $Xv'J'$ level for $\omega < D_0$. The calculated total fragments collected (S) with the PCE-laser on, showed a resonance peak at $\omega = \omega_0$. Observation of such peak would ensure the critical role of the $Xv'J'$ level and eliminate the possibility of other processes, as discussed under the fluorescence results. Figure 3 gives our results for the fragment enhancement ratio, $R = S \text{ (with PCE-laser on)}/S \text{ (without PCE-laser)}$. At

resonance, R reaches the value 2 at I as low as 10^5 W/cm^2 and the maximum value 152 at $I \sim 10^7 \text{ W/cm}^2$. At low intensity where the PCE is negligible, notice that R can be (slightly) less than 1 owing to laser-stimulated B-X population flopping. Observation of the resonance peak and of the intensity-dependent enhancement in I-atom fragments at the expected mass, translational energy, and angular distribution would constitute direct proof of the PCE.

Based on our earlier preliminary results on the fluorescence system, an experiment to observe the PCE was attempted by Brechignac, Cahuzac and Vetter,¹⁵ using a narrow-band (30 MHz), single-mode, YAG-pumped dye laser ($\tau \sim 10\text{ns}$). Only the fluorescence line (and not the fragments) was monitored in their cell experiment. The predicted resonance dip was observed. In the intensity study, they reported an IFS decrease of 40% at $2 \times 10^8 \text{ W/cm}^2$, of 20% and 10% at lower (but unmeasured) intensities, and no decrease below $2 \times 10^7 \text{ W/cm}^2$. We find that all their results can be accounted for by the $\Delta = 0.3 \text{ cm}^{-1}$ solid curve in Fig. 2. A detuning of 0.3 cm^{-1} might be due to a reported frequency-drift problem in their dye laser. If so, their data point with the highest intensity ($2 \times 10^8 \text{ W/cm}^2$) has just reached the region where the case with PCE begins to differ from the case with only stimulated emission (see Fig. 2). As such, their results probably could not be considered as clear evidence nor as a disproof of the existence of the PCE in I_2 (BvJ).

The study of Brechignac et al. prompted us to check the effects of spatial and spectral averagings of the pulses and of optical Stark shifts. Of these, only spectral averaging (over a Gaussian line profile of FWHM 0.03 cm^{-1} resulting from overlapping Doppler-broadened hyperfine lines of the B-X transitions¹⁶) changes significantly the approach to saturation for the $\Delta = 0$ curve, while leaving its

PCE-dominant region and the entire curves for $\Delta = 0.03$ and 0.3 cm^{-1} essentially the same as the unaveraged curves (see Fig. 2). Also, our calculations can reproduce quite satisfactorily the shapes of the three experimental saturation curves (each with 5 data points) in the ion-dip spectroscopy of I_2 .¹³ From these checks, we believe our present results are reliable. We hope these results would stimulate and aid experimental efforts to observe this effect. We also hope that this work would stimulate studies of PCE in other areas of physics and chemistry, since theories^{3,5} (without restricting the nature of the bound and the continuum states) indicate that the PCE is also applicable to other bound-continuum transitions: those involving electronic motion^{7,8} and those occurring in liquids and solids.^{2,17}

We wish to thank J. L. Picqué, J. Vigue, G. Mainfray, J. Wessel, S. Yang, J. Bernholc and the authors of Refs. 9(b)-(d), 12 and 15 for helpful discussions. This work is supported in part by the U. S. Office of Naval Research.

References

1. A. L 'Huillier, L. A. Lompre, G. Mainfray and C. Manus, Phys. Rev. Lett. 48, 1814 (1982).
2. C. L. Braun, T. W. Scott and A. C. Albrecht, Chem. Phys. Lett. 90, 81 (1982) and references therein.
3. For a review, see A.M.F. Lau in Dynamics of the Excited State (Adv. Chem. Phys., Vol. 50) edited by K. P. Lawley (Wiley, New York, 1982), pp. 191-253.
4. A. M. F. Lau, Phys. Rev. A22, 614 (1980).
5. A. M. F. Lau, Phys. Rev. A25, 363 (1982).
6. A. Lami and N. K. Rahman, Phys. Rev. A26, 3360 (1982).
7. S. N. Dixit and A. M. F. Lau, Bull. Am. Phys. Soc. 27, 882 (1982).
8. Y. S. Kim and P. Lambropoulos, Phys. Rev. Lett. 49, 1698 (1982); K. R. Dastidar and P. Lambropoulos, Chem. Phys. Lett 93, 273 (1982). Their "laser-intensity effect" is called the PCE here.
9. (a) J. Tellinghuisen, M. R. McKeever and A. Sur, J. Mol. Spectr. 82, 225 (1980), (b) P. Luc, J. Mol. Spectr. 80, 41 (1980). (c) S. Gerstenkorn and (d) R. Bacis, private communications.
10. J. B. Koffend, R. Bacis and R. W. Field, J. Chem. Phys. 70, 2366 (1979). J. Tellinghuisen, J. Chem. Phys. 76, 4736 (1982).
11. M. Broyer, J. Vigue and J. C. Lehmann, J. Chem. Phys. 63, 5428 (1975); J. Vigue et al., J. Phys. (Paris) 42, 937 (1981).
12. R. W. Field, private communications.
13. D. E. Cooper, C. M. Klimcak and J. E. Wessel, Phys. Rev. Lett. 46, 324 (1981).
14. R. K. Sanders and K. R. Wilson, J. Chem. Phys. 63, 4242 (1975).
15. C. Brechignac, P. Cahuzac and R. Vetter, private communications.
16. M. Kroll and K. K. Innes, J. Mol. Spectr. 36, 295 (1970).
17. J. M. Baranowski, J. M. Noras and J. W. Allen, J. Phys. C7, 4529 (1974) and references therein.

Figure Captions

Fig. 1. The photon-as-catalyst effect (the solid-line arrows) on I_2 in a BvJ level consists of the stimulated emission to an unpopulated intermediate level $Xv'J'$ and the absorption to the vibrational continua of lu and A states. ω , ω_p and ω_f are the PCE-laser, pump-laser and fluorescence frequencies, respectively.

Fig. 2. Integrated fluorescence signal versus laser intensity for 10-ns (unlabeled) and 1- μ s pulses, plotted relative to the natural fluorescence amount (normalized to the same dashed curve for both 10-ns and 1- μ s cases). Each pair consisting of a solid curve (case with PCE) and of a dotted curve (case with i-r bound-bound transition but without r-f bound-free transition) is labeled by the detuning in cm^{-1} . The pair labeled by $\bar{0}$ is for zero detuning with spectral averaging.

Fig. 3. Enhancement ratio of fragments versus laser intensity for 1- μ s pulses. Each curve is labeled by the detuning in cm^{-1} .

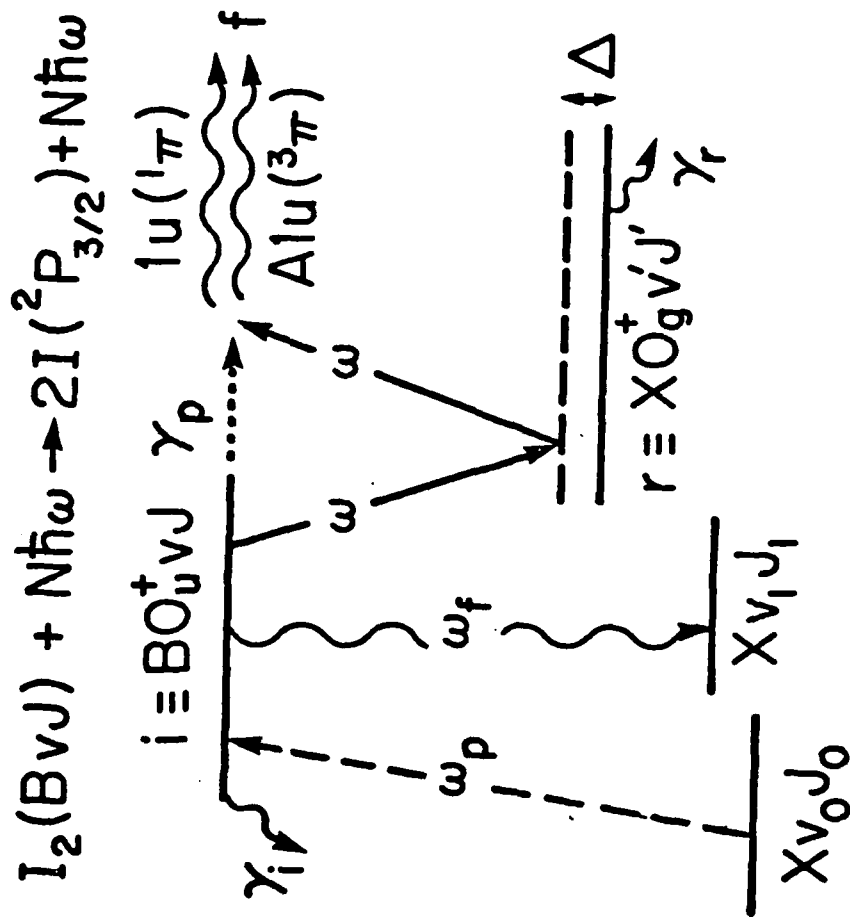


Fig. 1

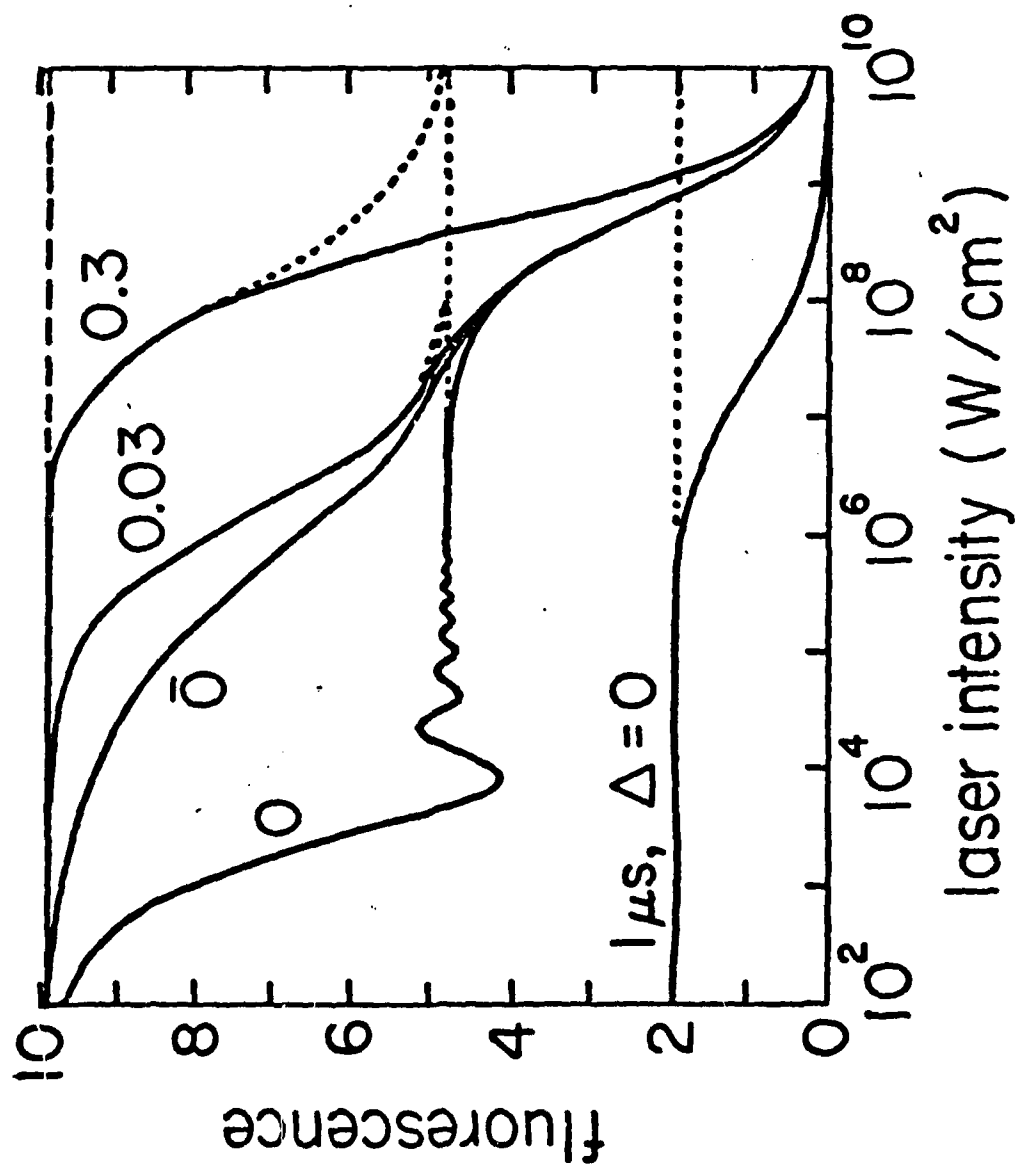


FIG. 2

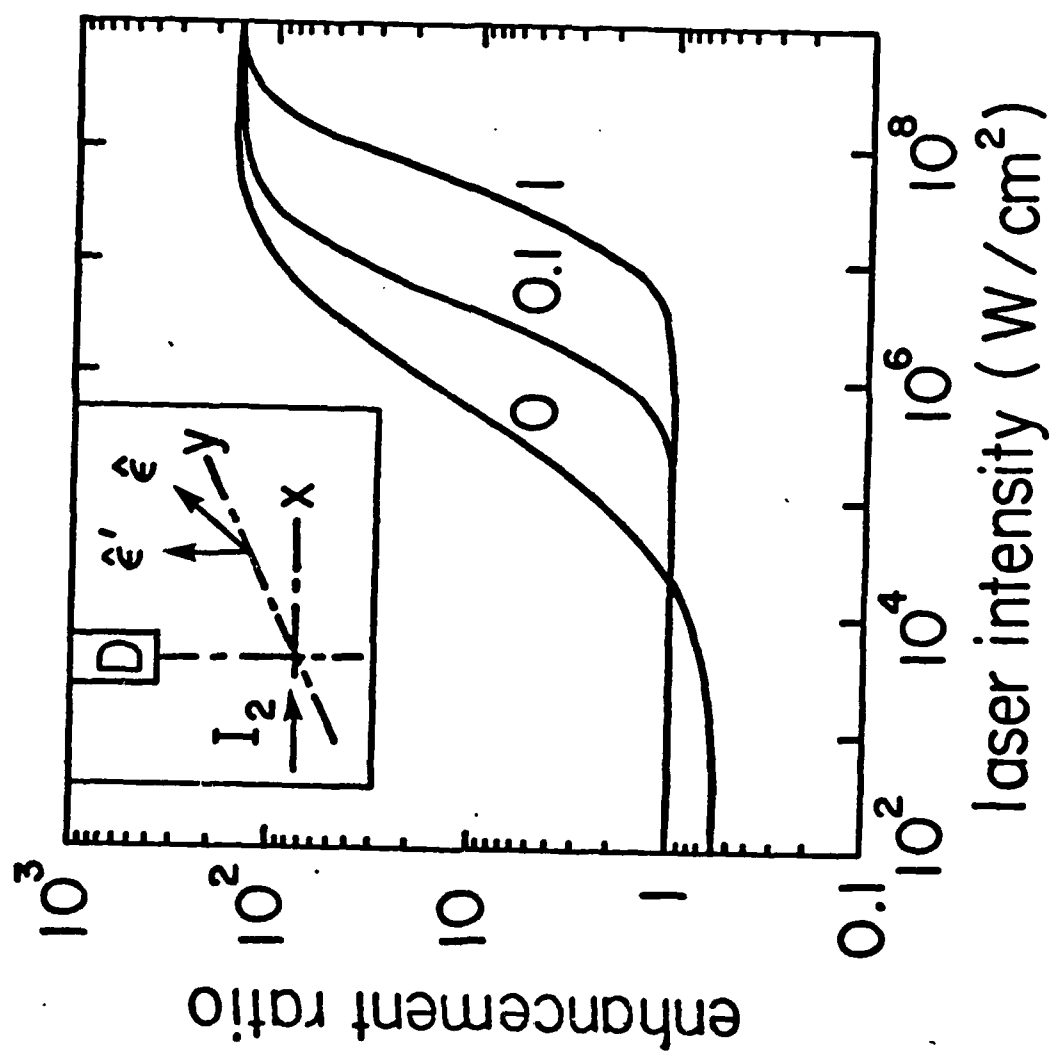


FIG. 3.

THE EIGENVALUE PROBLEM FOR TWO LEVEL SYSTEMS

E.J. Robinson

New York University
Physics Department
4 Washington Place
New York, N.Y. 10003 USA

INTRODUCTION

The study of two-level atoms coupled by external fields is more than 50 years old, but continues to be of interest.¹⁻¹⁰ Our purpose here is to deepen the A^2 eigenvalue method, an approach to this problem introduced recently.⁹

Except for a few potentials, closed-form solutions are not known.^{2,4} Recently, Bambini and Berman⁶ (B and B) found a class of coupling functions for which the two-state equations of motion could be solved analytically. The set includes the hyperbolic secant of Rosen and Zener as a special case.² Apart from this, all members of the set are temporally asymmetric. For these, B and B showed that there are no coupling strengths where the transition probability vanishes, except on resonance.⁸ This differs from the hyperbolic secant, where $P = 0$ for any pulse area A equal to an integral multiple of π , regardless of Δ .² It is also known that other temporally symmetric pulses have pulse areas for $P = 0$ off resonance.

This suggests that it may be true in general that symmetric (asymmetric) pulses possess (lack) nodes in $P(A)$. The author studied this point by regarding the equations of motion as an eigenvalue (EV) problem for A^2 .⁹ By determining when these EV were real or complex, he was able to generalize the B and B result, finding that symmetric pulses always have nodes, but asymmetric pulses do not, except under over-determined conditions.⁹

In the present paper, we direct our attention to actually determining EV and indicating how one may perform accurate approximate calculations of them. We shall present examples where this knowledge provides partial understanding of spectra. In addition, we shall demonstrate how to express transition amplitudes in terms of the EV and eigenfunctions and, in turn, will exhibit an approximation method for P.

THE EIGENVALUE PROBLEM AND ITS VARIATIONAL APPROXIMATION

The time-dependent Schrödinger equation for amplitudes a_1 and a_2 is, in RWA with detuning Δ ,

$$i \dot{a}_1 = V(t) e^{i\Delta t} a_2, \quad (1a)$$

$$i \dot{a}_2 = V(t) e^{-i\Delta t} a_1, \quad (1b)$$

for real potentials. Equivalently

$$\ddot{a}_1 - \left(\frac{\dot{V}}{V} + i\Delta\right) \dot{a}_1 + V^2 a_1 = 0, \quad (2a)$$

$$\ddot{a}_2 - \left(\frac{\dot{V}}{V} - i\Delta\right) \dot{a}_2 + V^2 a_2 = 0. \quad (2b)$$

Consider now envelope functions of a single algebraic sign, and define $z = \int_{-\infty}^t f(t') dt' - \frac{1}{2}$, where $f(t) = V(t)/\Lambda$, with $\Lambda = \int_{-\infty}^{\infty} V(t) dt$. Then

$$a_1'' - \frac{i\Delta}{f} a_1' + \Lambda^2 a_1 = 0, \quad (3a)$$

$$a_2'' + \frac{j\Delta}{f} a_2' + \Lambda^2 a_2 = 0. \quad (3b)$$

Writing

$$a_1 = b_1 e^{\frac{i\Delta t}{2}}, \quad a_2 = b_2 e^{\frac{-i\Delta t}{2}},$$

$$-b_1'' - \left(\frac{\Delta^2}{4f^2} - \frac{i\Delta f'}{2f^2}\right) b_1 = \Lambda^2 b_1, \quad (4a)$$

$$-b_2'' - \left(\frac{\Delta^2}{4f^2} + \frac{i\Delta f'}{2f^2}\right) b_2 = \Lambda^2 b_2. \quad (4b)$$

Eq. (3a) is subject to the initial conditions $a_2(-\frac{1}{2}) = 0$, $a_2'(-\frac{1}{2}) = -i\Lambda e^{\phi}$, ϕ real but arbitrary. For certain Λ^2 , (the EV Λ_n^2) $a_2(\frac{1}{2})$ also vanishes. We have previously shown that Λ_n^2 is real if $f(t)$ is temporally symmetric, while it is ordinarily complex for asymmetric potentials and $\Delta \neq 0$.⁹ The eigenfunctions corresponding to Λ_n^2 are a_{2n} and b_{2n} in the two representations.

We shall restrict the remainder of the discussion to potentials that are symmetric in the time (and in z).

Eq. (4b) resembles a one-dimensional, time-independent Schrödinger equation for a particle in a complex "potential." Because of the non-Hermiticity of the "Hamiltonian", a generalized form of the usual eigenfunction expansion is appropriate.¹¹ In particular, the correct normalization integral is $\int_{-\frac{1}{2}}^{\frac{1}{2}} b_n^2 dz$, not $\int_{-\frac{1}{2}}^{\frac{1}{2}} |b_n|^2 dz$, and matrix elements of operator O are given by $O_{mn} = \int_{-\frac{1}{2}}^{\frac{1}{2}} b_m^* O b_n dz$. Then A_n^2 is given by (b_n normalized to 1)

$$A_n^2 = - \int_{-\frac{1}{2}}^{\frac{1}{2}} b_n'' b_n dz - \int_{-\frac{1}{2}}^{\frac{1}{2}} b_n^2 \left(\frac{\Delta^2}{4f^2} + \frac{i\Delta f'}{2f^2} \right) dz. \quad (5)$$

If b_n is exact, Eq. (5) gives A_n^2 without error. One may also interpret it as a variational principal for A_n^2 , with b_n now a trial function, which, if arbitrarily flexible, generates an Euler-Lagrange equation that is Eq. (4b). If b_n is a function of a finite number of parameters, Eq. (5) provides a variational approximation for the eigenvalues of Eq. (4b).

APPLICATION OF THE EIGENVALUE METHOD

In this section, we shall demonstrate how the eigenvalue method can predict qualitative features of two-level spectra. We address the question of the validity of the Rosen-Zener conjecture² for Δ small. For the hyperbolic secant

$$P = 2\pi |\tilde{V}(\Delta)|^2 \sin^2 \Delta/\Delta^2, \quad (6)$$

where \tilde{V} is the Fourier transform of $V(t) = \Lambda f(t)$.² Rosen and Zener² surmised that Eq. (6) might be true for all smooth $V(t)$, replacing only the Fourier transform of the hyperbolic secant with that of V . Since the result holds for $\Delta = 0$, one might expect a region of approximate validity for symmetric pulses at small detunings. It can be established that this is indeed the case, in the sense that corrections are $O(\Delta^2)$ if \tilde{V} is differentiable at $\Delta = 0$. For the Lorentzian, \tilde{V} is not differentiable at $\Delta = 0$. By calculating an eigenvalue for that potential, the R-Z conjecture will be shown to be invalid for small Δ in that case.

On resonance, the first node in the transition amplitude occurs, for any pulse shape, at $\Delta = \pi$. For the purpose at hand, it is sufficient to demonstrate that, for small Δ , there is a linear correction in this first eigenvalue for the Lorentzian. Off-resonance, we choose a trial eigenfunction which reduces to the known resonant b_n as $\Delta \rightarrow 0$. This is

$$b_T = N e^{-\frac{1}{2}\Delta t} \frac{1}{\sqrt{1+t^2}} \frac{1}{\sqrt{1+\alpha^2 t^2}}$$

where N is a normalizing factor, and pass to the limit $\alpha \rightarrow 0$. This leads to

$$\Lambda_1^2 = \pi^2 \frac{1+3|\Delta|}{1+|\Delta|},$$

a correction to R-Z linear in Δ . A leading correction to the eigenvalue that is linear in Δ cannot be the signature of a leading quadratic correction to the transition amplitude. This crude trial function gives a result that is an excellent approximation to the true eigenvalue for $\Delta = 0.1$.

AN EIGENFUNCTION EXPANSION FOR TRANSITION AMPLITUDES

Since the b_n are complete, one may use them as a basis for expressing unknown functions. In particular, if b_2 is the solution to Eq. (4) for $\Lambda^2 \neq \Lambda_n^2$, we may expand b_2 in terms of the b_n for $-\frac{1}{2} \leq z < \frac{1}{2}$. Then $b_2(\frac{1}{2})$ may be deduced from the expansion by standard procedures.

Thus

$$b_2(z) = \sum \alpha_n b_n(z) = \sum b_n(z) \int_{-\frac{1}{2}}^{\frac{1}{2}} b_n(z') b_2(z') dz' . \quad (7)$$

Equations for b_n , b_2 are

$$-b_2'' - \left[\frac{1}{2} \frac{\Delta f'}{f^2} + \frac{\Lambda^2}{4f^2} \right] b_2 = \Lambda^2 b_2 , \quad (8a)$$

$$-b_n'' - \left[\frac{1}{2} \frac{\Delta f'}{f^2} + \frac{\Lambda_n^2}{4f^2} \right] b_n = \Lambda_n^2 b_n . \quad (8b)$$

Multiply Eq. (8a) by b_n , Eq. (8b) by b_2 , subtract and integrate over all allowed z . This yields, using Green's theorem,

$$[-(b_2' b_n - b_2 b_n')]_{-\frac{1}{2}}^{\frac{1}{2}} = (\Lambda^2 - \Lambda_n^2) \int_{-\frac{1}{2}}^{\frac{1}{2}} b_2(z) b_n(z) dz \quad (9)$$

and

$$\alpha_n = \frac{b_2(\frac{1}{2}) b_n'(\frac{1}{2})}{\Lambda^2 - \Lambda_n^2} ,$$

$$b_2(z) = \sum \alpha_n b_n(z) = b_2(\frac{1}{2}) \sum \frac{b_n'(\frac{1}{2}) b_n(z)}{\Lambda^2 - \Lambda_n^2}$$

or

$$b_2(z) = \frac{b_2(z)}{\sum \frac{b_n'(z) b_n(z)}{A^2 - \Lambda_n^2}} \quad (10)$$

As $A \rightarrow 0$, $b_2(z)$ is correctly given by first-order theory

$$b_2^{(1)}(z) = \frac{b_2^{(1)}(z)}{\sum \frac{b_n'(z) b_n(z)}{-\Lambda_n^2}}$$

Since first order theory is also exact for all A as $z \rightarrow -\frac{1}{2}$,

$$b_2(z) = b_2^{(1)}(z) \lim_{z \rightarrow -\frac{1}{2}} \sum \frac{b_n'(z) b_n(z)}{-\Lambda_n^2} \quad (11)$$

$$\sum \frac{b_n'(z) b_n(z)}{\Lambda^2 - \Lambda_n^2}$$

A summation of the form $\sum \frac{b_n(z) b_n(z')}{\lambda - \Lambda_n^2}$ is the Green's function

$G(\lambda, z, z')$, satisfying

$$\left[-\frac{d^2}{dz^2} - \frac{1}{2f^2} - \frac{\Delta^2}{4f^2} - \lambda \right] G = -\delta(z - z') \quad (12)$$

$$\text{Accordingly, } b_2(z) = b_2^{(1)}(z) \lim_{\substack{z \rightarrow -\frac{1}{2} \\ z' \rightarrow +\frac{1}{2}}} \frac{\frac{\partial}{\partial z'} G(0, z, z')}{\frac{\partial}{\partial z'} G(\Lambda^2, z, z')}$$

For problems whose exact solutions are not known, G may be approximated by means of a variational principle.

This work was supported by the Office of Naval Research.

1. Extensive bibliographies for the two-level problem are contained in L. Allen and J.H. Eberly, Optical Resonance and Two-Level Atoms (Wiley, New York, 1975), and M. Sargent III, M.O. Scully, and W.E. Lamb, Jr., Laser Physics, (Addison-Wesley, Reading, Mass. 1974).
2. N. Rosen and C. Zener, Phys. Rev. A 40, 502 (1932); R.T. Robiscoe, Phys. Rev. A 17, 247 (1978).
3. R.T. Robiscoe, Phys. Rev. A 27, 1365 (1983).
4. A.E. Kaplan, Sov. Phys. JETP 41, 409 (1976).
5. D.S.F. Crothers, J. Phys. B 6, 1418 (1973).
6. D.S.F. Crothers, J. Phys. B 11, 1025 (1978).
7. D.S.F. Crothers, and J.G. Hughes, J. Phys. B 10, L557 (1977).
8. A. Bambini and P.R. Berman, Phys. Rev. A 23, 2496 (1981).
9. E.J. Robinson, Phys. Rev. A 24, 2239 (1981).
10. E.J. Robinson and P.R. Berman, Phys. Rev. A 27, 1022 (1983).
11. P.M. Morse and H. Feshbach, Methods of Theoretical Physics, (McGraw-Hill New York, 1953).
12. P.R. Berman and S. Yeh, unpublished.
13. For a derivation of the variational principle for the Green's function, see, e.g., E.J. Robinson, Phys. Rev. A 18, 1334 (1978).

Production of "hot" excited-state atoms in collisionally aided radiative transitions

E. Giacobino,* M. Tawil, P. R. Berman, O. Redi, and H. H. Stroke

Supported by the U.S. Office of Naval Research, Physics Department, New York University, New York, New York 10003
under Contract No. N00014-77-C-0553.

(Received 13 June 1983)

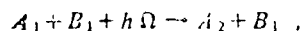
Reproduction in whole or in part is permitted for any purpose of the United States Government.

Collisionally aided radiative excitation of atoms using a laser detuned to the blue is shown to lead to heating of the external degrees of freedom. The velocity distribution of the excited atoms is studied experimentally and compared with theoretical predictions.

AFR233 1983 PACS numbers 34.50.Lf

XEROX COPY

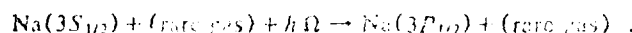
The combined effect of collisional and radiative interactions upon an atom in a vapor has been the subject of a great deal of theoretical and experimental activity in the past several years.^{1,2} A class of such reactions, commonly referred to as collisionally aided radiative excitation (CARE), can be described in a very general way as



where A_i and B_j represent atoms of different species A and B in states i and j , respectively. Experimental studies to date have mainly concentrated on measurements of either CARE cross sections or the frequency distribution of the reemitted light. However, as implied in most recent treatments of light scattering, this type of process also produces a change in the atomic velocities. The velocity changes can be viewed very easily: Let us consider radiation of frequency Ω acting on a two-level system whose Bohr frequency is ω (with $\Omega - \omega = \delta > 0$ Doppler width). As a result of the interaction with the field, the atom may undergo Rayleigh scattering or be excited to its upper state. The latter process, although possible without collision in the presence of a strong field, is greatly enhanced by collisions.³ Since the final energy level of the atom is different from the energy of the absorbed photon, the energy difference must be compensated by a change in the translational energy of the colliding atoms.

As pointed out previously,^{4,5} this process may have potential use as a method for heating or cooling an atomic vapor. Tuning with $\Omega > \omega$ produces heating whereas that with $\Omega < \omega$ produces cooling.

We have studied the case of the sodium-rare-gas system subjected to laser irradiation detuned from the sodium $3S \rightarrow 3P$ transition toward high frequencies:



The velocity distribution of the excited $3P$ sodium atoms was monitored by scanning a narrow-band probe laser through the Doppler-broadened resonance associated with absorption on the $3P_{1/2} \rightarrow 4D_{3/2}$ transition (Fig. 1).

The rare-gas perturbers used in our experiment were helium ($M=4$), argon ($M=40$), and xenon ($M=136$). The excess energy $h\Delta = h(\Omega - \omega)$ is distributed between the two partners of the collision, sodium ($M=23$) and rare gas according to the usual laws of classical mechanics. Consequently, we expect very small velocity changes for sodium in the helium-sodium collision, since the lighter helium atom carries off practically all the excess energy $h\Delta$. The velocity distribution of the $3P$ excited sodium atoms is that

case will be essentially identical to the Maxwellian velocity distribution in the ground state; this provides a control measurement to which the velocity changes obtained in collision with the heavier rare gases, argon and xenon, can be compared. In the latter cases, the velocities of the $3P$ excited sodium atoms will be nonthermal and characterized by a nonequilibrium distribution $\rho(\vec{v})$ which has been calculated using standard methods⁶:

$$\rho(\vec{v}) = \frac{P}{\gamma} W_0(\vec{v}) \int W(\vec{v}' \rightarrow \vec{v}) d\vec{v}',$$

where P is the excitation probability, γ^{-1} the lifetime of the $3P_{1/2}$ level, and $W_0(\vec{v})$ the Maxwellian distribution. The collisional kernel $W(\vec{v}' \rightarrow \vec{v})$ has been computed assuming a hard-sphere scattering potential. This can be justified because at the large blue detuning corresponding to our experimental situation, the main contribution comes from collisions with small impact parameters in which the repulsive core of the interacting potential is dominant. The theoretical $3P$ velocity distributions are shown in Fig. 2; the $3P_{1/2} \rightarrow 4D_{3/2}$ absorption profiles have essentially the same shape, with absolute area $(n_1/n_2)P/\gamma$. The curves deviate from Gaussian profiles since there are no "slow" atoms in the velocity of radiation. With $\Delta = 15.00 \times 10^3 \text{ GHz}$ at 250°C ($h\Delta = 1.6 \text{ eV}$) the full widths at $1/e^2$ maximum

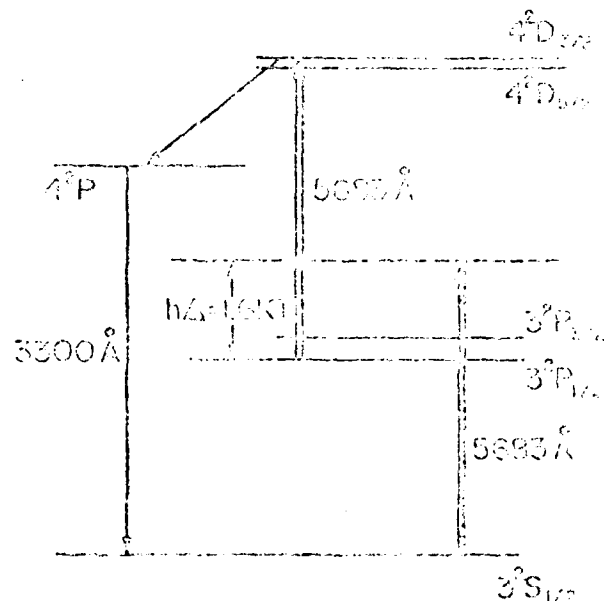


FIG. 1. Sodium energy-level diagram and excitation scheme.

*Present address: CNRS, 91190 Brunoy, France.

†Present address: Laboratoire de Physique, Université de Paris, 75231 Paris, France.

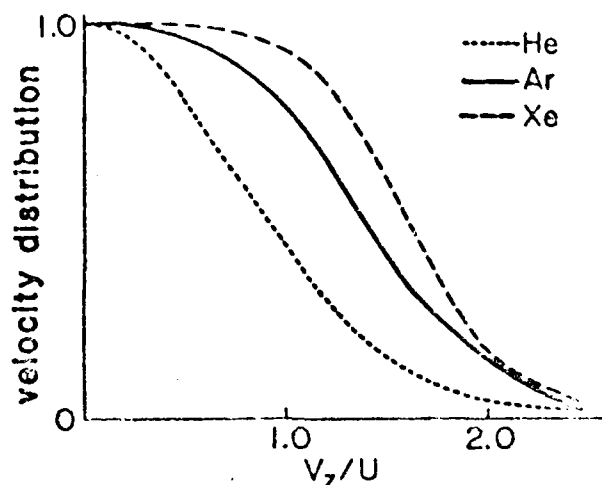


FIG. 2. Normalized theoretical velocity distributions after $3S \rightarrow 3P$ collisionally aided radiative excitation in the presence of helium, argon, and xenon (v_z is the velocity component along the laser beam, u the mean-square velocity.)

(FWHM's) are calculated to be, respectively, 1.9, 2.9, and 3.5 GHz for helium, argon, and xenon perturbers. The FWHM given by a Maxwellian velocity distribution at the same temperature is 1.6 GHz.

The experimental setup is shown in Fig. 3. The experiment was performed in an alkali-vacuum glass cell connected to a vacuum system, and kept by an oven at a temperature of about 250°C, producing a sodium density of 5×10^{13} cm^{-3} . Rare-gas (helium, argon, xenon) pressures between 5 and 20 Torr were used. The atoms were irradiated by laser light focused into the cell to a diameter of about 50 μm . The collisionally aided $3S \rightarrow 3P$ excitation and the probing on the $3P_{1/2} \rightarrow 4D_{3/2}$ transition were achieved with the same laser, tuned to the $3P_{1/2} \rightarrow 4D_{3/2}$ line (5893 Å). The corresponding detuning of the laser from the $3S_{1/2} \rightarrow 3P_{1/2}$ resonance (688 Å) is 19.09×10^3 GHz. The laser used is an argon-ion-pumped single-mode ring dye laser operated with rhodamine 6G at a power of 50 mW to avoid excessive saturation of the $3P \rightarrow 4D$ transition. The laser was scanned over 30 GHz across the $3P_{1/2} \rightarrow 4D_{3/2}$ resonance. (The magnitude of this scan over a range is very small compared with the frequency detuning Δ from the $3S \rightarrow 3P$ transition, and the resulting variation of Δ can be neglected.) The scan was calibrated by passing a small part

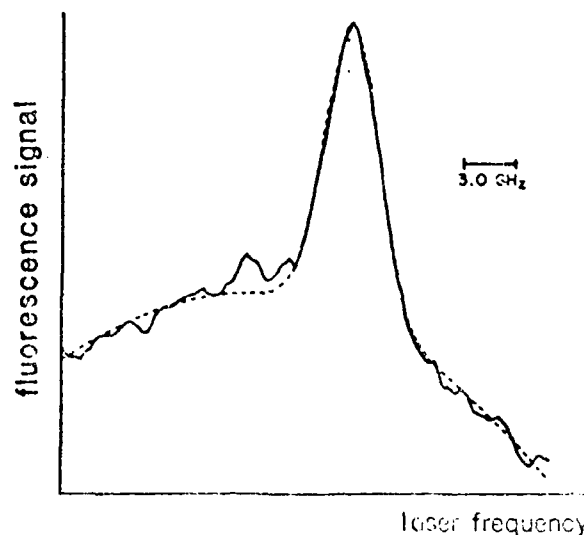


FIG. 4. Na-Xe collisional line shape recorded on the $4D \rightarrow 3P$ fluorescence (solid line). $T = 250^\circ\text{C}$, $p_{\text{Xe}} = 20$ Torr. Because of the low transmission of the alkali-resistant glass in the UV, we could not use the 3300-Å line associated with the $4D \rightarrow 4P \rightarrow 3S$ cascade. The $4D \rightarrow 3P$ fluorescence appears on the background laser light, which has been taken into account by including a broad parabola in the fitting function (dashed line).

of the laser beam through an iodine cell and recording the absorption spectrum.⁷ The $3P_{1/2} \rightarrow 4D_{3/2}$ transition line shape was measured by monitoring the fluorescence emitted from the $4D_{3/2}$ level on an x-y recorder or a data converter for computer analysis. An example of the latter is shown in Fig. 4.

As discussed above, the width of this Doppler-broadened absorption line gives a measurement of the mean speed of the $3P$ atoms along the laser propagation axis. Table I shows the FWHM measured in our experiments for various pressures of rare-gas perturbors. There is an obvious difference in the widths obtained for helium and the two heavy rare gases. However, these raw data actually include pressure and power broadening effects on the probe transition which we have extracted for a more quantitative comparison with the theoretical Doppler widths given above. This was done in this case by the use of the pressure and power broadening results obtained with helium as the perturber. The Doppler profile in this case is essentially the Gaussian curve associated with the Maxwellian distribution. The absorption line shape is a Voigt profile that results from the convolution of the Gaussian-Doppler line shape with a Lorentzian function, the width of which is determined by pressure and light-

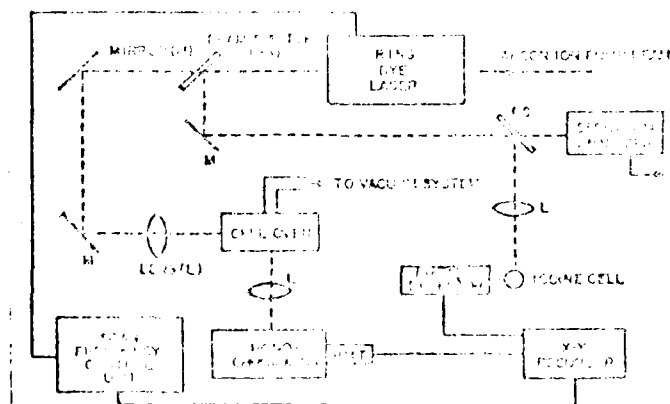


FIG. 3. Experimental setup.

TABLE I. Widths, in GHz, of the probe $3P \rightarrow 4D$ transition. The estimated errors are about 0.1 GHz.

Rare-gas pressure (Torr)	Na-He	Na-Ar	Na-Xe
5	2.7	3.0	
10	2.7		
20	3.1		
30	3.3		

AD-A134 299

THEORETICAL STUDIES RELATING TO THE INTERACTION OF
RADIATION WITH MATTER... (U) NEW YORK UNIV NY DEPT OF
PHYSICS P R BERMAN 15 SEP 83 N00014-77-C-0553

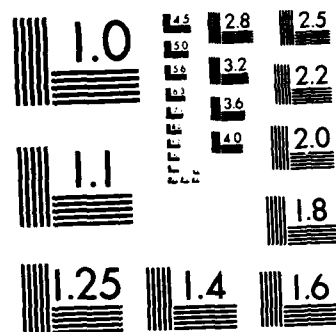
2/2

UNCLASSIFIED

F/G 20/8

NL





MICROCOPY RESOLUTION TEST CHART
NATIONAL BUREAU OF STANDARDS-1963-A

power broadening (the natural width and lfs can be neglected here). Study of the dependence of the widths upon laser power shows that the power broadening is significant. However, at a laser power of 50 mW, which was used in all the experimental runs, it is rather small and is accounted for in our data processing at the same time as pressure broadening, as shown below. For the analysis of pressure broadening effects, we rely on previous experimental studies^{8,9} which indicate that the pressure broadening coefficients for helium, argon, and xenon are the same within 15% for the $3P \rightarrow 4D$ transition. We have thus assumed the same Lorentzian widths for the heavy rare gases as for helium at the same pressure, and we have used the values of the Lorentzian widths experimentally determined by the deconvolution of the curves obtained with helium to interpret the absorption curves obtained with argon and xenon. We obtained the Doppler contributions to the linewidths for the latter two gases by a deconvolution also assuming a Voigt profile (this assumption will be discussed below). Thus we obtained values for the Doppler widths which are no longer dependent on the foreign gas pressure.

These are shown in Table II, along with the theoretical predictions. For both argon and xenon, it can be seen that the experimental values are significantly larger than the thermal Doppler widths. This gives evidence for the predicted "heating" effect. Nevertheless, the effect is smaller than theoretically calculated. One can account for this if one considers the processes that thermalize the atoms in the $3P$ state. First, once excited to the $3P$ state and before absorbing a second laser photon, the sodium atoms may undergo collisions with the perturbers which tend to return the velocity distribution to the thermal one. We note that the laser power density is large enough for the $3P \rightarrow 4D$ transition to be partly saturated, which reduces these velocity changes. Second, the reabsorption of resonance photons, which provides an alternative mechanism to excite atoms from the ground state, has the same effect of washing out the particular velocity distribution of the $3P$ atoms by CARE. Although we work at densities of sodium where the optical depth for resonant light is high, the transit time of an atom excited by CARE through the laser beam is small, so that reabsorption events take place mainly outside of the laser beam, where we do not detect them. These ef-

TABLE II. Comparison of the experimentally obtained widths with theory (power and pressure broadening extracted). All values are in GHz.

Gas	Thermal Doppler width	Theoretical width including heating	Experimental Doppler width
Ar	1.8	2.9	2.4
Xe	1.8	3.5	2.8

fects are very difficult to estimate quantitatively. In order to study them it would be necessary to perform experiments at lower sodium and rare-gas pressures, which we were unable to do because of signal-to-noise ratio considerations. The partial thermalization in the $3P$ level may also explain why the experimental absorption line shape (Fig. 4) for the $3P \rightarrow 4D$ transition differs from the theoretically predicted one (Fig. 2), and justifies our use of a Voigt profile in fitting the data.

In conclusion, our experiment has shown evidence for significant "heating" associated with the collisionally aided radiative excitation of the $3P$ atoms using a laser detuned to be blue. If a large enough fraction of the atoms in the laser beam undergoes such a transition, this effect might lead to measurable temperature variations in the vapor, providing a new method of laser heating or cooling. [We wish to point out that cooling cannot be observed in the excited state, or least after one absorption process: If the laser is tuned to the red side of the line, only fast atoms can be excited from the ground state, and are slowed down, resulting in a velocity distribution which can be shown to be identical to the Maxwellian one.¹⁰ In this case, the ground state is cooled.]

One of us (E.G.) would like to thank P. R. Berman and H. H. Strobe for the kind hospitality during her stay at New York University. We wish to thank W. Happer, Princeton University, for providing us with alkali-resistant cells during the initial stages of this work. This work was supported by the U.S. Office of Naval Research, and NSF under Grants No. 7921530 and No. PHY8204402-01.

*Permanent address: Laboratoire de Spectroscopie Hertzienne de l'Ecole Normale Supérieure, Université Pierre et Marie Curie, 4 Place Jussieu, F-75239 Paris, Cedex 05 France.

¹J. L. Carlsten and A. Szöke, Phys. Rev. Lett. **36**, 667 (1976); J. L. Carlsten, A. Szöke, and M. G. Raymer, Phys. Rev. A **15**, 1029 (1977).

²S. Yeh and P. R. Berman, Phys. Rev. A **19**, 1106 (1979); P. R. Berman and F. J. Robinson, in *Photon Assisted Collisions and Related Topics*, edited by N. K. Bahner and C. Guidotti (Harwood Academic Publishers, Chur, Switzerland, 1982), pp. 15-33.

³S. Reynaud and C. Cohen-Tannoudji, J. Phys. (Paris) **43**, 1021 (1982).

⁴P. R. Berman and S. Stenholm, Opt. Commun. **24**, 155 (1978).

⁵E. Giacobino and P. R. Berman, Proceedings of the Workshop on Spectroscopic Applications of Slow Atomic Beams, Nat. Bur. Stand. (U.S.) Publication No. 88 (unpublished).

⁶M. Tawil, Ph.D. thesis (New York University, 1983) (unpublished).

⁷S. Gerstenkorn and P. Luc, *Atlas du Spectre d'Absorption de la Molecule d'Iode* (Editions du CNRS, Paris, 1978).

⁸R. Walkup, A. Spielhiedel, D. Fly, W. D. Phillips, and D. E. Pritchard J. Phys. B **20**, 1953 (1981).

⁹A. Flusberg, T. Mossberg, and S. R. Hartmann, Opt. Commun. **24**, 207 (1978).

¹⁰P. Berman (unpublished).

Cooling of Vapors Using Collisionally Aided Radiative Excitation*

E. Giacobino and P.R. Berman

Physics Department, New York University, New York, N.Y. 10003

Collisionally aided radiative excitation (CARE) is proposed as a mechanism for cooling an atomic vapor. With a CW laser power of 1.0 W/cm^2 and the resonant dipole-dipole interaction providing the collision mechanism, we estimate that temperature gradients of tens of degrees per cm can be achieved at vapor densities of order $10^{16} \text{ atoms/cm}^3$.

Key words: cooling, collisions, resonant broadening, laser assisted collisions.

1. Introduction

Over the past several years, there has been considerable interest in collisional processes that occur in the presence of radiation fields such as reactions of the form



(A_1 , atom A in state 1; B_1 , atom B in state 1), which are commonly referred to as collisionally aided radiative excitation (CARE) [1]. Most experimental studies to date have concentrated on measurements of either the CARE cross sections or the frequency distribution of the reemitted light. However, it can easily be seen that CARE also produces a change in the atoms' translational energy and, as such may have potential use as a method for heating or cooling an atomic vapor [2].

*Supported in part by NSF Grant INT 7921530 and by the U.S. Office of Naval Research.

Let us consider radiation of amplitude E and frequency Ω acting on a two-level atomic system whose Bohr frequency is $\omega = \Omega - \Delta$ ($|\Delta| \gg$ Doppler width). As a result of the interaction with the field, the atom may scatter a Rayleigh photon or be excited to its upper state. The latter process, although possible without collisions in strong fields, is greatly enhanced by collisions [1]. Since the final energy level of the atom is different from the energy of the absorbed photon, the energy difference must be compensated by a change in the translational energy of the colliding atoms. As pointed out previously [2] the net result is a cooling or a heating of the vapor. Tuning with $\Omega > \omega$ produces heating and that with $\Omega < \omega$ produces cooling.

2. Expected Cooling

The magnitude of the effect depends strongly on the detuning $\Delta = \Omega - \omega$: each time an atom interacts with a photon the energy $\hbar\Delta$ is removed or added to the vapor. One may choose $\hbar\Delta$ to be an appreciable fraction of kT (at 500°K kT corresponds to a frequency of 10^4 GHz or a wave number of $3 \times 10^2 \text{ cm}^{-1}$), so that velocity changes are large compared with those of order 1.0 cm/sec which occur as a result of photon-recoil processes.

Of course, the process considered here involves a non-resonant atom-field interaction and the rate of excitation is reduced compared to a resonant excitation by a factor Γ^2/Δ^2 where Γ is the collision rate. (For the sake of simplicity we use expressions calculated using the impact limit of line broadening). We shall consider the case of resonant broadening; i.e. the resonant dipole-dipole interaction between two atoms of the species gives rise to the rate Γ .

The rate of excitation to level 2 from level 1, is given by

$$\dot{n}_2 = \frac{2\chi^2\Gamma}{\Delta^2} (n_1 - n_2) \quad (1)$$

where n_1 is the population of state 1, χ is the Rabi frequency defined by

$$\chi = \frac{\mu E}{\hbar} \quad (2)$$

and μ is the dipole matrix element for the transition. If $n_1 \gg n_2$, the steady-state upper population of state 2 is

$$n_2 = \frac{2\chi^2\Gamma}{\gamma\Delta^2}, \quad (3)$$

where γ is the decay rate of the upper level. For cooling to actually occur, the atom must decay back to the ground state via spontaneous emission rather than via stimulated emission (stimulated emission would "heat" the atom if absorption cools it). This means that it is advisable to restrict the laser power such that

$$\frac{2\chi^2\Gamma}{\Delta^2} < \gamma. \quad (4)$$

Beyond this limit, any additional laser power is useless since there is as much stimulated emission as absorption.

For an atomic density N and cylindrical interaction volume of length L and cross-sectional area A , the power dH/dt removed from the sample is

$$\frac{dH}{dt} = \hbar\Delta \frac{2\chi^2\Gamma}{\Delta^2} NAL, \quad (5)$$

which may be rewritten as

$$\frac{dH}{dt} = \frac{\hbar\Delta}{1/\gamma} \frac{P}{P_m} NAL, \quad (P < P_m) \quad (6)$$

where P is the laser power and P_m is the maximum laser power consistent with condition (4). This result suggests a potentially large heating or cooling effect. Taking

$$\begin{aligned} \hbar\Delta/kT &= 0.1 \quad (\Delta/2\pi = 10^3 \text{ GHz}) ; \quad \gamma/2\pi = 10 \text{ MHz}; \\ P/P_m &\approx 10^{-7} \quad (P \approx 5.0 \text{ W/cm}^2 ; N \approx 10^{15} \text{ cm}^{-3}), \end{aligned}$$

one finds

$$\frac{1}{NAL} \frac{dH}{dt} \approx 6 \hbar\Delta \text{ sec}^{-1} \quad (7)$$

Under such conditions, the time scale at which the energy is removed or doubled is

1.0 sec. In calculating dH/dt , we assumed the medium to be optically thin.

The above calculation has to be modified when effects of radiation trapping are taken into account. Equation (4) must be replaced by

$$\frac{2\chi^2\Gamma}{\Delta^2} < \gamma' , \quad (8)$$

where γ' is the effective upper state decay rate in the presence of radiation trapping. Typically, one finds [3]

$$\gamma' \approx \gamma / [KL (\pi \ln KL)^{1/2}], \quad (KL \gg 1) \quad (9)$$

where

$$K = N\sigma_0 (\gamma/\omega_D) \quad (10)$$

is the absorption coefficient for resonant radiation in a Doppler broadened medium (ω_D = Doppler width). The cross section σ_0 is given by

$$\sigma_0 = \frac{2\Omega}{\epsilon_0 c} \frac{\mu^2}{\hbar\gamma} \approx \lambda^2/2 , \quad (11)$$

where μ is the dipole matrix element and λ the wavelength for the transition.

The rate of energy loss for the sample is now given by

$$\frac{dH}{dt} = \frac{\hbar\Delta}{1/\gamma'} \frac{P}{P_m'} NAL, \quad (P < P_m') \quad (12)$$

where P_m' is the maximum laser power consistent with condition (8). Note that P_m' may be considerably less than P_m . However, since $P_m'/\gamma' = P_m/\gamma$, Eq. (12) may be recast in the form

$$\frac{dH}{dt} = \frac{\hbar\Delta}{1/\gamma} \frac{P}{P_m} NAL . \quad [P < P_m' = P_m(\gamma'/\gamma)] \quad (13)$$

Equation (13) is identical to the result (6) which we found in the absence of radiation trapping, except that P is limited to a smaller value.

Even though P is limited to a value equal to P'_m , significant cooling can still be achieved. For example, for the parameters chosen above, one can use Eqs. (9-11) to estimate $P'_m/P_m = \gamma'/\gamma \approx 10^{-6}$, assuming a cell length on the order of 5cm. Since P/P_m was taken equal to 10^{-7} , one finds $P \approx 10^{-1} P'_m$ which does not violate the condition $P < P'_m$. Thus, the expected cooling is the same as that found in Eq. (7).

3. Temperature Gradient

We can now estimate the temperature gradient in a cell created by this cooling. Considering that the atoms are perfectly thermalized on the wall of the cell, the amount of energy we must remove per second, to keep a temperature gradient dT/dr between the laser interaction region and walls is

$$\frac{1}{S} \frac{dH}{dt} = \kappa \frac{dT}{dr} , \quad (14)$$

where S is the surface of the laser beam [$S = 2\sqrt{\pi AL} = 2L$; beam circumference = $2L$] and κ is the thermal conductivity of the gas approximately given by

$$\kappa \approx ku/\sigma_c \quad (15)$$

where k is the Boltzmann constant, u a mean speed, and σ_c a collision cross section.

Combining Eqs. (14) and (13) and dividing by the wall temperature T_w we obtain

$$\frac{L}{T_w} \frac{dT}{dr} = \frac{\sigma_c}{(u/\gamma)L} \left(\frac{\hbar\Delta}{kT_w} \right) \left(\frac{P}{P_m} \right) NAL . \quad (P < P'_m) \quad (16)$$

We may also note that the limiting value P_m determined from condition [4] is given by

$$P_m = 2 \frac{\hbar\Delta^2 \Omega}{\Gamma \sigma_o} A . \quad (17)$$

To optimize the temperature gradient which can be obtained, we proceed as follows:

(1) We choose a density N such that the optical depth for the laser radiation is

equal to unity. That is, we set

$$K_L L = 1 = \frac{N \sigma_o \Gamma \gamma}{2 \Delta^2} L ;$$

$$N = 2 \Delta^2 / (\sigma_o L \Gamma \gamma) \quad (18)$$

For $L = 5 \text{ cm}$, and Γ determined from theories of resonance broadening [4] (i.e. $\Gamma = 0.023 N \lambda^3 \gamma$), $\lambda = 600 \text{ nm}$, and the values of Δ and γ used above, one finds $N = 2 \times 10^{16} \text{ atoms/cm}^3$. By choosing an optical depth of unity, we ensure that each photon "does its duty" in removing energy from the sample. (2) For this value of N , Eq. (9) yields a value $\gamma'/\gamma = P'_m/P_m \approx 10^{-7}$ (3) Using Eq. (17), we estimate the maximum allowed value P'_m for P to be

$$\frac{P'_m}{A} \approx 1 \times 10^{-7} \frac{P_m}{A} \approx 0.2 \text{ W/cm}^2 .$$

(4) Since this value of P'_m/A is readily obtainable with a CW laser for $A < 5 \text{ cm}^2$ we set P/P_m equal to its maximum allowed value (P'_m/P_m) in Eq. (16). Moreover, we take $N \sigma_c \approx 0.1 \Gamma/u^*$ to finally obtain

$$\frac{l}{T_W} \frac{dT}{dr} = 0.1 \left(\frac{\hbar \Delta}{k T_W} \right) \frac{\Gamma \gamma A}{u^2} \cdot (1 \times 10^{-7}) . \quad (19)$$

For $A \approx 4.0 \text{ cm}^2$, $\Gamma = 0.6 \times 10^{10} \text{ sec}^{-1}$, $u^2 = 10^{10} \text{ cm/sec}$, $(\hbar \Delta/kT) = 0.1$,

$$\frac{l}{T_W} \frac{dT}{dr} \approx 0.1 \quad (20)$$

The temperature gradients predicted by Eq. (19) (of order 10 degrees/cm) may be somewhat optimistic. However, this order of magnitude calculation does seem to indicate that significant cooling can be achieved using collisionally aided radiative excitation.

One of us (E.G.) would like to thank Dr. F. Laloe for stimulating discussions on this subject.

*We assume that the excited state population is close enough to saturation to ensure that it is resonant collisions that provide the major contribution to the thermal conductivity.

4. References

- [1] See, for example, the review article by P.R. Berman and E.J. Robinson in Photon-Assisted Collisions and Related Topics edited by N.K. Rahman and C. Guidotti, (Harwood Academic Pub., Chur, Switz. , 1982) pp.15-34 and other articles in this book.
- [2] P.R. Berman and S. Stenholm, Opt. Comm. 24, 155 (1978).
- [3] M.I. Dyakonov and V.I. Perel, Sov. Phys. - JETP 20, 997 (1965).
- [4] A recent review is given by E.L. Lewis [E.L. Lewis, Phys. Rep. 58, 3 (1980)].

Heating of Atoms by Collisionally Assisted Radiative Excitation

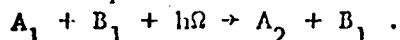
E. Giacobino*, M. Tawil, O. Redi, R. Vetter**, R.H. Stroke and P.R. Berman

Department of Physics, New York University, 4 Washington Place, New York, N.Y. 10003, U.S.A.

*Permanent address: Laboratoire de Spectroscopie Hertzienne de l'ENS, Paris, France

**Permanent address: Laboratoire Aimé Cotton, Orsay, France

Over the past several years there has been considerable interest in collisional processes that occur in the presence of laser fields [1] such as,



This class of reactions is commonly referred to as CARE (Collisionally Aided Radiative Excitation). If the laser is detuned from the 1-2 transition frequency by Δ , the collision provides translational kinetic energy to compensate for the mismatch $h\Delta$ between the field and the atomic transition, which leads to a corresponding change in the velocity of the atoms involved in the process. This change in translational energy is distributed between the active atom (A) and the perturber (B) depending on their relative masses.

We have studied the case of the sodium-rare gas system subjected to laser irradiation detuned from the 3S - 3P transition toward high frequencies. The velocity distribution of sodium excited 3P atoms has been calculated for various rare gases using a hard sphere collision kernel. The distribution obtained with helium perturbers is very close to the initial Maxwellian distribution, since helium is much lighter than sodium and takes practically all the excess energy. In contrast, when argon or xenon is used, the sodium atoms are predicted to undergo large velocity changes, and the Doppler lineshape deviates from a Gaussian lineshape.

Experimentally, the velocity distribution of the 3P atoms was monitored by looking at the Doppler broadened resonance associated with the absorption on a second transition 3P \rightarrow 4D.

We observed a significant difference between the Doppler width of the 3P - 4D transition for helium, argon and xenon perturbers (see Table I).

Table 1: Widths of the absorption resonance on the probe 3P \rightarrow 4D in GHz. The accuracy is about 0.1 GHz.

Rare Gas Pressure-Torr	Na-He	Na-Ar	Na-Xe
5	2.7	3.0	
10	2.7	3.2	3.5
20	3.1	3.3	4.0
30	3.3	3.6	

To precisely check by how much the Doppler width was modified by the "heating" effect, we had to extract the effect of pressure and power broadening on the 3P \rightarrow 4D probe transition. These were determined in the case of helium, where there is no heating, from the deconvolution of the experimental Voigt

Supported by the U.S. Office of Naval Research under Contract NO. N00014-77 C 0053.

Reproduction in whole or in part is permitted for any part of the United States Government

END

FILMED

11/13

EDITION